

FILE COPY

ESD-TR-75-80

MTR-2968

CHARACTERIZATION OF THE DIGITAL HIGH-SPEED
AUTOVON CHANNEL - FINAL REPORT

AUGUST 1975

SD ACCIDENT LIST

AFRI Call No.

83339

Copy No.

1 of 2 cys.

Prepared for

DEPUTY FOR COMMAND AND MANAGEMENT SYSTEMS

ELECTRONIC SYSTEMS DIVISION

AIR FORCE SYSTEMS COMMAND

UNITED STATES AIR FORCE

Hanscom Air Force Base, Bedford, Massachusetts



Approved for public release;
distribution unlimited.

Project No. 6190

Prepared by

THE MITRE CORPORATION

Bedford, Massachusetts

Contract No. F19628-75-C-0001

BEST AVAILABLE COPY

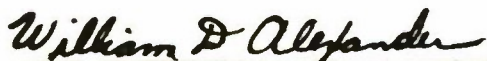
ADA016402

When U.S. Government drawings, specifications, or other data are used for any purpose other than a definitely related government procurement operation, the government thereby incurs no responsibility nor any obligation whatsoever; and the fact that the government may have formulated, furnished, or in any way supplied the said drawings, specifications, or other data is not to be regarded by implication or otherwise, as in any manner licensing the holder or any other person or corporation, or conveying any rights or permission to manufacture, use, or sell any patented invention that may in any way be related thereto.

Do not return this copy. Retain or destroy.

REVIEW AND APPROVAL

This technical report has been reviewed and is approved for publication.

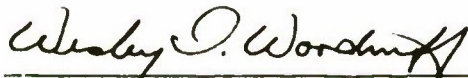


WILLIAM D. ALEXANDER, Captain, USAF
Project Engineer, Equipment Branch
SATIN IV Engineering Division



ARTHUR J. ROSCOE, JR., Lt. Colonel, USAF
Acting Chief
SATIN IV Engineering Division

FOR THE COMMANDER



WESLEY D. WOODRUFF, Colonel, USAF
System Program Director
SATIN IV System Program Office
Deputy for Command and Management Systems

UNCLASSIFIED

SECURITY CLASSIFICATION OF THIS PAGE (When Data Entered)

REPORT DOCUMENTATION PAGE		READ INSTRUCTIONS BEFORE COMPLETING FORM
1. REPORT NUMBER ESD-TR-75-80	2. GOVT ACCESSION NO.	3. RECIPIENT'S CATALOG NUMBER
4. TITLE (and Subtitle) CHARACTERIZATION OF THE DIGITAL HIGH-SPEED AUTOVON CHANNEL		5. TYPE OF REPORT & PERIOD COVERED FINAL REPORT
		6. PERFORMING ORG. REPORT NUMBER MTR-2968
7. AUTHOR(s) Kenneth Brayer		8. CONTRACT OR GRANT NUMBER(s) F19628-75-C-0001
9. PERFORMING ORGANIZATION NAME AND ADDRESS The MITRE Corporation Box 208 Bedford, MA 01730		10. PROGRAM ELEMENT, PROJECT, TASK AREA & WORK UNIT NUMBERS Project No. 6190
11. CONTROLLING OFFICE NAME AND ADDRESS Deputy for Command and Management Systems Electronic Systems Division, AFSC Hanscom Air Force Base, Bedford, MA 01731		12. REPORT DATE AUGUST 1975
		13. NUMBER OF PAGES 131
14. MONITORING AGENCY NAME & ADDRESS (if different from Controlling Office)		15. SECURITY CLASS. (of this report) UNCLASSIFIED
		15a. DECLASSIFICATION DOWNGRADING SCHEDULE
16. DISTRIBUTION STATEMENT (of this Report) Approved for public release; distribution unlimited.		
17. DISTRIBUTION STATEMENT (of the abstract entered in Block 20, if different from Report)		
18. SUPPLEMENTARY NOTES		
19. KEY WORDS (Continue on reverse side if necessary and identify by block number) AUTOVON CHANNEL MODELING DATA COMMUNICATION ERROR PATTERN ANALYSIS MARKOV CHAIN MODELS		
20. ABSTRACT (Continue on reverse side if necessary and identify by block number) AUTOVON, a voice telephone communication system available to U.S. Government agencies, can be used for the transmission of high-speed digital data. In this paper, the performance of AUTOVON in passing 4800 b/s and 9600 b/s digital data is evaluated in terms of the residual channel error distributions associated with the use of the state-of-the-art Codex 9600 modem. It is demonstrated that the channel is a burst error channel and will support data transmission with bit error rates in		

20. ABSTRACT

the order of 10^{-4} to 10^{-5} . In addition, channel models are presented that can be used to predict the performance and design of error-detecting/correcting codes.

FOREWORD

The research reported in this paper was performed by the MITRE Corporation in conjunction with the Digital Communications Experimental Facility (DICEF) of the Rome Air Development Center (RADC), Griffiss AFB. Channel tests of the AUTOVON network were conducted by RADC and the digital data was analyzed by MITRE. Special appreciation must be given to Mr. J. McEvoy of RADC/DCLD who helped organize the tests and placed many of the test requirements in proper perspective, and to Capt. C. Lownes RADC/DCLD who was test director.

The Codex 9600 modem was used solely because it was readily available at RADC. This study was in no way intended as an evaluation of the Codex 9600 modem. The AUTOVON switches used for creating tandem links were selected only because dial-thru units were available at these switches at the time the tests started. The tests were conducted on a one-to two-day per week basis from August 1973 to April 1974.

An interim analysis of the error pattern data available part way through the test program was reported in ESD-TR-75-79, Characterization and Modeling of the Digital High-Speed AUTOVON Channel-Interim Report, August 1975. The results in this paper supersede and replace the earlier results.

TABLE OF CONTENTS

		<u>Page</u>
	LIST OF ILLUSTRATIONS	5
	LIST OF TABLES	13
SECTION I	INTRODUCTION	15
	AUTOVON	15
	The Codex 9600 Modem	17
	Test Procedure	18
	Summary of Data	19
SECTION II	4800 VS. 9600 B/S DATA ANALYSIS	21
	INTER-ERROR PROBABILITIES	21
	BURST DEFINITIONS	25
	Definition of a Burst	25
	Definition of an Interval	28
	BURST ANALYSIS	29
	Burst Distributions	29
	Interval Distributions	29
	MARKOV CHANNEL MODEL	33
	The MARKOV Chain Model	33
	Data-Derived Channel Models	36
SECTION III	ANALYSIS BY SWITCH CONFIGURATION	39
	INTER-ERROR DISTRIBUTIONS	39
	BURST DISTRIBUTIONS	42

TABLE OF CONTENTS (Concluded)

	<u>Page</u>
SECTION IV	
ANALYSIS ACCORDING TO CIRCUIT MILEAGE	57
INTER-ERROR DISTRIBUTIONS	57
BURST DISTRIBUTIONS	61
SECTION V	
ANALYSIS ACCORDING TO NUMBERS OF TRUNKS	73
INTER-ERROR DISTRIBUTIONS	73
BURST DISTRIBUTIONS	77
SECTION VI	
CONCLUSIONS	89
APPENDIX I	
TULLY ACCESS LINE ERROR PATTERNS	91
APPENDIX II	
COMPARATIVE ERROR PATTERNS OF BELL AND CODEX MODEMS	99
LOOP TO ARLINGTON, VIRGINIA	99
LOOP TO SANTA ROSA, CALIFORNIA	102
LOOP TO ROCKDALE, GEORGIA	110
CONCLUSIONS	110
APPENDIX III	
CODEX SCRAMBLER MODE VS. CODEX SELF-SYNC MODE	123
Comparative Error Distributions	123
REFERENCES	133

LIST OF ILLUSTRATIONS

<u>Figure</u>		<u>Page</u>
1	Cumulative Distribution of Consecutive Errors — Codex Modem Data	23
2	Cumulative Distribution of Error-Free Gaps — Codex Modem Data	23
3	Relative Frequency of Errors — All 4800 b/s Data 2048 Bits/Block	24
4	Relative Frequency of Errors — All 9600 b/s Data 2048 Bits/Block	24
5	Probability of at Least E Errors in an M Bit Block — 4800 b/s All Data	26
6	Probability of at Least E Errors in an M Bit Block — 9600 b/s All Data	27
7	Cumulative Distribution on Lengths of Bursts — Codex Modem Data	30
8	Cumulative Distribution on Burst Densities — Codex Modem Data	30
9	Cumulative Distribution on Lengths of Intervals — Codex Modem Data	31
10	Cumulative Distribution on Interval Densities — Codex Modem Data	31
11	Interval to Burst Ratios — Codex Modem Data	32
12	Cumulative Distribution of Consecutive Errors — 4800 b/s Data	41
13	Cumulative Distribution of Consecutive Errors — 9600 b/s Data	41
14	Cumulative Distribution of Error-Free Gaps — 4800 b/s Data	43
15	Cumulative Distribution of Error-Free Gaps — 9600 b/s Data	43
16	Probability of at Least E Errors in an M Bit Block — Loop to 1 Switch/4800 b/s	44

LIST OF ILLUSTRATIONS (Continued)

<u>Figure</u>		<u>Page</u>
17	Probability of at Least E Errors in an M Bit Block — Loop to 2 Switches/4800 b/s	45
18	Probability of at Least E Errors in an M Bit Block — Loop to 3 Switches/4800 b/s	46
19	Probability of at Least E Errors in an M Bit Block — Loop to 4 Switches/4800 b/s	47
20	Probability of at Least E Errors in an M Bit Block — Loop to 1 Switch/9600 b/s	48
21	Probability of at Least E Errors in an M Bit Block — Loop to 2 Switches/9600 b/s	49
22	Probability of at Least E Errors in an M Bit Block — Loop to 3 Switches/9600 b/s	50
23	Cumulative Distribution on Lengths of Bursts — 4800 b/s Data	51
24	Cumulative Distribution on Lengths of Bursts — 9600 b/s Data	51
25	Cumulative Distribution on Burst Densities — 4800 b/s Data	52
26	Cumulative Distribution on Burst Densities — 9600 b/s Data	52
27	Cumulative Distribution on Lengths of Intervals — 4800 b/s Data	53
28	Cumulative Distribution on Lengths of Intervals — 9600 b/s Data	53
29	Cumulative Distribution on Interval Densities — 4800 b/s Data	54
30	Cumulative Distribution on Interval Densities — 9600 b/s Data	54
31	Interval to Burst Ratios — 4800 b/s Data	55
32	Interval to Burst Ratios — 9600 b/s Data	56

LIST OF ILLUSTRATIONS (Continued)

<u>Figure</u>		<u>Page</u>
33	Cumulative Distribution of Consecutive Errors — 4800 b/s Data	59
34	Cumulative Distribution of Consecutive Errors — 9600 b/s Data	59
35	Cumulative Distribution of Error-Free Gaps — 4800 b/s Data	60
36	Cumulative Distribution of Error-Free Gaps — 9600 b/s Data	60
37	Probability of at Least E Errors in an M Bit Block — Circuit ≤ 1000 MI/4800 b/s	62
38	Probability of at Least E Errors in an M Bit Block — 1000 MI < Circuit < 3000 MI/4800 b/s	63
39	Probability of at Least E Errors in an M Bit Block — Circuit ≥ 3000 MI/4800 b/s	64
40	Probability of at Least E Errors in an M Bit Block — Circuit ≤ 1000 MI/9600 b/s	65
41	Probability of at Least E Errors in an M Bit Block — 1000 MI < Circuit < 3000 MI/9600 b/s	66
42	Probability of at Least E Errors in an M Bit Block — Circuit ≥ 3000 MI/9600 b/s	67
43	Cumulative Distribution on Lengths of Bursts — 4800 b/s Data	68
44	Cumulative Distribution on Lengths of Bursts — 9600 b/s Data	68
45	Cumulative Distribution on Burst Densities — 4800 b/s Data	69
46	Cumulative Distribution on Burst Densities — 9600 b/s Data	69
47	Cumulative Distribution on Lengths of Intervals — 4800 b/s Data	70

LIST OF ILLUSTRATIONS (Continued)

<u>Figure</u>		<u>Page</u>
48	Cumulative Distribution on Lengths of Intervals — 9600 b/s Data	70
49	Cumulative Distribution on Interval Densities — 4800 b/s Data	71
50	Cumulative Distribution on Interval Densities — 9600 b/s Data	71
51	Interval to Burst Ratios — 4800 b/s Data	72
52	Interval to Burst Ratios — 9600 b/s Data	72
53	Cumulative Distribution of Consecutive Errors — 4800 b/s Data	75
54	Cumulative Distribution of Consecutive Errors — 9600 b/s Data	75
55	Cumulative Distribution of Error-Free Gaps — 4800 b/s Data	76
56	Cumulative Distribution of Error-Free Gaps — 9600 b/s Data	76
57	Probability of at Least E Errors in an M Bit Block — Loop on 2 Trunks/4800 b/s	78
58	Probability of at Least E Errors in an M Bit Block — Loop on 4 Trunks/4800 b/s	79
59	Probability of at Least E Errors in an M Bit Block — Loop on 5 or More Trunks/4800 b/s	80
60	Probability of at Least E Errors in an M Bit Block — Loop on 2 Trunks/9600 b/s	81
61	Probability of at Least E Errors in an M Bit Block — Loop on 4 Trunks/9600 b/s	82
62	Probability of at Least E Errors in an M Bit Block — Loop on 6 Trunks/9600 b/s	83
63	Cumulative Distribution on Lengths of Bursts — 4800 b/s Data	84

LIST OF ILLUSTRATIONS (Continued)

<u>Figure</u>		<u>Page</u>
64	Cumulative Distribution on Lengths of Bursts — 9600 b/s Data	84
65	Cumulative Distribution on Burst Densities — 4800 b/s Data	85
66	Cumulative Distribution on Burst Densities — 9600 b/s Data	85
67	Cumulative Distribution on Lengths of Intervals — 4800 b/s Data	86
68	Cumulative Distribution on Lengths of Intervals — 9600 b/s Data	86
69	Cumulative Distribution on Interval Densities — 4800 b/s Data	87
70	Cumulative Distribution on Interval Densities — 9600 b/s Data	87
71	Interval to Burst Ratios — 4800 b/s Data	88
72	Interval to Burst Ratios — 9600 b/s Data	88
73	Cumulative Distribution of Consecutive Errors — DICEF to Tully Access Line	92
74	Cumulative Distribution of Error-Free Gaps — DICEF to Tully Access Line	92
75	Probability of at Least E Errors in an M Bit Block — DICEF to Tully Access Line 4800 b/s	93
76	Probability of at Least E Errors in an M Bit Block — DICEF to Tully Access Line 9600 b/s	94
77	Cumulative Distribution on Lengths of Bursts — DICEF to Tully Access Line	96
78	Cumulative Distribution on Burst Densities — DICEF to Tully Access Line	96
79	Cumulative Distribution on Lengths of Intervals — DICEF to Tully Access Line	97

LIST OF ILLUSTRATIONS (Continued)

<u>Figure</u>		<u>Page</u>
80	Cumulative Distribution on Interval Densities — DICEF to Tully Access Line	97
81	Interval to Burst Ratios — DICEF to Tully Access Line	98
82	Cumulative Distribution of Consecutive Errors — Loop to Arlington 4800 b/s	101
83	Cumulative Distribution of Error-Free Gaps — Loop to Arlington 4800 b/s	101
84	Cumulative Distribution on Lengths of Bursts — Loop to Arlington 4800 b/s	103
85	Cumulative Distribution on Burst Densities — Loop to Arlington 4800 b/s	103
86	Cumulative Distribution on Lengths of Intervals — Loop to Arlington 4800 b/s	104
87	Cumulative Distribution on Interval Densities — Loop to Arlington 4800 b/s	104
88	Interval to Burst Ratios — Loop to Arlington 4800 b/s	105
89	Probability of at Least E Errors in an M Bit Block — Loop to Arlington/Bell 4800 b/s	106
90	Probability of at Least E Errors in an M Bit Block — Loop to Arlington/Codex 4800 b/s	107
91	Cumulative Distribution of Consecutive Errors — Loop to Santa Rosa 4800 b/s	108
92	Cumulative Distribution of Error-Free Gaps — Loop to Santa Rosa 4800 b/s	108
93	Cumulative Distribution on Lengths of Bursts — Loop to Santa Rosa 4800 b/s	109
94	Cumulative Distribution on Burst Densities — Loop to Santa Rosa 4800 b/s	109
95	Cumulative Distribution on Lengths of Intervals — Loop to Santa Rosa 4800 b/s	111

LIST OF ILLUSTRATIONS (Continued)

<u>Figure</u>		<u>Page</u>
96	Cumulative Distribution on Interval Densities — Loop to Santa Rosa 4800 b/s	111
97	Interval to Burst Ratios — Loop to Santa Rosa 4800 b/s	112
98	Probability of at Least E Errors in an M Bit Block — Loop to Santa Rosa/Bell/4800 b/s	113
99	Probability of at Least E Errors in an M Bit Block — Loop to Santa Rosa/Codex/4800 b/s	114
100	Cumulative Distribution of Consecutive Errors — Loop to Rockdale/4800 b/s	115
101	Cumulative Distribution of Error-Free Gaps — Loop to Rockdale/4800 b/s	115
102	Cumulative Distribution on Lengths of Bursts — Loop to Rockdale/4800 b/s	116
103	Cumulative Distribution on Burst Densities — Loop to Rockdale/4800 b/s	116
104	Cumulative Distribution on Lengths of Intervals — Loop to Rockdale/4800 b/s	117
105	Cumulative Distribution on Interval Densities — Loop to Rockdale/4800 b/s	117
106	Interval to Burst Ratios — Loop to Rockdale 4800 b/s	118
107	Probability of at Least E Errors in an M Bit Block — Loop to Rockdale/Bell 4800 b/s	119
108	Probability of at Least E Errors in an M Bit Block — Loop to Rockdale/Codex 4800 b/s	120
109	Probability of at Least E Errors in an M Bit Block — Loop to 1 Switch/Codex 4800 b/s	121
110	Probability of at Least E Errors in an M Bit Block — Loop to 1 Switch/Bell 4800 b/s	122
111	Cumulative Distribution of Consecutive Errors — Codex SS vs. Codex SCR Data	125

LIST OF ILLUSTRATIONS (Concluded)

<u>Figure</u>		<u>Page</u>
112	Cumulative Distribution of Error-Free Gaps — Codex SS vs. Codex SCR Data	125
113	Cumulative Distribution on Lengths of Bursts — Codex SS vs. Codex SCR Data	126
114	Cumulative Distribution on Burst Densities — Codex SS vs. Codex SCR Data	126
115	Cumulative Distribution on Lengths of Intervals — Codex SS vs. Codex SCR Data	127
116	Cumulative Distribution on Interval Densities — Codex SS vs. Codex SCR Data	127
117	Interval to Burst Ratios — Codex SS vs. Codex SCR Data	128
118	Probability of at Least E Errors in an M Bit Block — Loop to 2 Switches/4800 b/s	129
119	Probability of at Least E Errors in an M Bit Block — Loop to 2 Switches/Codex SS 4800 b/s	130
120	Probability of at Least E Errors in an M Bit Block — Loop to 2 Switches/9600 b/s	131
121	Probability of at Least E Errors in an M Bit Block — Loop 2 Switches/Codex SS 9600 b/s	132

LIST OF TABLES

<u>Table</u>		<u>Page</u>
I	Bell System Circuit Parameters	16
II	Data Summary - All Data	22
III	Data Summary - By Switches	40
IV	Data Summary - By Miles	58
V	Data Summary - By Trunks	74
VI	Data Summary - Tully Access Line	91
VII	Data Summary - BELL Modem vs. Codex Modem	100
VIII	Data Summary - Codex Scrambler vs. Self-Sync	124

SECTION I

INTRODUCTION

In recent years there has been, within the civilian and military worlds, a drive toward the use of voice grade circuits (nominally 2400 Hz of usable bandwidth) for high-speed digital data transmission. This drive has developed because of the need to interconnect computers and computer-like devices on existing communication circuits at data rates sufficiently high for the achievement of operational computer efficiency. A natural outgrowth of efforts in this direction is the use of the AUTOVON common-user voice grade circuits for digital data transmission at the state-of-the-art speed of 9600 b/s.

The Electronic Systems Division of the Air Force is presently developing with MITRE's technical support a new CONUS record data communication system for SAC called the SAC Automated Total Information Network (SATIN IV). Since AUTOVON is the primary candidate for use as the backbone transmission facility for SATIN IV, a study was undertaken to determine the digital characteristics of AUTOVON in light of the SATIN IV system performance requirements. As a first step in this study, digital error patterns obtained during channel tests on AUTOVON are being analyzed. In this paper, a description of the AUTOVON channel tests results is provided using an analysis technique previously developed^[1] for such error pattern tests.

AUTOVON

AUTOVON is a network of telephone circuits traversing wireline and microwave links crisscrossing the country in the same fashion as the

commercial telephone system. AUTOVON is, however, limited in its use to authorized agencies of the U.S. Government. It uses switches (i. e., ESS and CROSSBAR) of the same type employed in commercial communications networks. These switches perform the call routing and interconnection functions of AUTOVON. The network is made up of unconditioned Common Grade Leased Lines.^[2] These Common Grade Leased Lines are similar in their analog characteristics to leased lines that meet C2 specifications. The access lines into the network are conditioned C3 (referred to as S3 by the government). A brief summary of the nominal conditioning levels is given in Table I.

Table I
Bell System Circuit Parameters

Frequency Range	C2 Amplitude Variation (dB)		C3
			Amplitude Variation (dB)
0.3 - 3.0 kHz	-2 to +6		-0.8 to +2
0.5 - 2.8 kHz	-1 to +3		-0.5 to +1
	Envelope Delay Distortion (μ sec)		
	0.5 - 2.8 kHz	3000	650
	0.6 - 2.6 kHz	1500	300
	1.0 - 2.6 kHz	500	110

The nominal conditioning levels, although useful in evaluating the performance of analog systems, are not generally relevant to digital data transmission performance. Such performance is more dependent on channel noise and phase jitter and how the decision algorithm of the modem responds to these channel conditions. Thus, the true digital data channel is not AUTOVON alone, but rather AUTOVON in conjunction with the modem used. The modem chosen for the tests reported herein was the Codex 9600

modem. This modem was chosen because it was the only on-hand government-owned 9600 b/s telephone line data modem available at the RADC test site during the test period.

The Codex 9600 Modem

The Codex 9600 modem is designed to transmit 4800, 7200 or 9600 bps serial, synchronous digital data at a 2400 baud signaling rate over a dedicated type 3002, C2 conditioned 4-wire telephone circuit. It is a full-duplex, double-sideband, suppressed-carrier modem using a combination of amplitude- and phase-shift keying and transversal equalization. The transmitted signal occupies a 2400 Hz spectrum centered at 1706 Hz. Each baud contains information from a 4-bit sample of 9600 bps, a 3-bit sample of 7200 bps, or a 2-bit sample of 4800 bps input data. Input data is scrambled before transmission to prevent the receiver from becoming sensitive to data patterns and to provide a uniform line-signal spectrum for the equalization process. Receiver-carrier and timing-recovery circuits use information contained in the transmitted data to eliminate the need for the transmission of pilot tones.

The modem employs a digital adaptive equalizer that is equivalent to a tapped-transversal delay-line filter without feedback. The equalizer performs a complex-valued digital filtering operation on the most recent thirty-one samples of the in-phase and quadrature components of the received signal. At each baud time, it provides a pair of outputs that correspond to the in-phase and quadrature components of the equalized received signal. The data decision logic also generates in-phase and quadrature error signals; these error signals are the difference between the equalizer output signals and the selected data point. These error signals are fed back to the equalizer and used to update the tap coefficients.

The magnitude of the error signal from the data decision logic also provides an indication of the reliability of the data. When the average magnitude of the error signal exceeds a preset threshold, the modem automatically initiates a training mode to reinitialize the equalizer parameters. During re-training, a known sequence is transmitted and the equalizer adjusts its taps by using knowledge of the transmitted sequence during this period rather than making decisions on the received data. The training mode takes approximately 280 milliseconds during which the output of the modem is either all ones or zeros depending on how it was strapped.

The modem has two data transmission modes: scrambler and self-synchronization. In the scrambler mode, the digital data is added (modulo 2) to the output of a pseudo-random sequence generator prior to transmission. At the receiver, this sequence is subtracted out. The objective of this scrambling is to eliminate any periodic patterns of bits that may exist in the source data which the modulation-equalization technique may be sensitive to. In the self-synchronization mode, the generator polynomial of the pseudo-random sequence is used to divide the data at transmission and the inverse operation is performed upon reception.

Test Procedure

The AUTOVON performance was measured by establishing a communication facility at the RADCD/DICEF and transmitting through the Codex 9600 modem. When the signal was received by the receive modem and its decisions as to bit values were made, the received bit sequence (suitably delayed to account for transmission delay) was added modulo 2 with no carry to the transmitted sequence. This summation (a bit-by-bit error pattern) was then recorded on computer compatible magnetic tape

in a suitable format for later statistical analysis. While dialing was to target switches, the trunks were randomly selected by the inherent nature of call dialing.

In all cases, data transmission originated at RADC and proceeded via access line to the Tully, N. Y. AUTOVON switch. From Tully, connections were made to the switches at Pottstown, PA., Arlington, VA., Rockdale, GA., and Santa Rosa, CA. (in varying orders and combinations). The return connection was back to RADC via Tully. Of the switches used, only Arlington, VA. was an ESS. Testing was conducted at all times of the day and test runs were, for the most part, 30 minutes or 1 hour in duration with redialing between runs. The retraining mode of the Codex modem was disabled. In almost all of the testing, the Codex scrambler mode was used.

Summary of Data

Data was collected at 4800 b/s and 9600 b/s on combinations of AUTOVON links, the access line to Tully and with the modem in its self-synchronization mode as opposed to its scrambler mode. The data will be analyzed in four ways:

- 1) All 4800 b/s data versus all 9600 b/s data,
- 2) Analysis as a function of the number of switches dialed through,
- 3) Analysis as a function of circuit miles,
- 4) Analysis as a function of the number of AUTOVON trunks.

Additionally, appendices are presented containing the analysis of the access line data and a comparison of the Codex 9600 modem performance to that of the BELL 208 modem on some circuits where BELL modem data was available.

Appendix III presents a comparison of data collected using the self-synchronization mode of the modem to data collected on similar circuits using the scrambler mode.

SECTION II

4800 VS. 9600 B/S DATA ANALYSIS

INTER-ERROR PROBABILITIES

The most valuable probabilities that can be obtained from the analysis of the patterns of errors occurring in digital data transmission are the average error rate and the inter-error probability distribution functions. It is these distributions (the consecutive error distributions and consecutive error-free gap distributions) that are commonly used to develop channel models from which communications systems can be analyzed. Along with these, another interesting probability, commonly used in coding system design and channel modeling, is the probability of at least E errors in a block of M bits, $P(\geq E, M)$. The probability of at least one error in a block is the probability that a message block will be received in error. This probability defines the retransmission rate of a retransmission error control system. Other values taken from the $P(\geq E, M)$ curves are useful in calculating the performance of forward error correction block codes.

The amount of data collected and reported on herein is summarized in Table II. Over 3 billion bits were collected at 4800 b/s and almost 4 billion bits were collected at 9600 b/s. The first interesting point to note is that the error rate at 9600 b/s is almost double that at 4800 b/s. This tends to imply that the errors that occurred were time dependent. As will be demonstrated later in this paper, errors occurred in bursts with long error-free intervals separating the bursts.

Table II
Data Summary - All Data

Data Rate	Total Bits	Total Errors	Bit Error Rate
4800 b/s	3,074,760,833	129,742	4.3 E-5
9600 b/s	3,996,064,721	325,130	8.1 E-5

As can be seen in Figure 1, the predominant type of error at 4800 b/s was the single error. The errors, while they occurred in bursts, occurred singly within the burst. At 9600 b/s, while single errors still predominate, double errors are almost as common.

The distribution of error-free gaps is indicative of the complexity of the data channel. A large number of gaps in the range of zero to thirty bits are usually seen on microwave circuits and are indicative of short dense bursts. When gaps are most commonly long (thousands of bits), the channel is generally random with a bit error rate in the neighborhood of the inverse of the mean gap length. As can be seen from Figure 2, the AUTOVON channel is very complex. There are microwave type short gaps and more random error-related long gaps. This complexity will be better understood in later sections of this paper where the data is subdivided by circuit complexity (number of switches, miles, or trunks).

Figures 3 and 4 exemplify an interesting characteristic of the Codex modem; that is, when errors occur, they tend to occur in even numbers. This shows up for a large range of numbers of errors in a block at 4800 b/s. At 9600 b/s, fully 70% of the blocks with errors have either two or four errors. This characteristic makes the Codex modem/AUTOVON channel combination a difficult channel to code since most coding techniques depend on some form of majority logic scheme for their success.

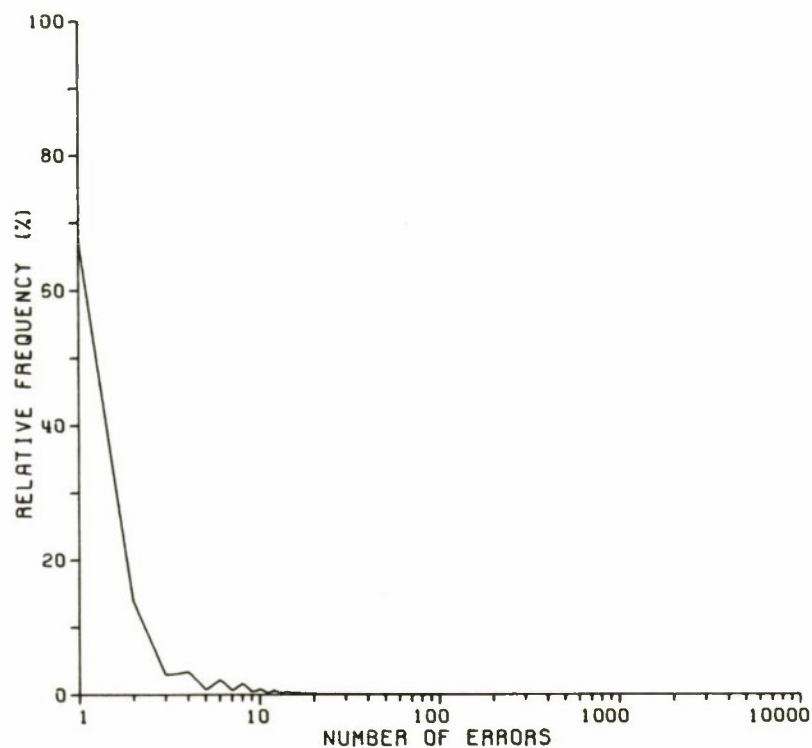


Figure 3. Relative Frequency of Errors — All 4800 b/s Data 2048 Bits/Block

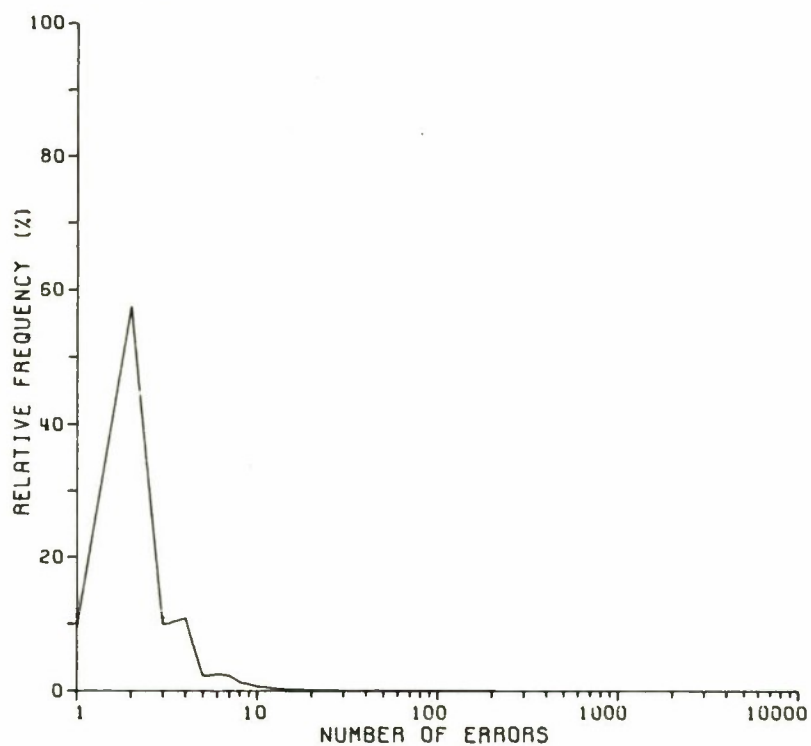


Figure 4. Relative Frequency of Errors — All 9600 b/s Data 2048 Bits/Block

The most commonly used error probabilities in the design of error control coding systems (forward error correction or retransmission) are the probabilities of at least E errors in an M bit block. For any value of M , the probability of at least one error is the block retransmission rate for a retransmission system (assuming perfect error detection) and the uncorrected block error rate for a forward error correction system. For a code that detects (or corrects) $E-1$ errors in an M bit block, the probability of at least E errors is the post-detection (or correction) block error rate. On Figures 5 and 6, these probabilities are presented for a wide range of block lengths and error values. For almost any block length and error value, the block error rate is no more than one-half order of magnitude higher at 9600 b/s than at 4800 b/s. The shapes of the curves are essentially the same for all values displayed, and it can be concluded that in a system that uses error control (of some type), a design performed against the 9600 b/s results would give the same or better performance at 4800 b/s.

BURST DEFINITIONS

The previous discussion of error pattern distributions does not present the complete picture. There is no information about length of bursts, nor is there information relative to the interval between bursts (guard space). For this reason and as an aid in narrowing choices in coding system design, the data shall be evaluated in terms of burst distributions.

Definition of a Burst

A burst is defined as a region of the serial data stream where the following properties hold. A minimum number of errors, M_e , are contained in the region and the minimum density of errors in the region

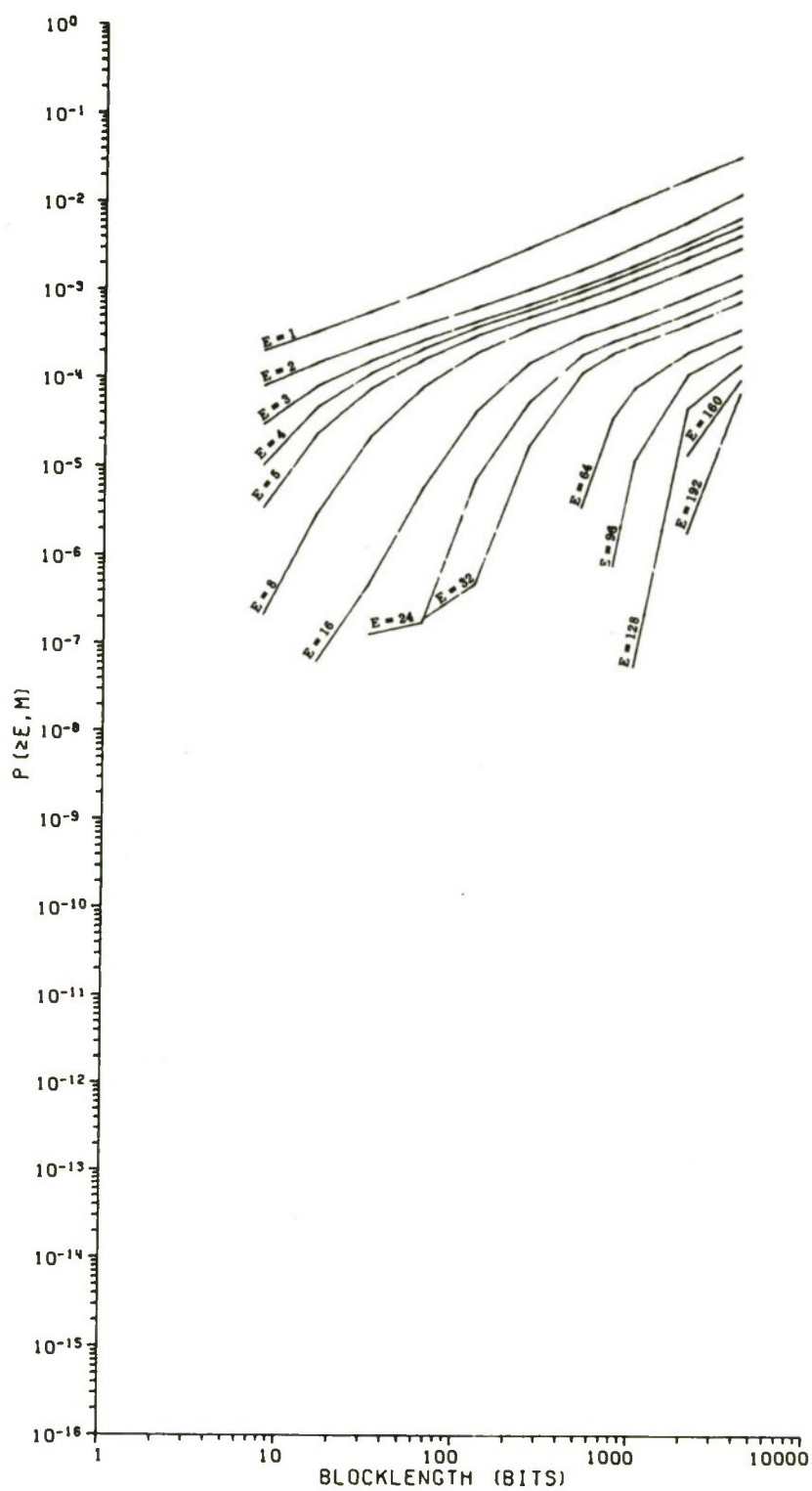


Figure 5. Probability of at Least E Errors in an M Bit Block — 4800 b/s All Data

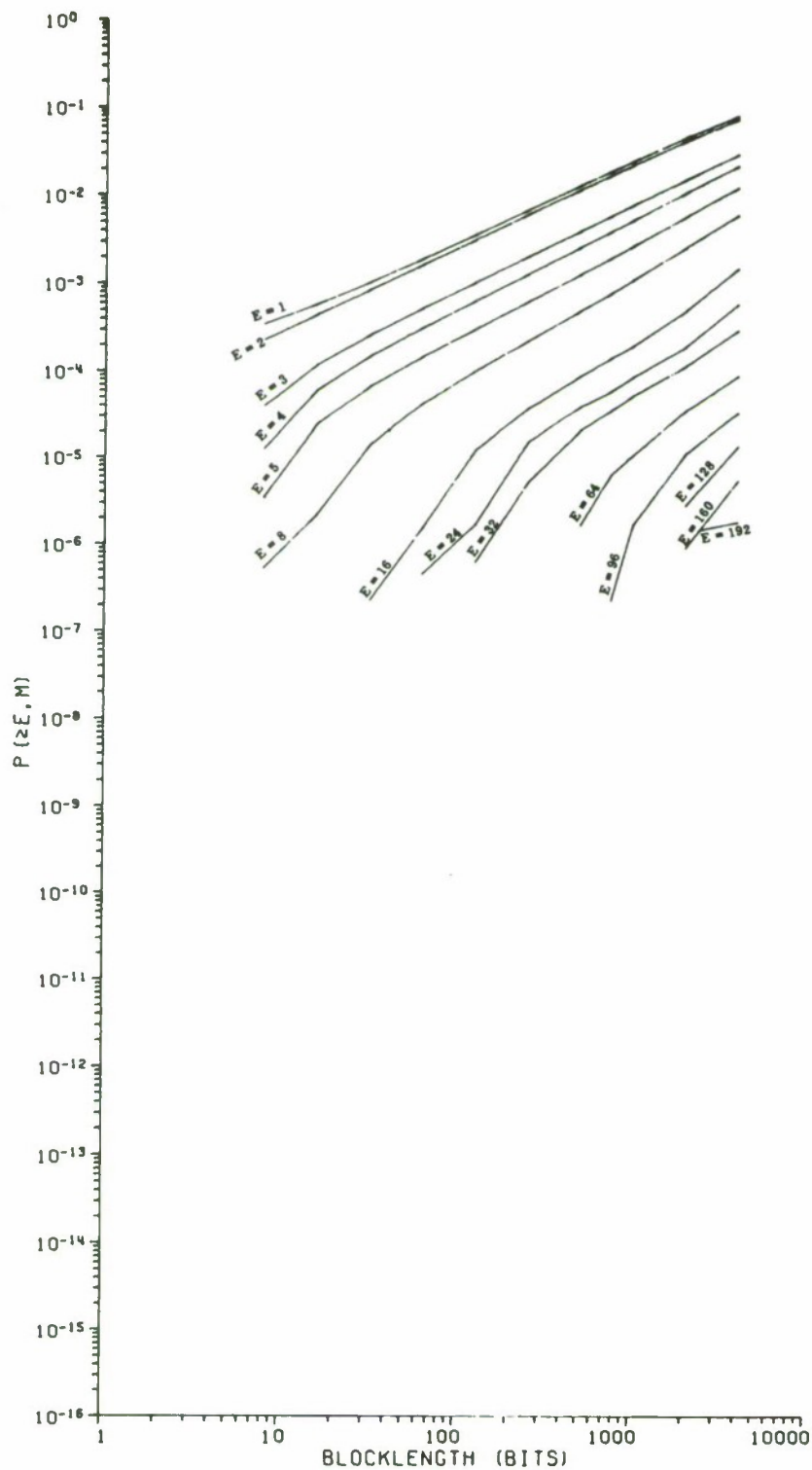


Figure 6. Probability of at Least E Errors in an M Bit Block — 9600 b/s All Data

is Δ . Both of these conditions must be satisfied for the chosen values of M_e and Δ for the region to be defined as a burst. The density of errors is defined as the ratio of bits-in-error to the total number of bits in the region.

The following properties hold for the burst. The burst always begins with a bit-in-error and ends with a bit-in-error. A burst may contain correct bits. Each burst is immediately preceded and followed by an interval in which the density of errors is less than Δ .

The burst probability density function is defined as the probability of occurrence of a burst of length N where N is any positive integer. The burst length is measured in terms of the total number of bits in the burst. A separate burst probability density function may be determined for each pair of Δ and M_e values.

The minimum number of errors in a burst has been chosen to be two for all the data included here. Experience^[1] indicates that larger values of M_e would not change the values of burst length significantly. When a value of one is selected for M_e , every error becomes a burst and the requirement that a burst begin and end in different errors is violated. Consequently, the burst distribution reduces to the consecutive error distribution. While a minimum value Δ is used in defining bursts, the actual burst error density is calculated. The algorithm has the effect of maximizing this error density.

Definition of an Interval

The interval is defined as the region, bounded by correct bits, in the serial data stream where the following property holds. The maximum density of errors is less than Δ . An interval may contain errors and is

always immediately preceded and followed by a burst. Thus, each and every bit in the data stream must lie in either a burst region or an interval region.

The interval probability density function is defined as the probability of occurrence of an interval of length L , where L is any positive integer. The interval probability density is a joint function of both Δ and M_e . Use of $M_e = 1$ has the effect of reducing the interval distribution to the error-free gap distribution.

The guard space ratio is defined as the ratio of an interval length to the burst length preceding it.

BURST ANALYSIS

Burst Distributions

Examining the burst distribution functions in Figure 7, it is evident that errors generally occur in bursts of less than 1000 bits duration. The 4800 b/s channel exhibits bursts that are almost one order of magnitude shorter than those of the 9600 b/s channel for the same cumulative frequency. The 9600 b/s bursts are both longer than those at 4800 b/s and denser in errors (Figure 8).

Interval Distributions

Intervals between bursts are generally very long at either data rate (Figure 9) and a greater percentage of the intervals, 90% versus 83%, are error-free (Figure 10) at 4800 b/s than at 9600 b/s; that is, when random errors between bursts occur, they are more likely to occur at 9600 b/s than at 4800 b/s. The exact relationship of bursts and intervals is shown in Figure 11, from which it can be seen that a burst at 4800 b/s is followed

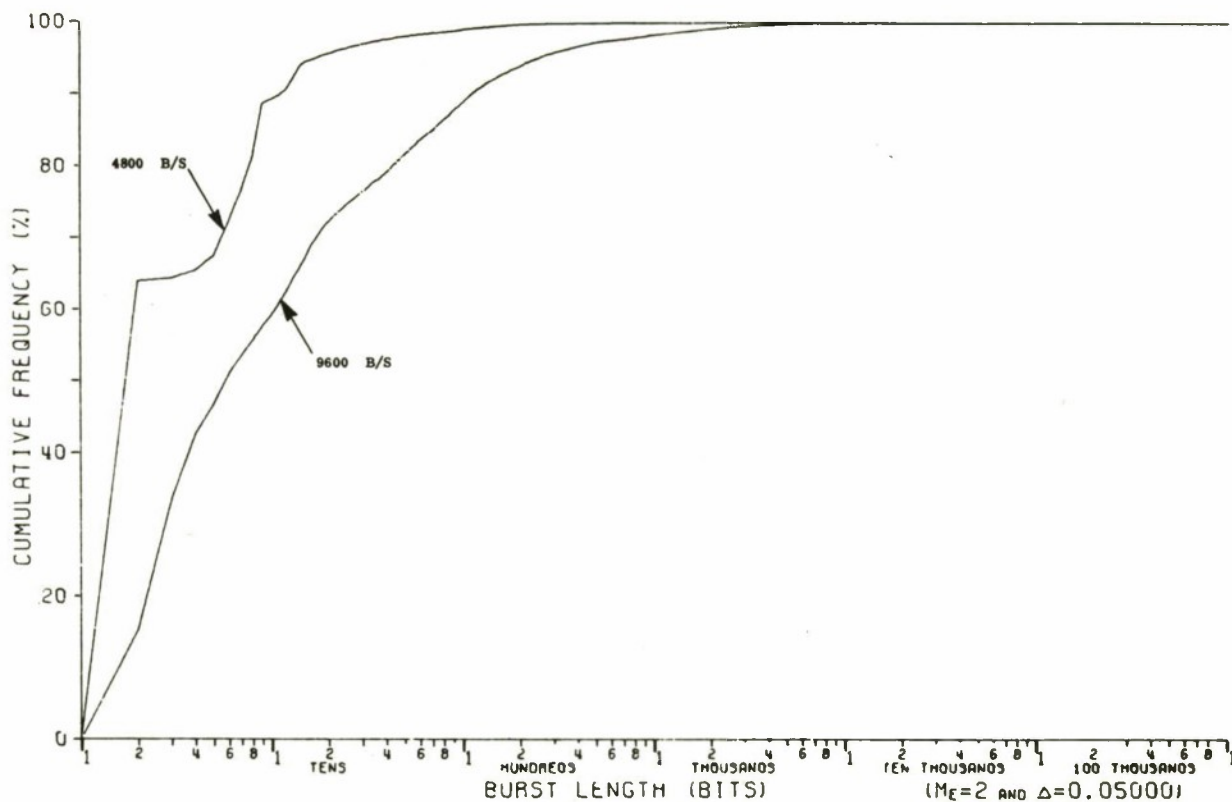


Figure 7. Cumulative Distribution on Lengths of Bursts — Codex Modem Data

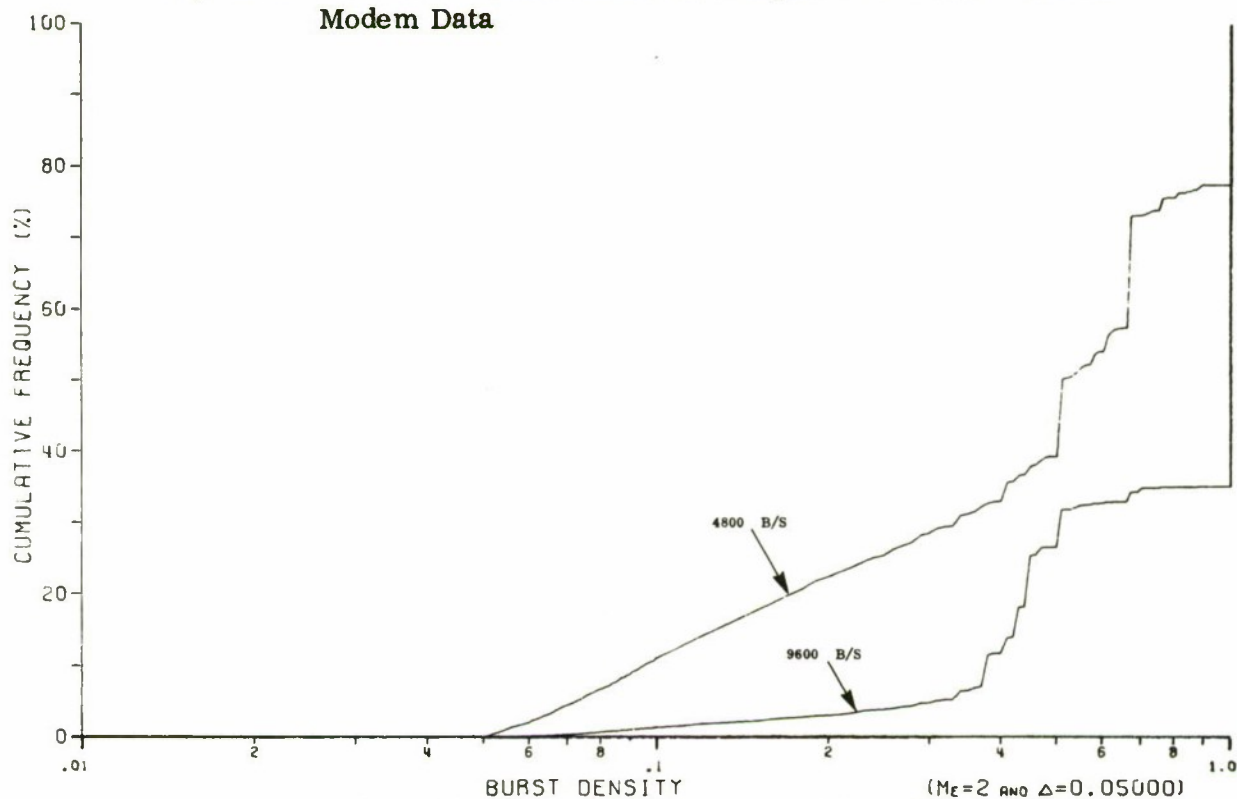


Figure 8. Cumulative Distribution on Burst Densities — Codex Modem Data

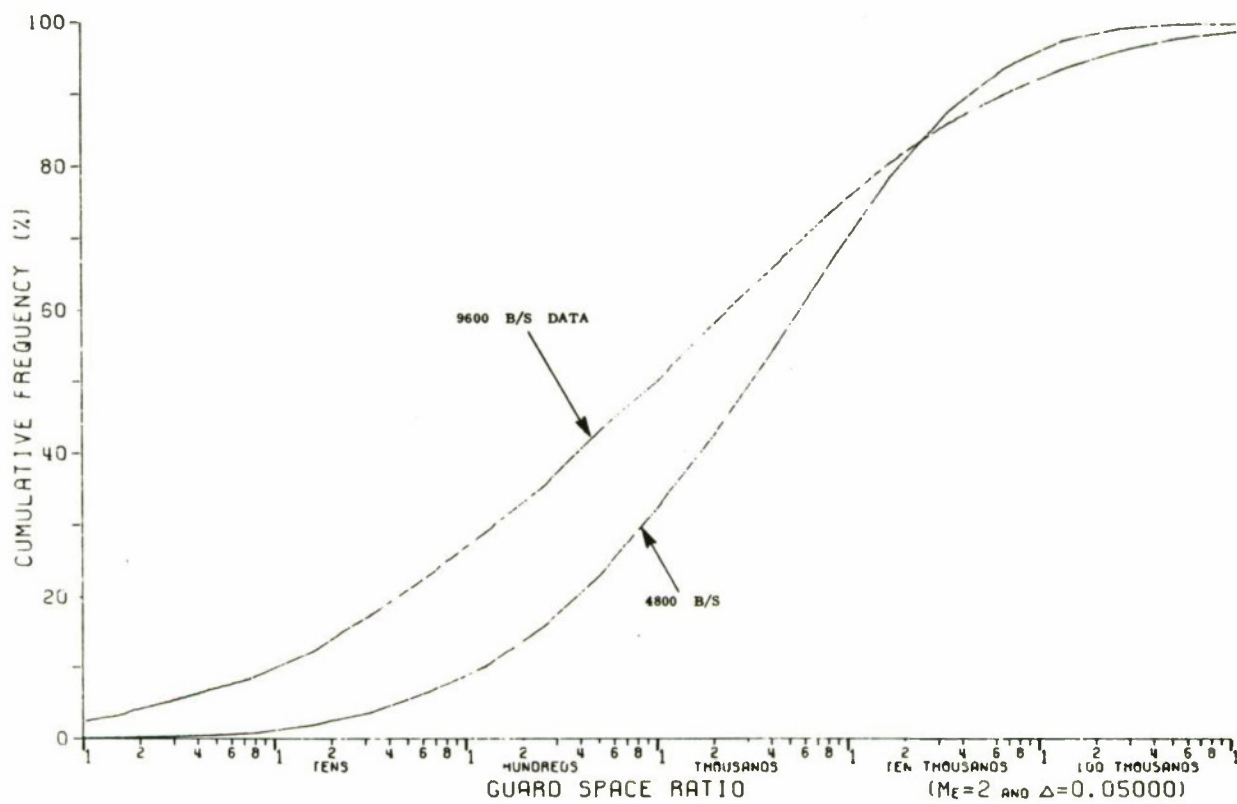


Figure 11. Interval to Burst Ratios — Codex Modem Data

by a longer interval than one at 9600 b/s. This result is very important for forward error correction systems since about 6% of the bursts cannot be randomized by interleaving due to the insufficient length (less than 3 times burst length) of the following interval.

MARKOV CHANNEL MODEL

The channel data collected is very useful for evaluating the performance of various techniques for error detection and correction that might be applied to the channel. Unfortunately, the channel data is most useful to those who have access to it along with large amounts of computer time and sophisticated computer programs. It is, however, possible to calculate the performance of such techniques [3] if a channel model is available. One such model is the MARKOV chain model.

The MARKOV Chain Model

Consider the output y_k of the digital communication channel to be the resultant summation of the input x_k and the noise e_k . Assume that the noise is independent of the input x_k . Since the noise and, in turn, the error sequence is assumed to be independent of the input sequence, the channel may be completely characterized by its error sequence $E = (e_k : k=1, 2, \dots)$. The error sequence is a bit stream of 0's and 1's where an error bit is represented by a 1, and an error-free bit is represented by a 0.

A distribution function which can be calculated for such an error sequence is the error-free run distribution, $P(0^m | 1)$. This distribution is the conditional probability that an error will be followed by at least m consecutive error-free bits. The error-free run distribution, which is closely related to the error-free gap distribution, is used to obtain the channel model. In obtaining the model, it is further assumed that the error sequence

has a limited number of states and the probability of being in any particular state at the n th bit decision is conditionally dependent only upon the state during the $(n-1)$ th bit decision. Such a process is called a MARKOV process of order one and can be represented by an N state MARKOV chain.

Fritchman [4] has developed a model for an N state MARKOV chain that partitions the N states into two groups of states, A and B. The K ($K < N$) states in group A correspond to K states where errors cannot occur. The $N-K$ states in group B correspond to the states in which errors can occur. In order to simplify the mathematics, Fritchman made two restrictions on the model. First, he did not allow transitions among the error states or among the error-free states. Second, he limited the model to a single error state, $K = N-1$. The state transition matrix for the MARKOV chain then becomes:

Diagram illustrating a sparse matrix structure, likely representing a banded matrix. The matrix is defined by indices p_{11} through p_{NN} . The structure shows a main diagonal of dots, with additional dots indicating non-zero elements. The matrix is labeled with p_{11} at the top-left, p_{1N} at the top-right, p_{N1} at the bottom-left, and p_{NN} at the bottom-right. The diagonal is labeled with p_{22} at the second row, second column, and $p_{N-1,N-1}$ at the (N-1)th row, (N-1)th column. The first row is labeled with 0 at the first column, and the first column is labeled with 0 at the first row. The last row is labeled with 0 at the last column, and the last column is labeled with 0 at the last row.

where p_{ij} is the probability of transition from state S_i to state S_j . Fritchman has shown that, for this model, the p_{ij} can be uniquely determined from the

error-free run distribution, since for a stochastic matrix, $\sum_{j=1}^N p_{ij} = 1$, $i = 1, 2, \dots, N$, there are only $2(N-1) = 2K$ unknowns. By fitting a sum of K exponentials to the error-free run distribution, the $2K$ unknowns may be determined. If the error-free run distribution can be approximated by

$$P(0^m | 1) = A_1 e^{a_1(m)} + A_2 e^{a_2(m)} + \dots + A_K e^{a_K(m)}$$

then, Fritchman has shown that the transition matrix is given by

$$\begin{bmatrix} e^{a_1} & 0 & \dots & \dots & \dots & \dots & \dots & \dots & \dots & 1-e^{a_1} \\ 0 & e^{a_2} & \dots & \dots & \dots & \dots & 0 & \dots & \dots & 1-e^{a_2} \\ \vdots & \vdots & \ddots & \ddots & \ddots & \ddots & \vdots & \vdots & \vdots & \vdots \\ \vdots & \vdots & \vdots & \ddots & \ddots & \ddots & \vdots & \vdots & \vdots & \vdots \\ \vdots & \vdots & \vdots & \vdots & \ddots & \ddots & \vdots & \vdots & \vdots & \vdots \\ \vdots & \vdots & \vdots & \vdots & \vdots & \ddots & \vdots & \vdots & \vdots & \vdots \\ \vdots & \vdots & \vdots & \vdots & \vdots & \vdots & \ddots & \vdots & \vdots & \vdots \\ \vdots & \vdots & \vdots & \vdots & \vdots & \vdots & \vdots & \ddots & \vdots & \vdots \\ \vdots & \vdots & \vdots & \vdots & \vdots & \vdots & \vdots & \vdots & \ddots & \vdots \\ \vdots & \vdots & \vdots & \vdots & \vdots & \vdots & \vdots & \vdots & \vdots & \ddots \\ A_1 e^{a_1} & A_2 e^{a_2} & \dots & \dots & \dots & \dots & \dots & \dots & A_K e^{a_K} & 1 - \sum_{j=1}^K A_j e^{a_j} \end{bmatrix}$$

The matrix is determined by applying a computer program to calculate the values of the A's and a's that best fit the data error-free run distribution. The program starts by assuming a two state model (K=1) and increments K until a fit to the data error-free run distribution is achieved by the exponential polynomial expression.

Data-Derived Channel Models

The error-free run distributions (derived from the gap distributions) for the 4800 b/s and 9600 b/s data were fitted by sums of exponentials and the state transition matrices were calculated. The results are presented in Model 1 and 2. Since there is only one error state, $K=N-1$, the conditional probability of error is the probability p_N of being in state N, and an average bit error probability [4] is found to be given by

$$p_e \cong \left[1 + \sum_{j=1}^{N-1} \left(\frac{p_{Nj}}{p_{jN}} \right) \right]^{-1} .$$

For each of the transition matrices, the bit-error probability is given for the model, and the goodness of fit of the model is reported. In both cases, the RMS error between the data error-free run distribution and the model-predicted distribution is less than .10, and the model was validated to that level of RMS error by using the model to generate error pattern data and comparing the gap distribution functions to those of the raw data.

MODEL 1

4800 b/s AUTOVON Data

$$\begin{bmatrix} .999699 & 0 & .0003010 \\ 0 & .9999974 & .0000026 \\ .3669279 & .0443345 & .5887375 \end{bmatrix}$$

Model predicted error rate = 5.52 E-5

RMS error between model and data gap distributions = .088

MODEL 2

9600 b/s AUTOVON Data

$$\begin{bmatrix} .8656363 & 0 & 0 & .1343637 \\ 0 & .9994334 & 0 & .0005666 \\ 0 & 0 & .9999943 & .0000057 \\ .3668136 & .1796088 & .0640107 & .3895669 \end{bmatrix}$$

Model predicted error rate = 8.68 E-5

RMS error between model and data gap distributions = .095

SECTION III

ANALYSIS BY SWITCH CONFIGURATION

The AUTOVON data was collected by connecting a series of AUTOVON switches together to form circuits. The question, therefore, naturally arises as to what the impact of a series of switches is on the circuit connection error performance. The average error rates seen on various switch connections are reported in Table III. By one switch, we define a circuit from RADC through the Tully, N. Y., switch out to one switch, and back to RADC via Tully. Thus, the Tully switch and the access line from Tully to RADC appear twice in every configuration. At 4800 b/s, the error rate almost doubles as one switch is added (from one to three). This does not occur for four switches, but here the data is a more restricted sample. At 9600 b/s, it was very difficult to connect through more than one switch and successfully pass data. Thus, no error rate versus switch connectivity conclusions can be drawn.

INTER-ERROR DISTRIBUTIONS

The consecutive error distributions (Figures 12 and 13) demonstrate that at 4800 b/s, the consecutive error occurrences differ between one switch and more than one switch, but there are no variations among higher numbers of switches. At 9600 b/s, the frequency of occurrence of double errors decreases with increasing numbers of switches. This result may only be a function of the inability to obtain large amounts of data for higher levels of switch connectivity.

Table III

Data Summary - By Switches

Connectivity	Data Rate	Total Bits	Total Errors	Bit Error Rate
One switch	4800 b/s	1,497,691,646	40,327	2.7 E-5
Two switches	4800 b/s	838,324,834	34,840	4.2 E-5
Three switches	4800 b/s	607,158,553	48,697	8.0 E-5
Four switches	4800 b/s	131,585,800	5,878	4.5 E-5
One switch	9600 b/s	3,878,827,265	309,188	8.0 E-5
Two switches	9600 b/s	100,240,103	13,551	1.4 E-4
Three switches	9600 b/s	16,997,353	2,391	1.4 E-4

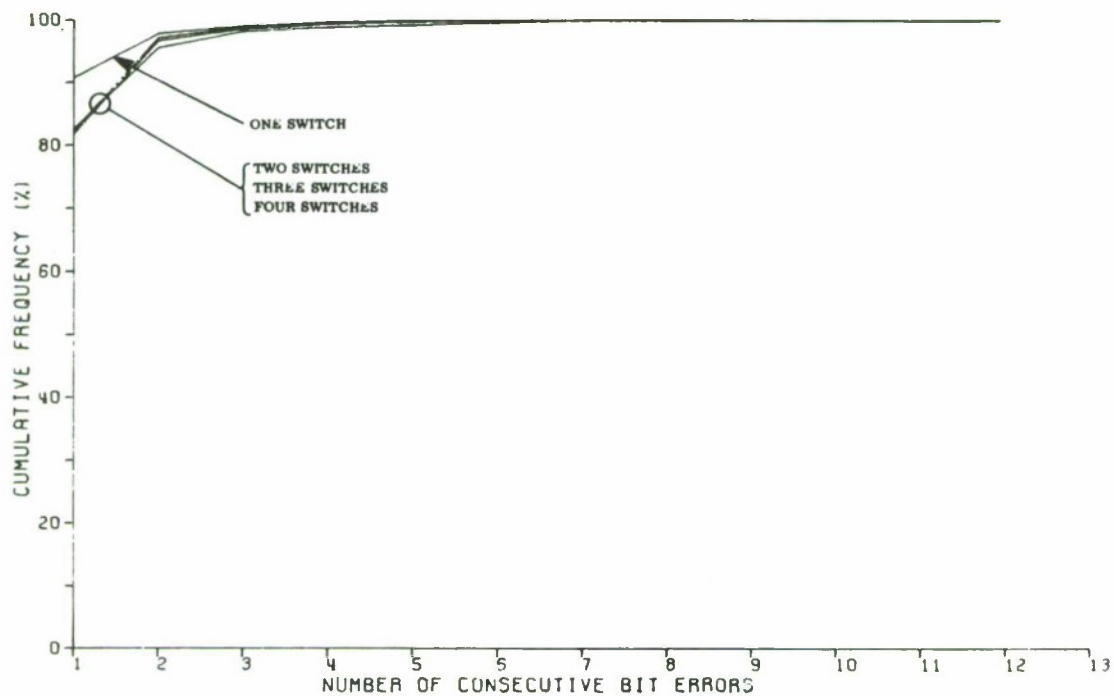


Figure 12. Cumulative Distribution of Consecutive Errors — 4800 b/s Data

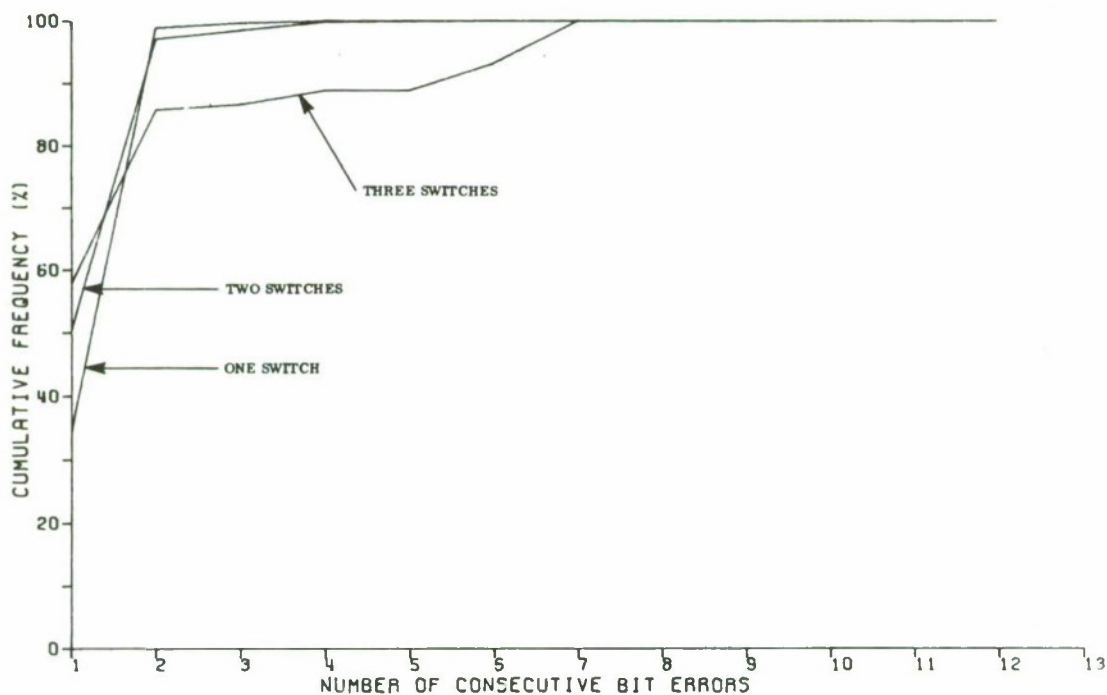


Figure 13. Cumulative Distribution of Consecutive Errors — 9600 b/s Data

It will be recalled that the error-free gap distributions were very complex for the overall data. It is clear from Figure 14, that there is a switch dependency in this distribution at 4800 b/s. The one switch circuit exhibits short dense bursts and random errors. As more switches are added to the connection, the random errors gradually disappear and the predominant characteristic is one of short bursts. At 9600 b/s (Figure 15), no such switch dependency appears.

The probabilities of at least E errors in an M bit block for the 4800 b/s data (Figures 16 through 19) generally show an upward compression with switch connectivity indicating that for a given block length more errors will occur within a block as more switches are included in the circuit. This same effect appears in the 9600 b/s one- and two-switch connections (Figures 20 and 21). The three-switch connection curves in Figure 22 are presented only for completeness. Since it was difficult to obtain data on such circuits, it is not clear that conclusions can be drawn from this figure.

BURST DISTRIBUTIONS

Separating the bursts from the random errors, it can be observed that there are no great variations of burst length with switch connectivity (Figures 23 and 24). However, it is interesting to note that burst error density decreases with increasing switch connectivity at 4800 b/s while it increases at 9600 b/s (Figures 25 and 26). At both data rates, there is no appreciable variation in interval length distribution with switch connectivity (Figures 27 and 28), and the percentage of error-free intervals increases with decreasing switch connectivity (Figures 29 and 30). Clearly, adding more switches tends to break up intervals, but only the very long intervals

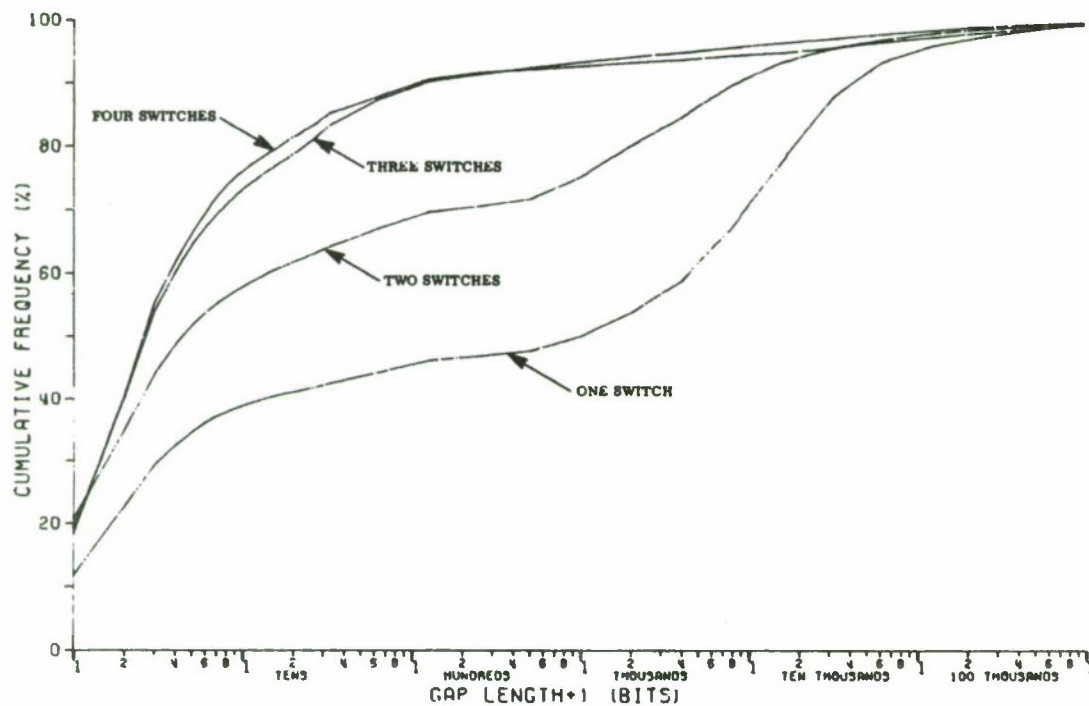


Figure 14. Cumulative Distribution of Error-Free Gaps — 4800 b/s Data

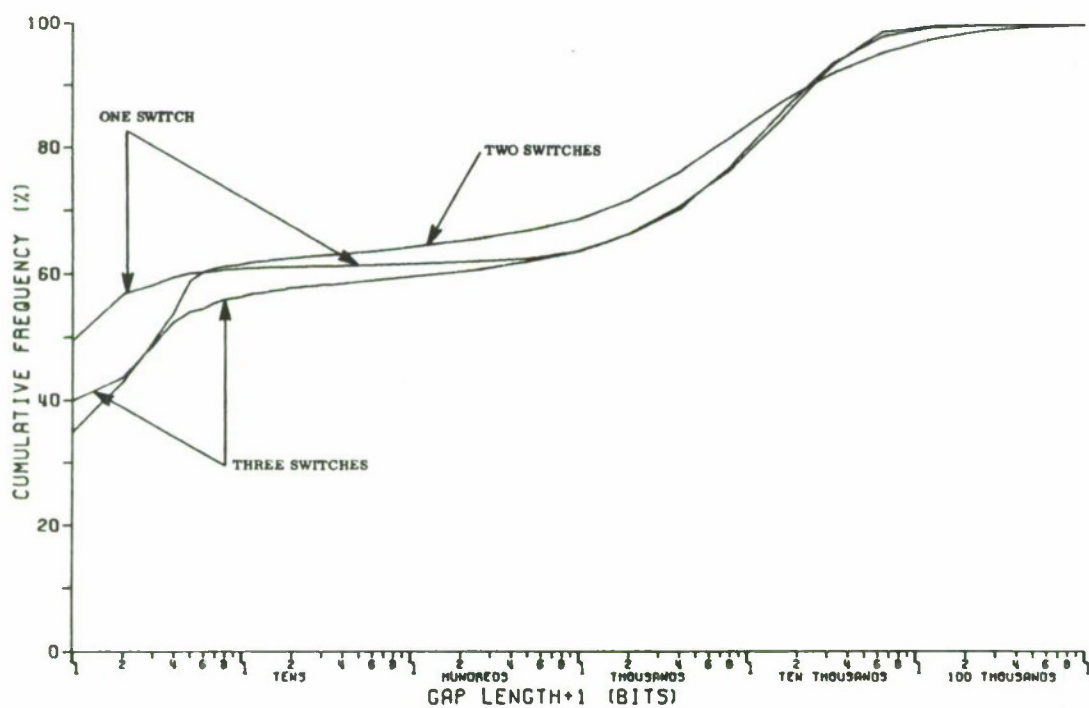


Figure 15. Cumulative Distribution of Error-Free Gaps — 9600 b/s Data

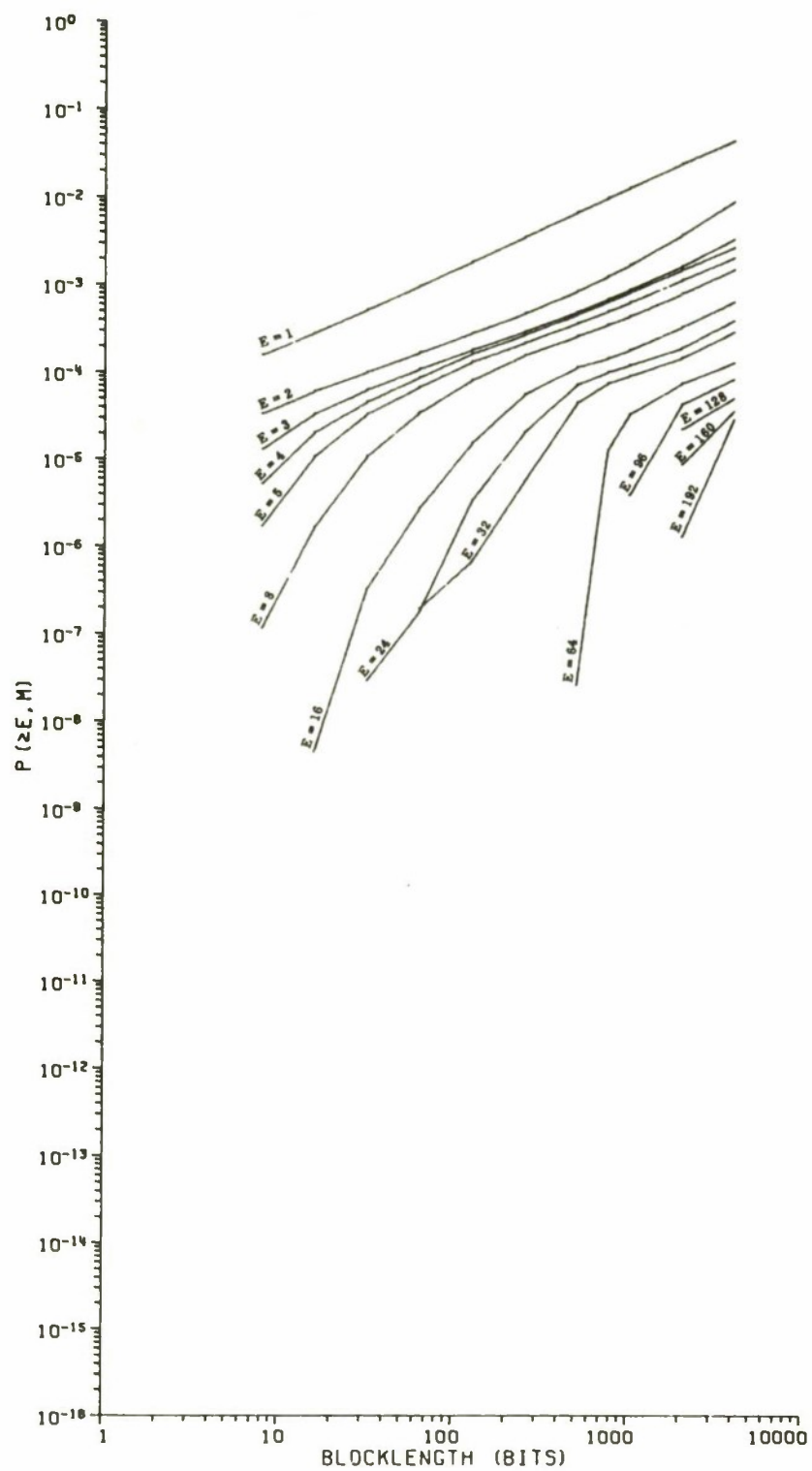


Figure 16. Probability of at Least E Errors in an M Bit Block — Loop to 1 Switch/4800 b/s

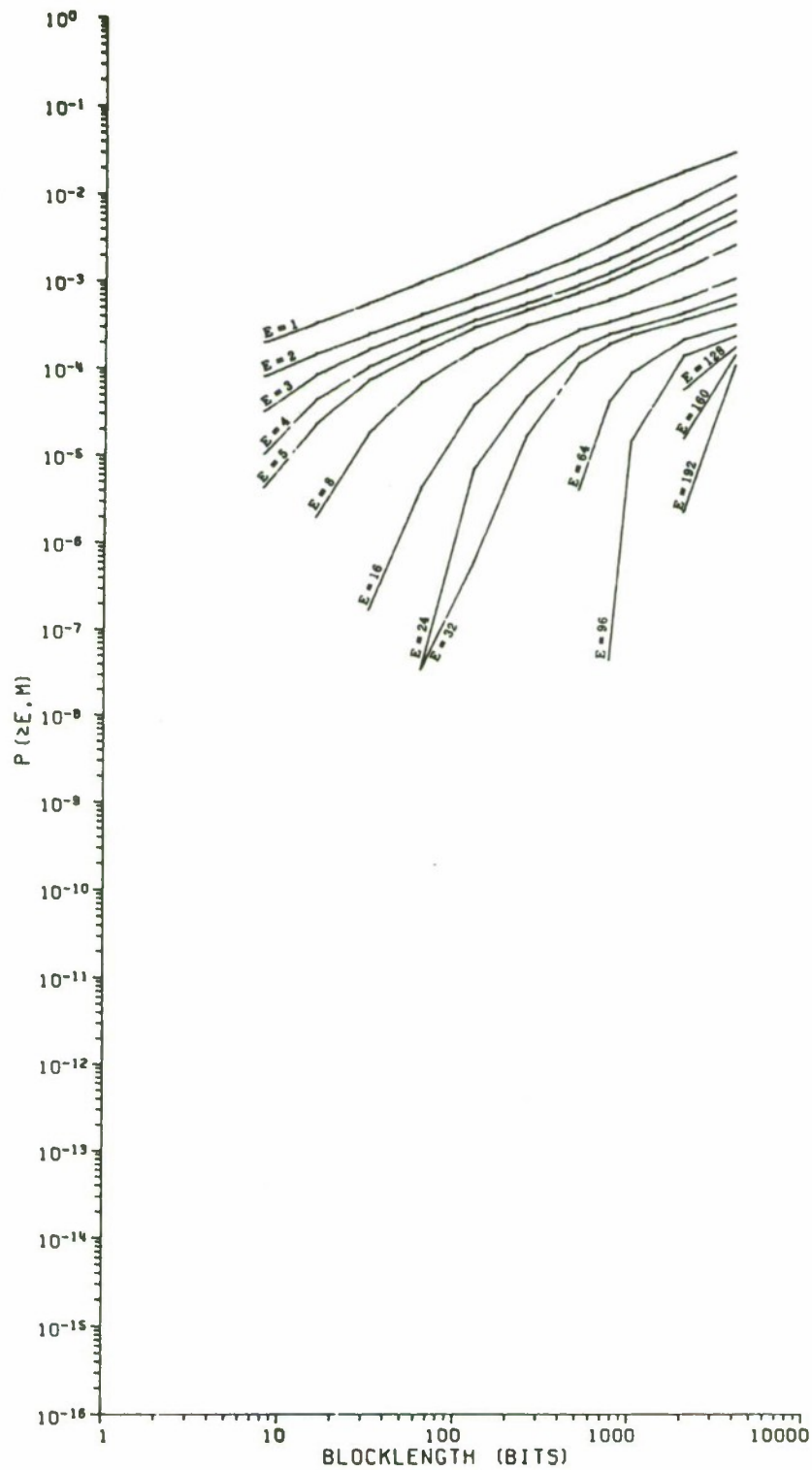


Figure 17. Probability of at Least E Errors in an M Bit Block — Loop to 2 Switches/4800 b/s

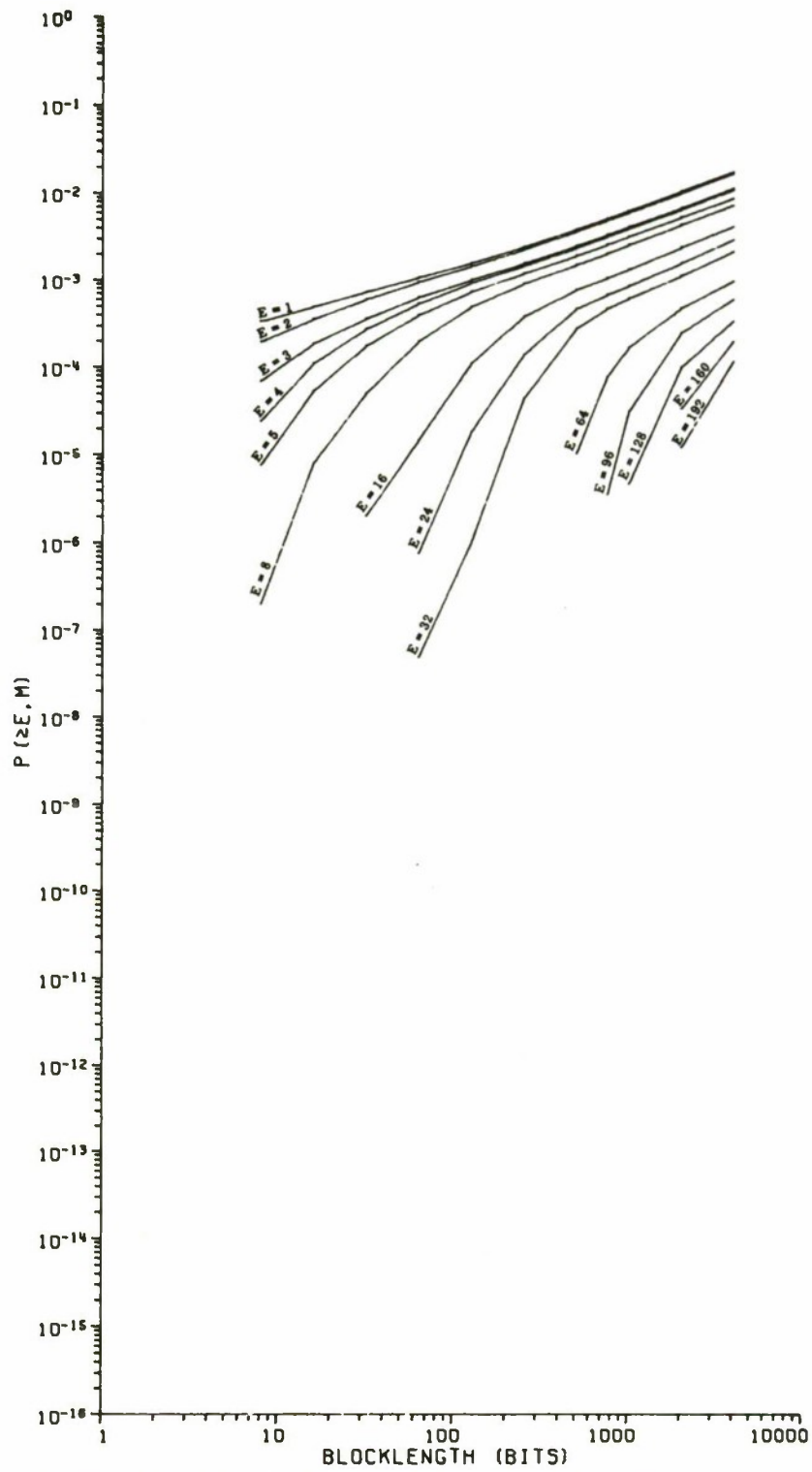


Figure 18. Probability of at Least E Errors in an M Bit Block — Loop to 3 Switches/4800 b/s

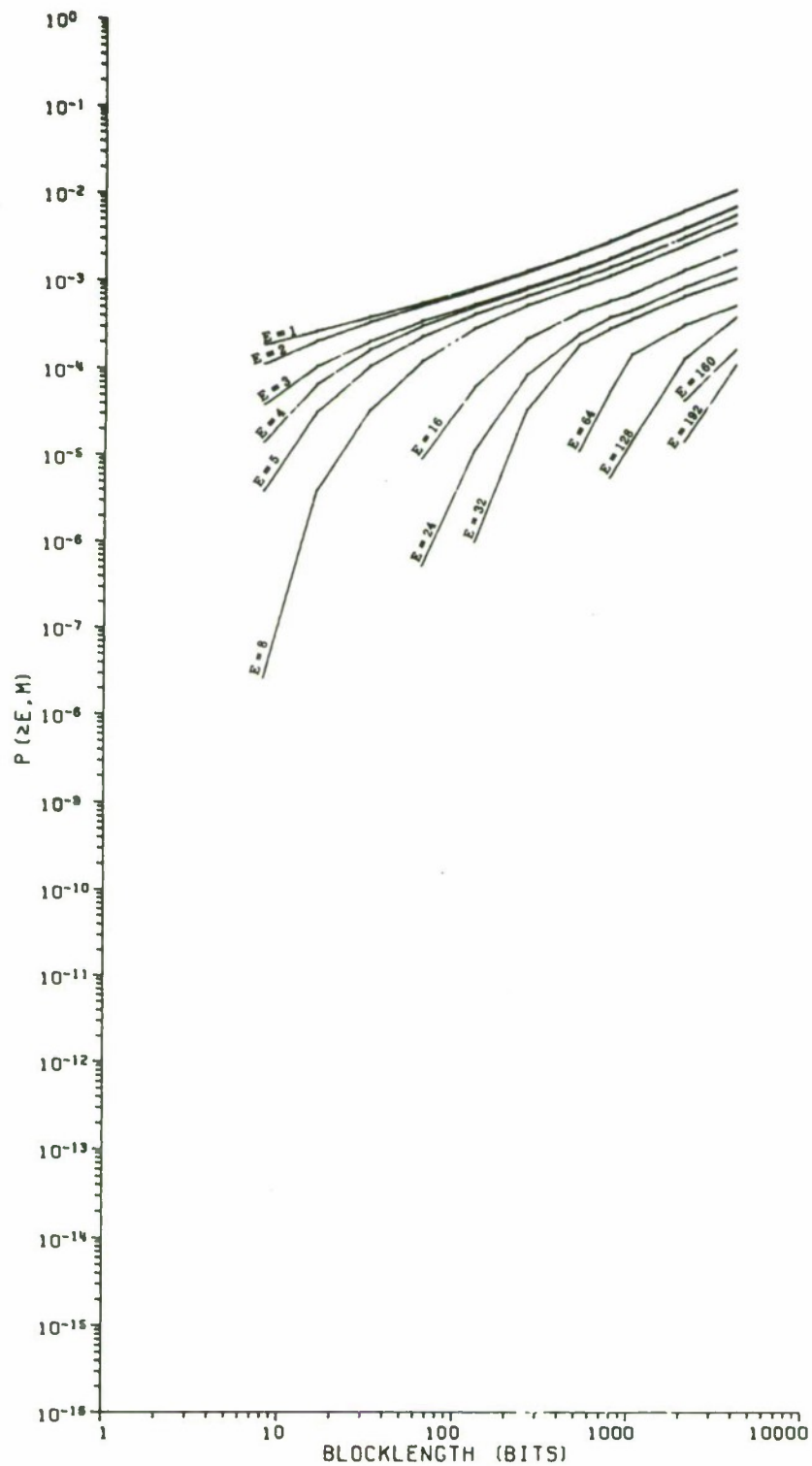


Figure 19. Probability of at Least E Errors in an M Bit Block — Loop to 4 Switches/4800 b/s

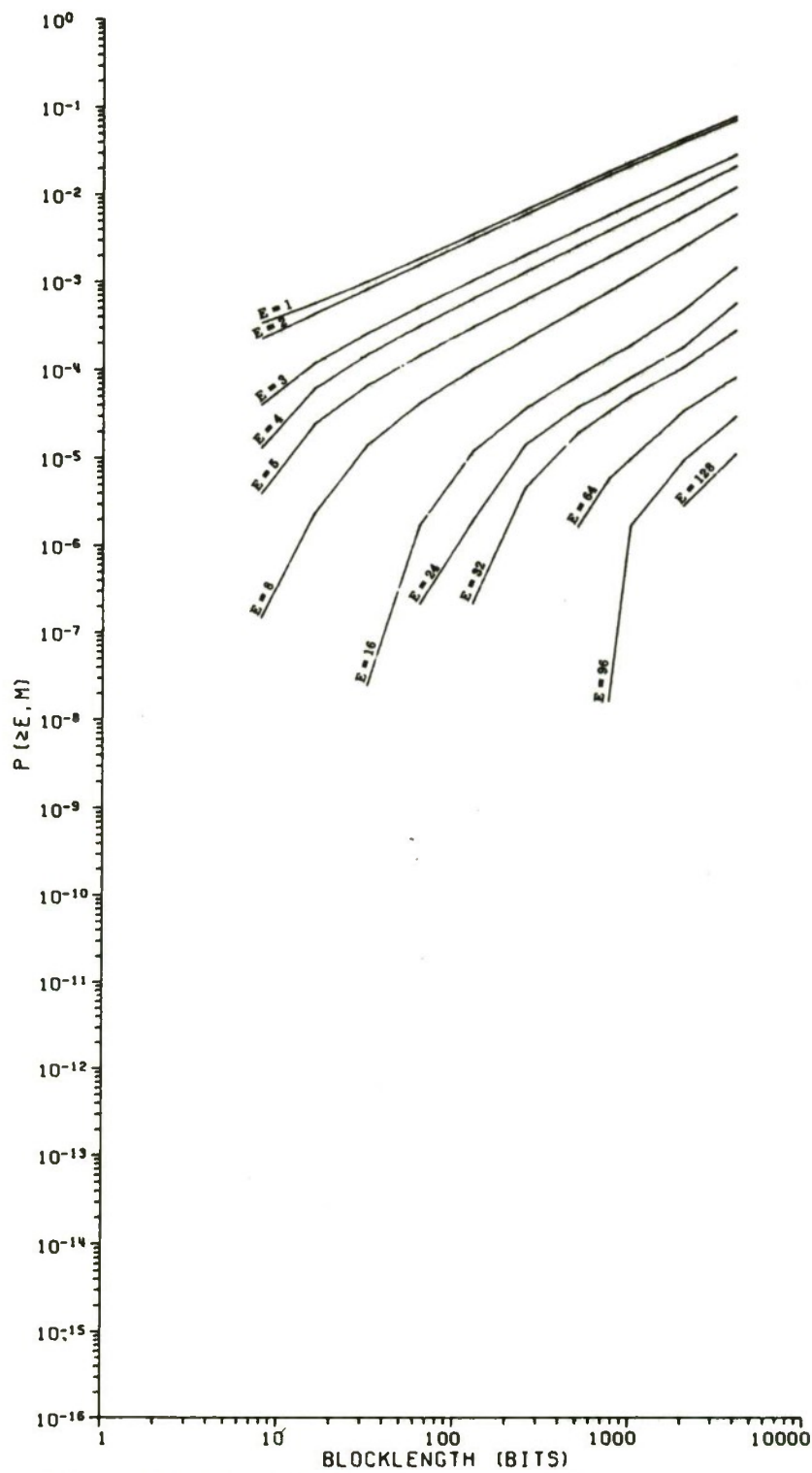


Figure 20. Probability of at Least E Errors in an M Bit Block — Loop to 1 Switch/9600 b/s

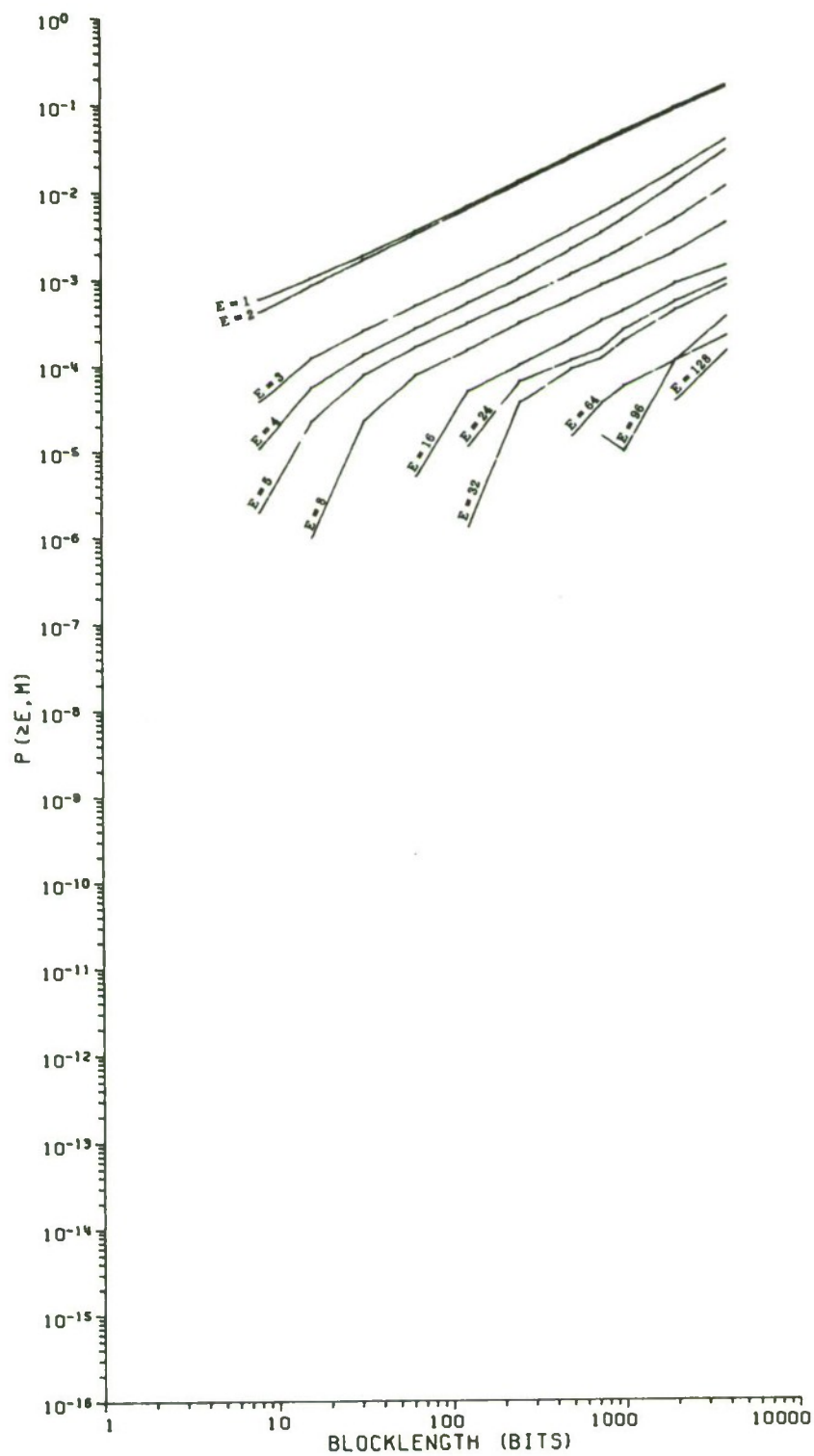


Figure 21. Probability of at Least E Errors in an M Bit Block — Loop to 2 Switches/9600 b/s

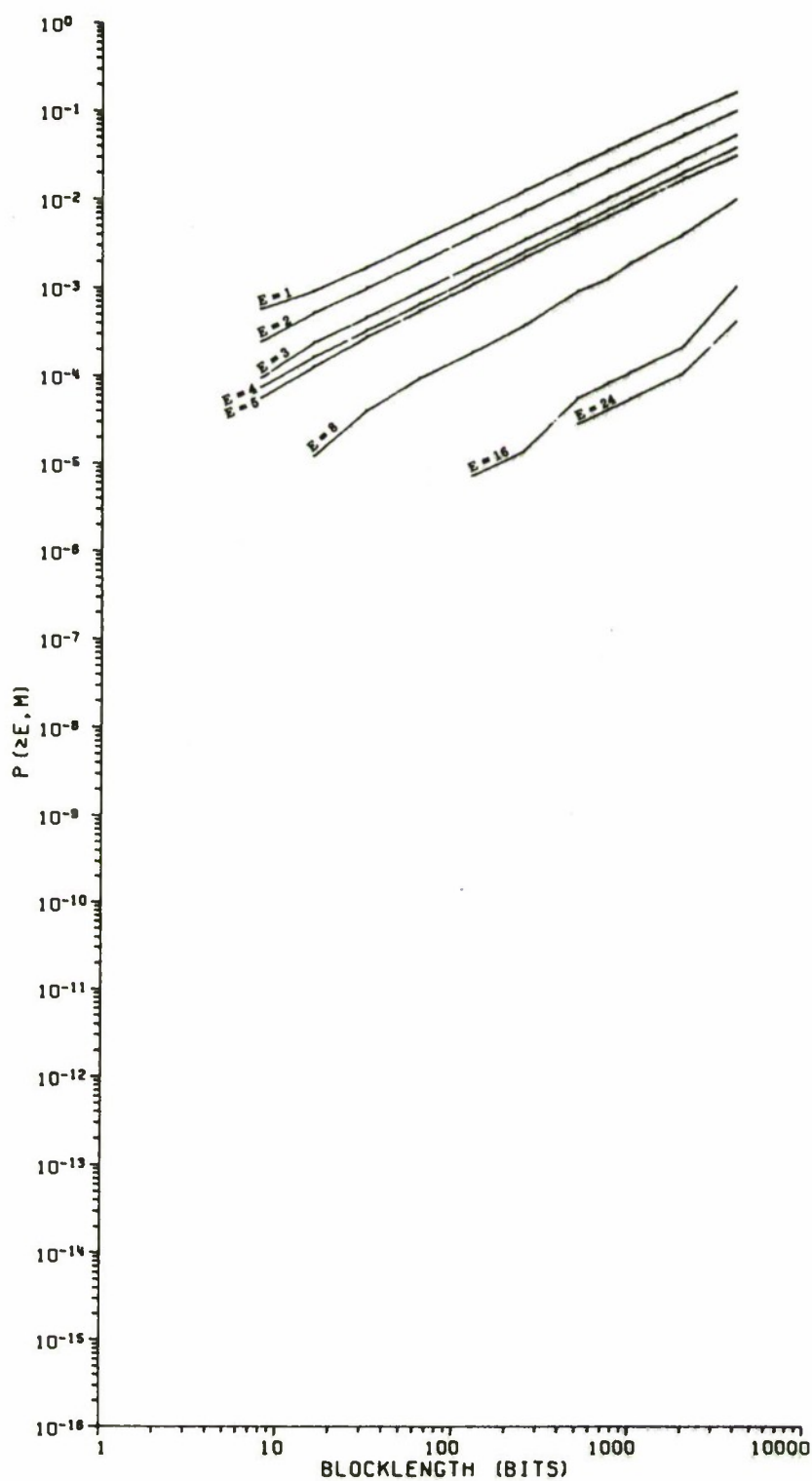


Figure 22. Probability of at Least E Errors in an M Bit Block — Loop to 3 Switches/9600 b/s

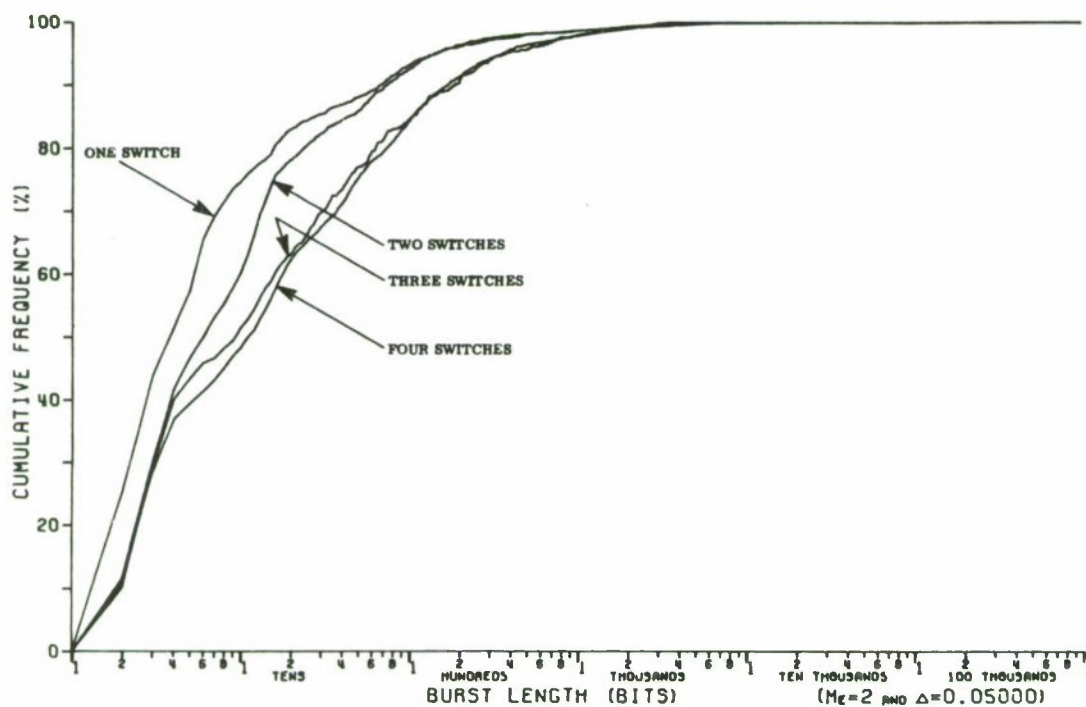


Figure 23. Cumulative Distribution on Lengths of Bursts — 4800 b/s Data

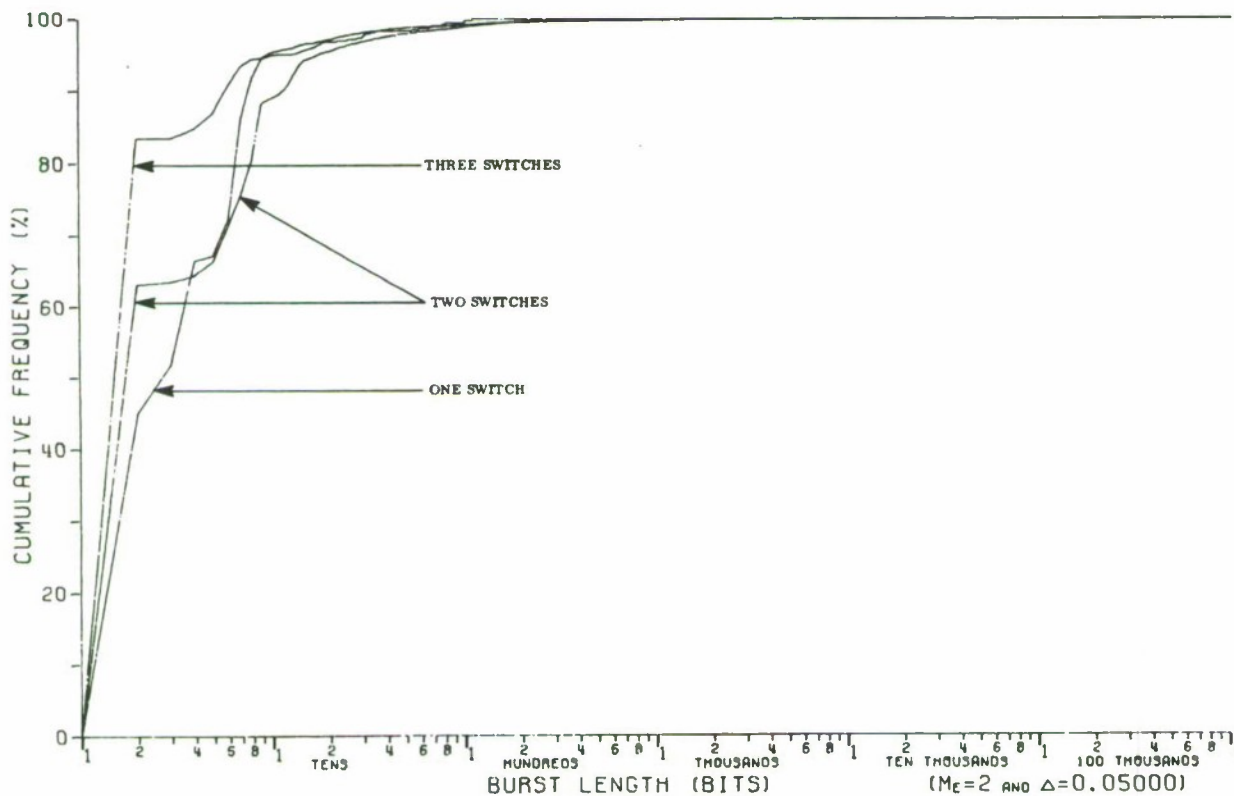


Figure 24. Cumulative Distribution on Lengths of Bursts — 9600 b/s Data

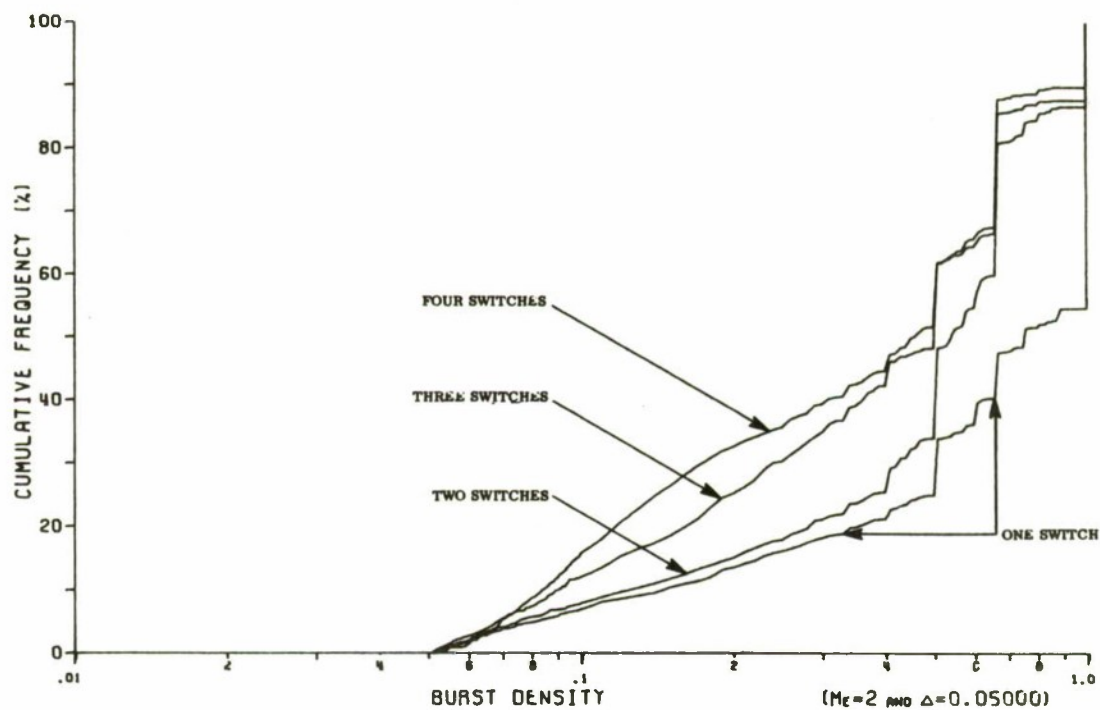


Figure 25. Cumulative Distribution on Burst Densities — 4800 b/s Data

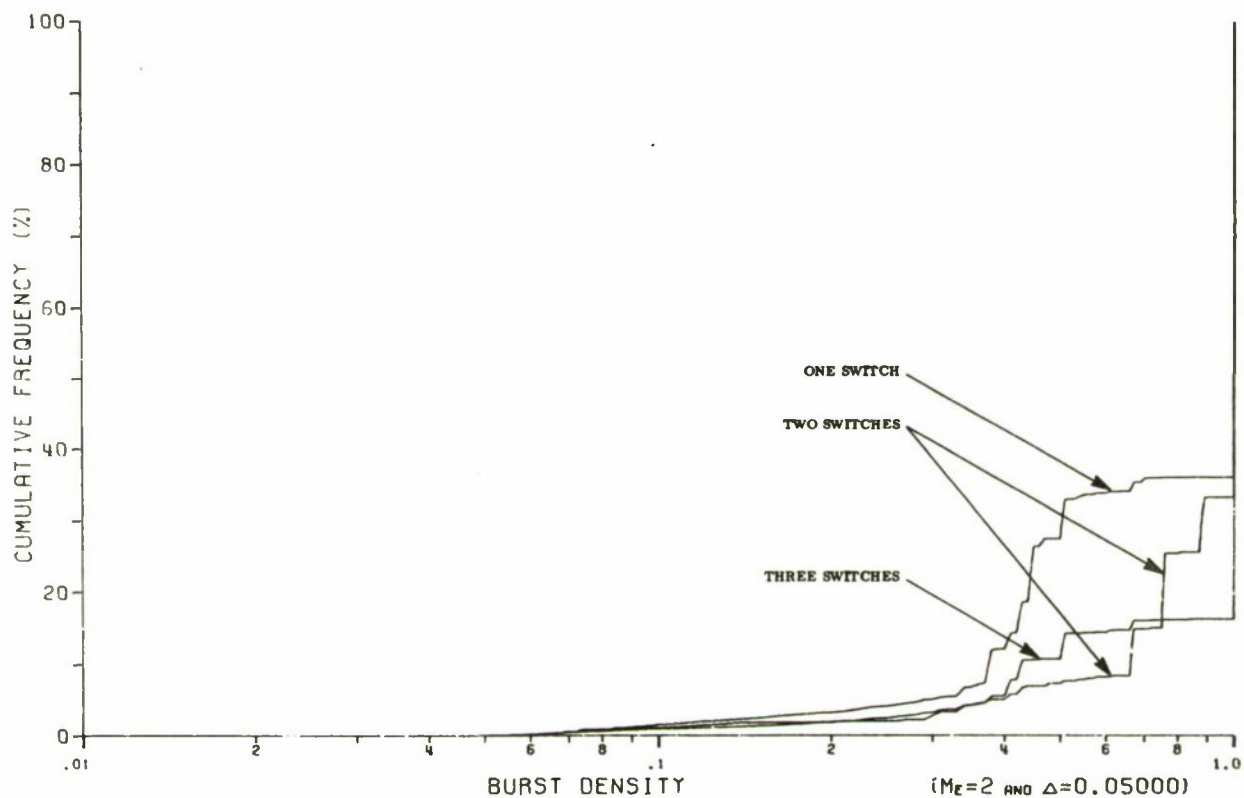


Figure 26. Cumulative Distribution on Burst Densities — 9600 b/s Data

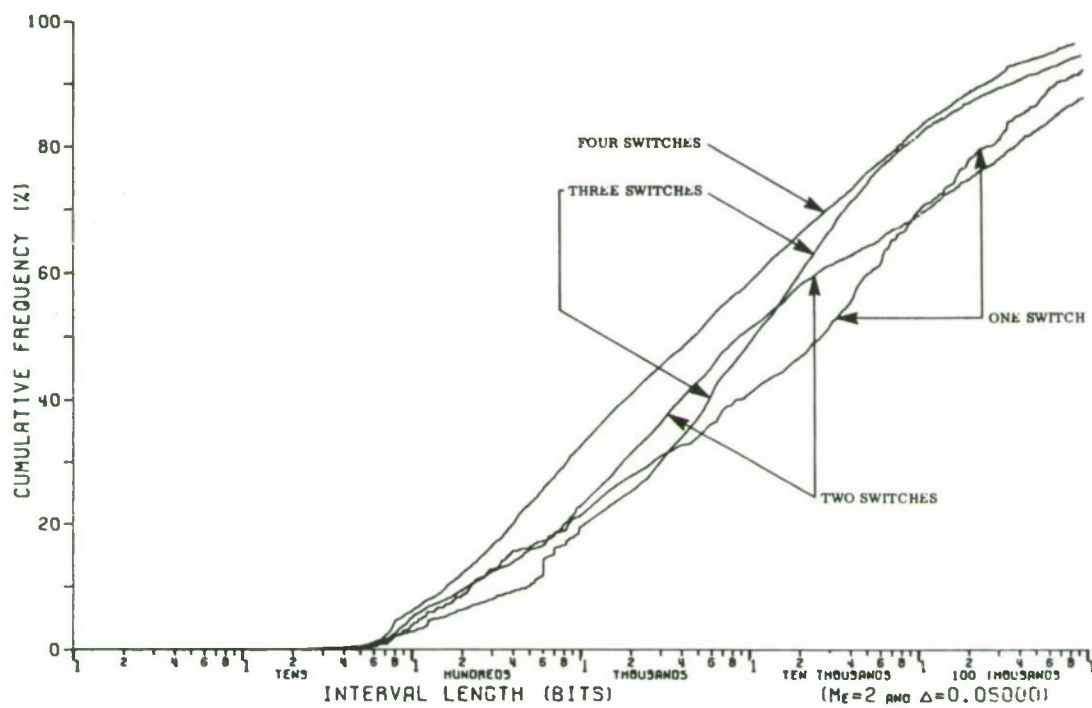


Figure 27. Cumulative Distribution on Lengths of Intervals — 4800 b/s Data

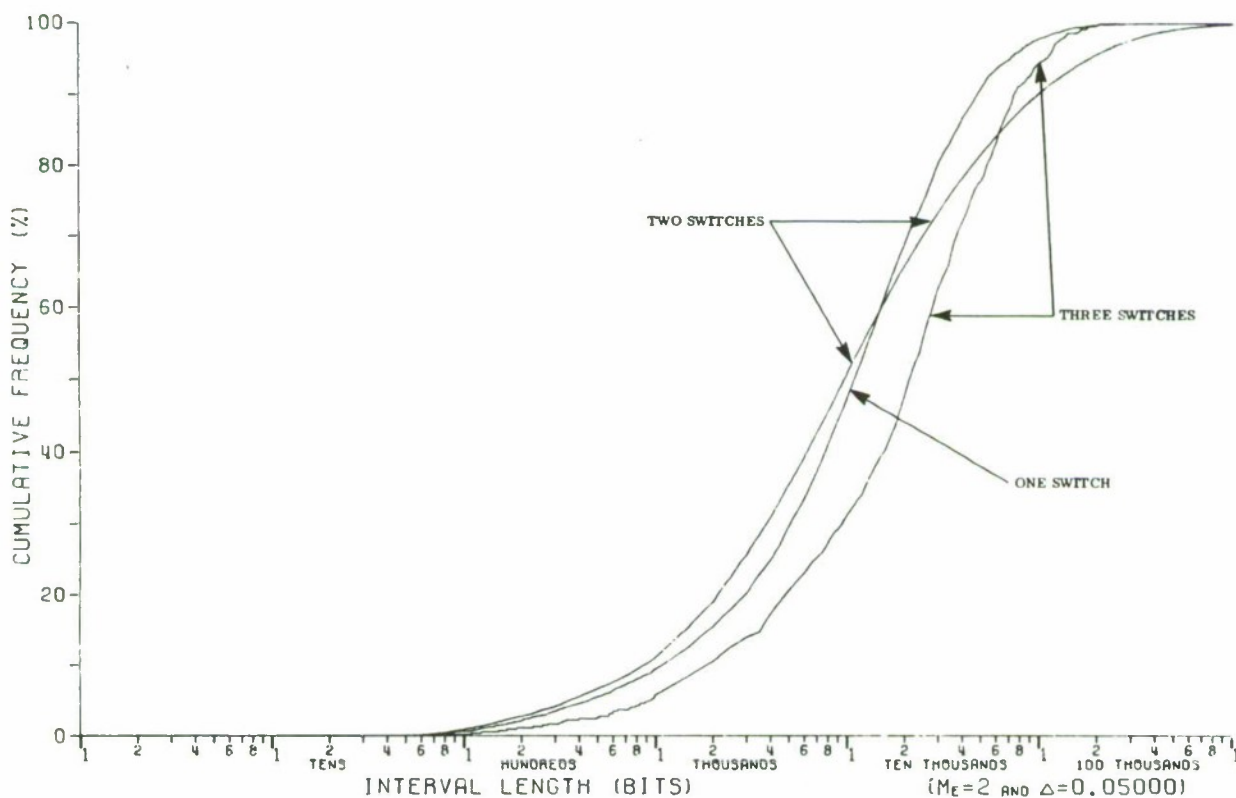


Figure 28. Cumulative Distribution on Lengths of Intervals — 9600 b/s Data

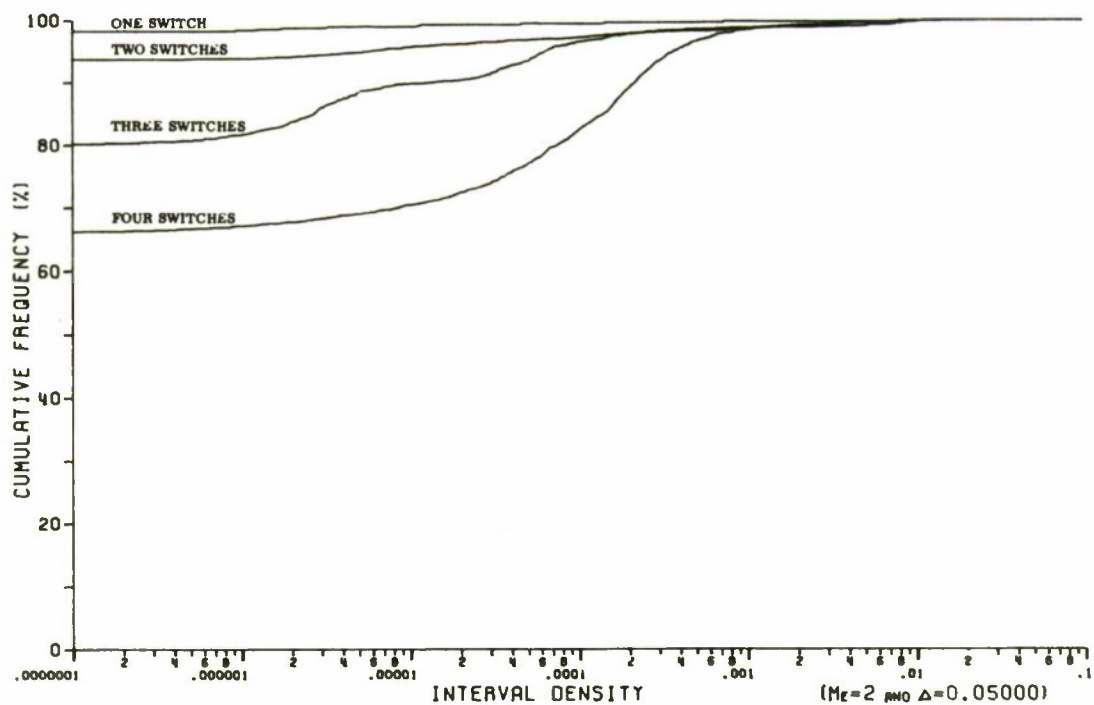


Figure 29. Cumulative Distribution on Interval Densities — 4800 b/s Data

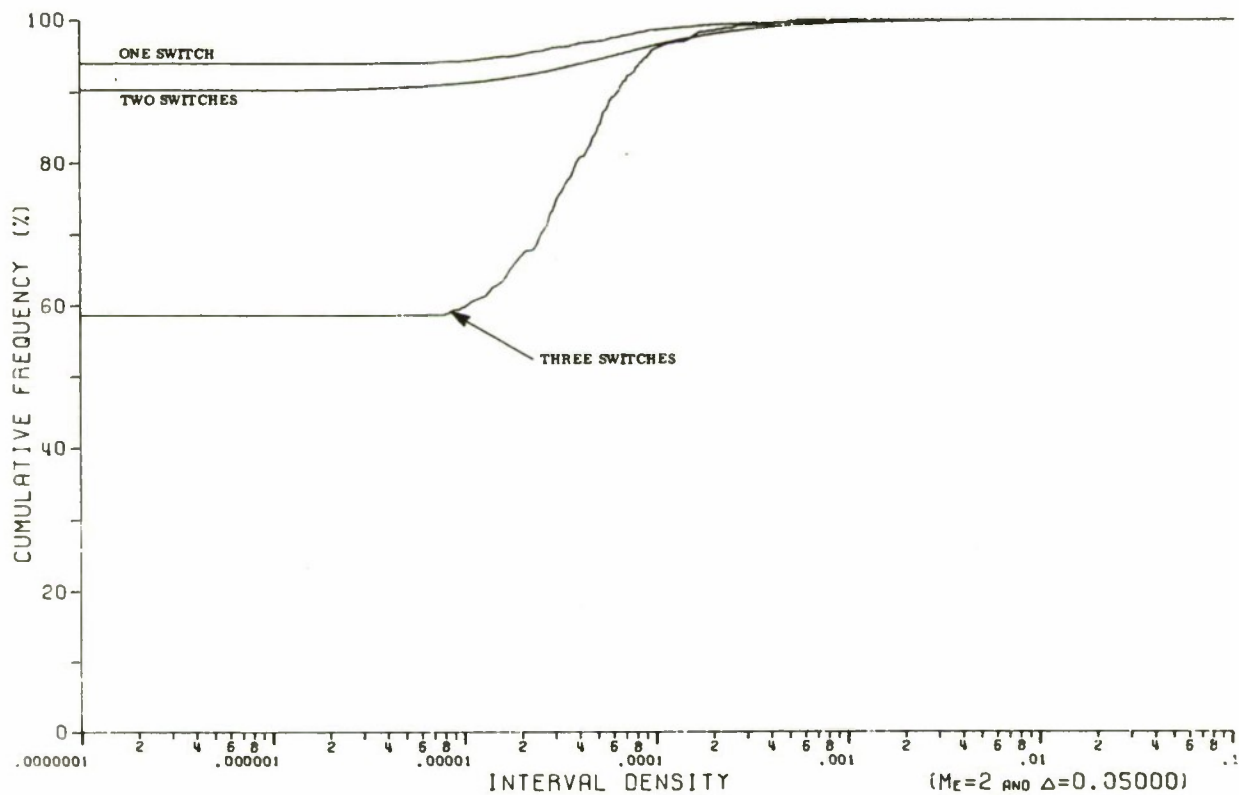


Figure 30. Cumulative Distribution on Interval Densities — 9600 b/s Data

are affected, thus causing little variation in the interval densities. The relationship of bursts to following intervals, in terms of length (Figures 31 and 32), is little affected by the number of switches in the circuit.

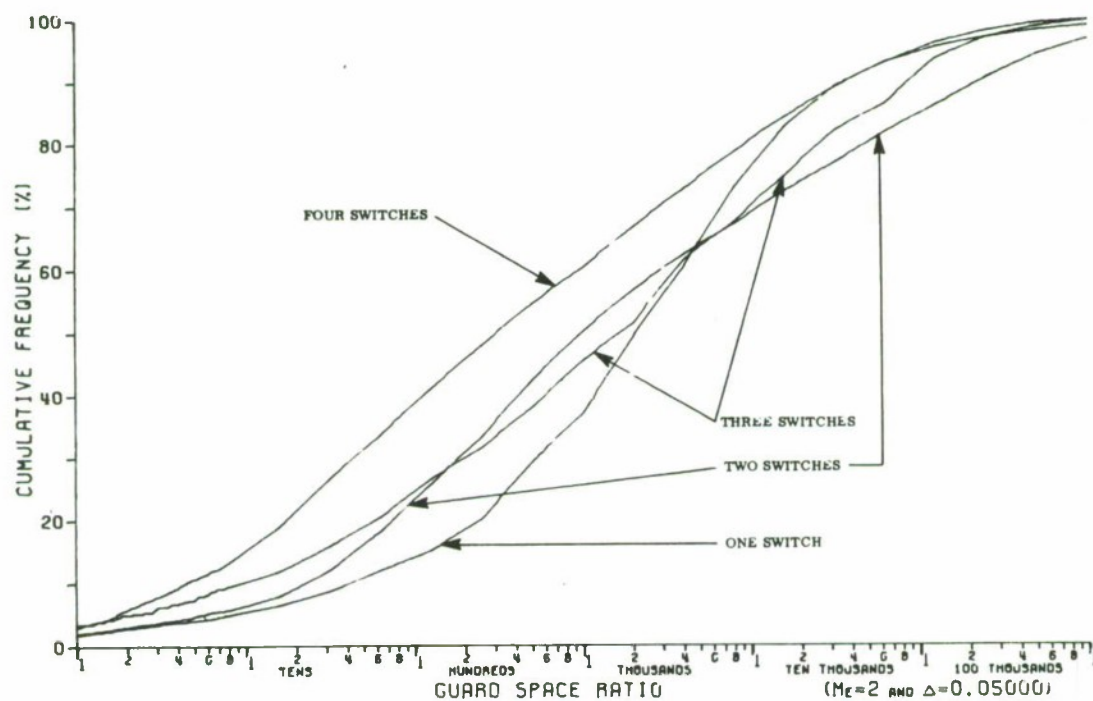


Figure 31. Interval to Burst Ratios — 4800 b/s Data

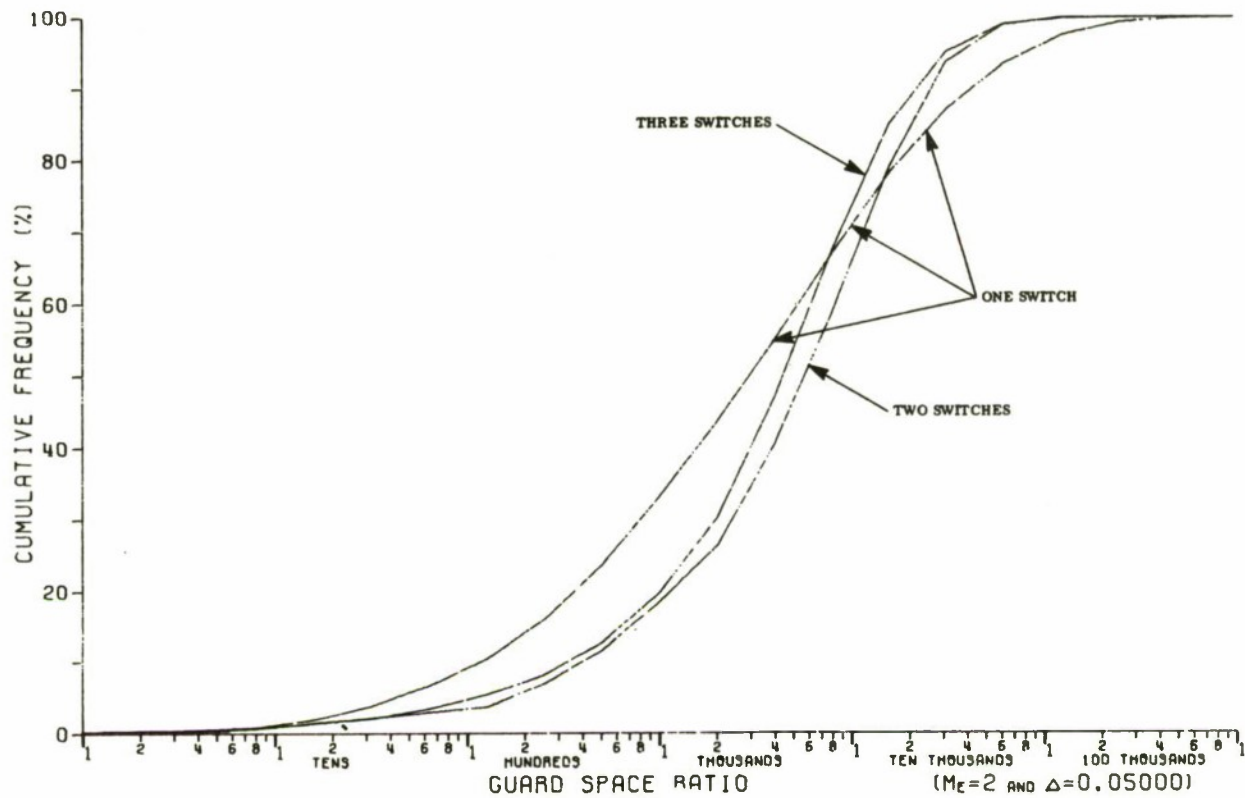


Figure 32. Interval to Burst Ratios — 9600 b/s Data

SECTION IV

ANALYSIS ACCORDING TO CIRCUIT MILEAGE

In the past, telephone channel error patterns have frequently been analyzed according to circuit mileage. The AUTOVON error patterns have thus been grouped according to circuit miles in order to determine whether there are any distance-related effects.

The data was divided into three classes:

- Less than 1,000 miles,
- Less than 3,000, but more than 1,000 miles,
- More than 3,000 miles.

The data, so subdivided, is summarized in Table IV. It should be apparent from this table that, at least in terms of an average error rate, circuit miles are not important.

INTER-ERROR DISTRIBUTIONS

The distributions of consecutive errors at 4800 b/s show a clear dichotomy between less than 1,000 miles and more than 1,000 miles. For the short circuits, errors are generally single errors while on the longer circuits the frequency of double errors becomes significant (Figure 33). The 9600 b/s consecutive errors are double error dominant (Figure 34) at all distances. Similarly, in the error-free gap distributions, the shorter range 4800 b/s circuits exhibit the random error characteristic while the greater than 1,000 mile circuits exhibit bursts as would be expected in view of their double error occurrences (Figure 35). The 9600 b/s gaps exhibit the same complex structure as the total 9600 b/s data (Figure 2) at all circuit distances (Figure 36).

Table IV
Data Summary - By Miles

Connectivity	Data Rate	Total Bits	Total Errors	Bit Error Rate
< 1000 MI 1000 ≤ MI < 3000 MI ≥ 3000	4800 b/s	963, 720, 407	22, 363	2.3 E-5
	4800 b/s	531, 400, 197	7, 079	1.3 E-5
	4800 b/s	1, 579, 640, 229	100, 300	6.3 E-5
< 1000 MI 1000 ≤ MI < 3000 MI ≥ 3000	9600 b/s	2, 641, 195, 208	117, 745	4.5 E-5
	9600 b/s	962, 022, 012	67, 607	7.0 E-5
	9600 b/s	392, 847, 501	139, 778	3.6 E-4

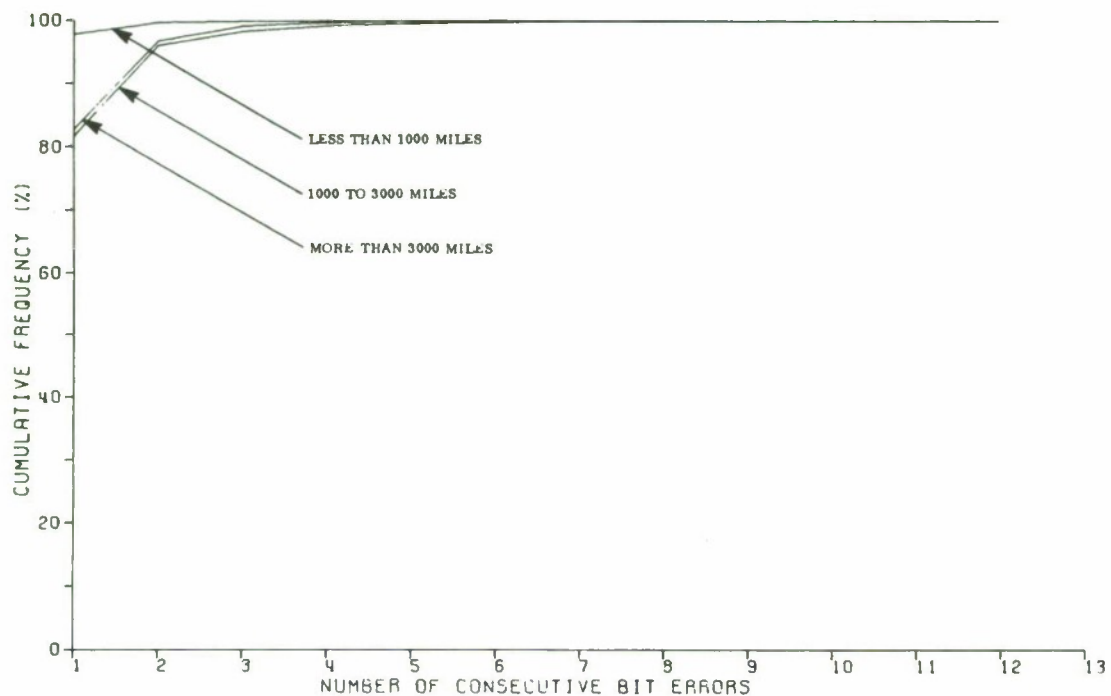


Figure 33. Cumulative Distribution of Consecutive Errors — 4800 b/s Data

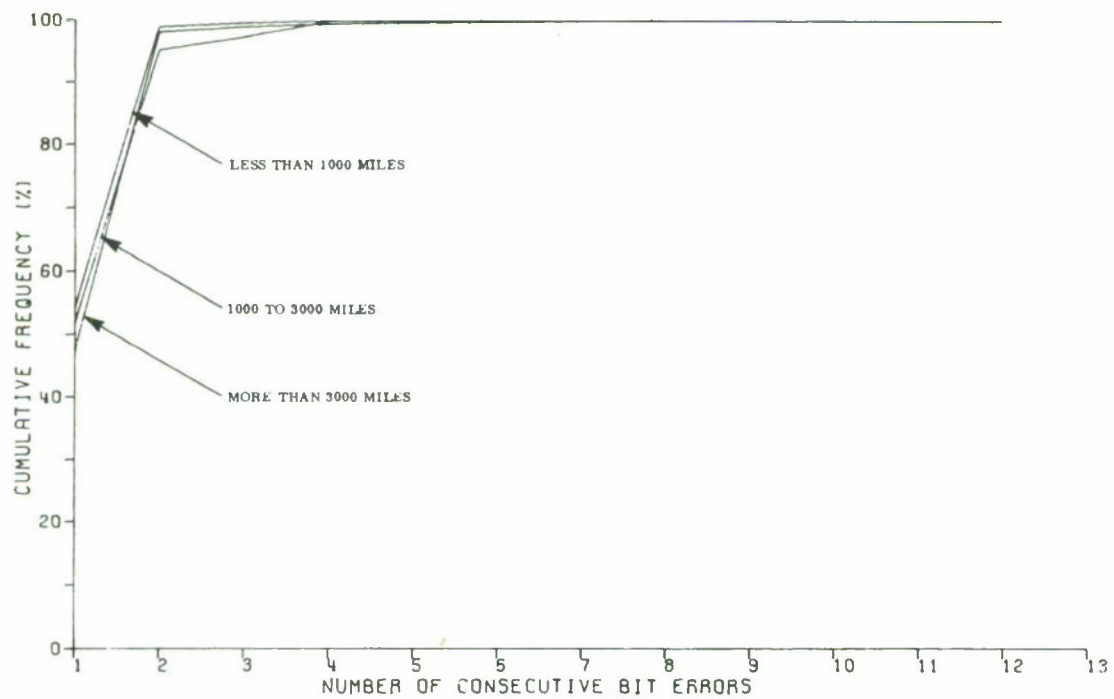


Figure 34. Cumulative Distribution of Consecutive Errors — 9600 b/s Data

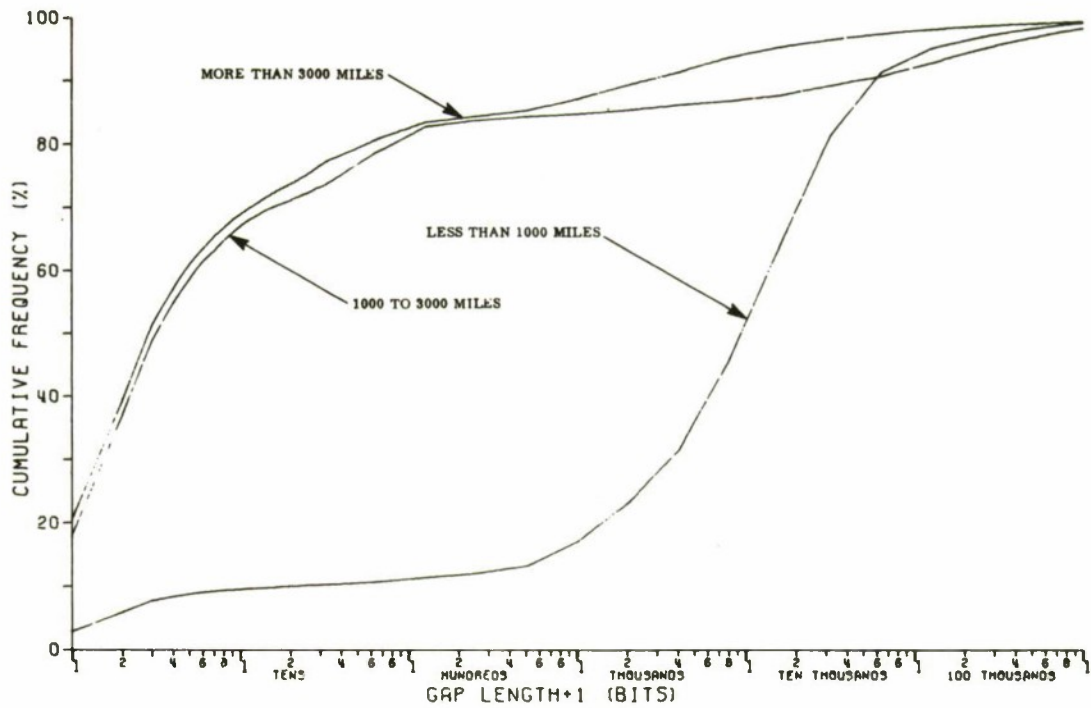


Figure 35. Cumulative Distribution of Error-Free Gaps — 4800 b/s Data

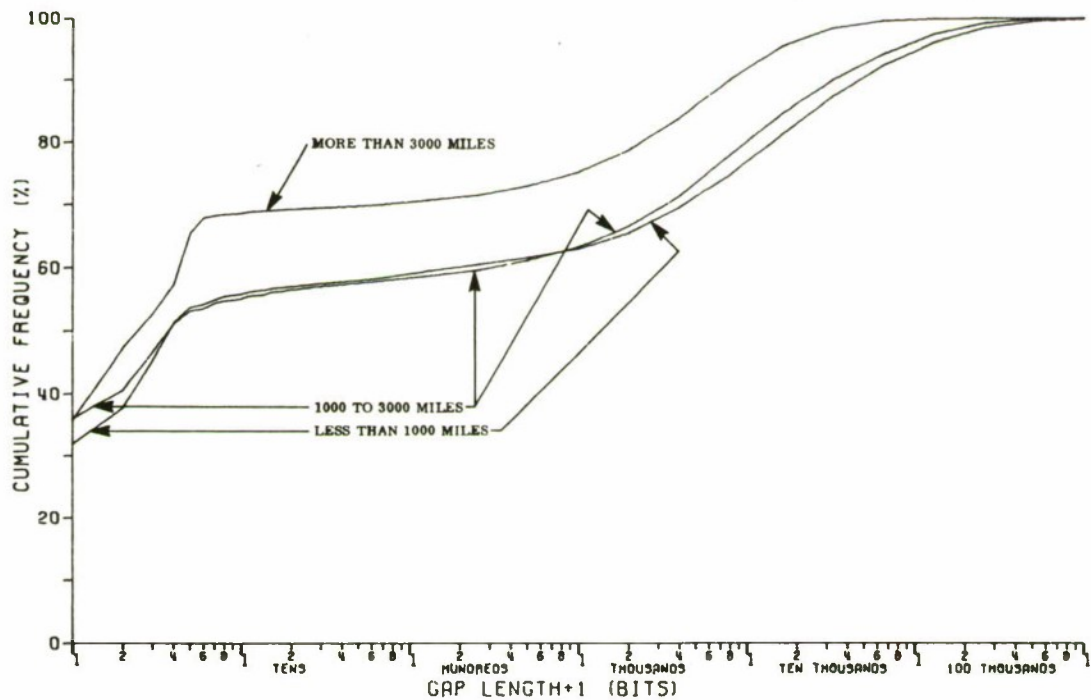


Figure 36. Cumulative Distribution of Error-Free Gaps — 9600 b/s Data

The $P(\geq E, M)$ curves exhibit the same upward compression toward probability one as a function of milage as has been seen previously, at 4800 b/s, with block error probability at less than 1,000 miles being greater than that at the other distances. (Figures 37 to 39.) This is consistent with a more random nature of the errors at this distance. The same probabilities at 9600 b/s indicate increasing numbers of errors and probabilities of errors at a given block length as the circuit mileage increases (Figures 40 to 42).

BURST DISTRIBUTIONS

The dichotomy previously seen at 4800 b/s in the consecutive errors and error-free gaps appears in the burst distributions, although here the 1,000 to 3,000 milc group is more closely allied to the less than 1,000 mile group. The 9600 b/s data shows generally longer and denser bursts as mileage increases. Based on the inter-error distributions, there are no new results to be drawn from the analysis of the data according to mileage. Therefore, the burst distributions, Figures 43 through 52, are presented only for the purpose of consistency in the data description.

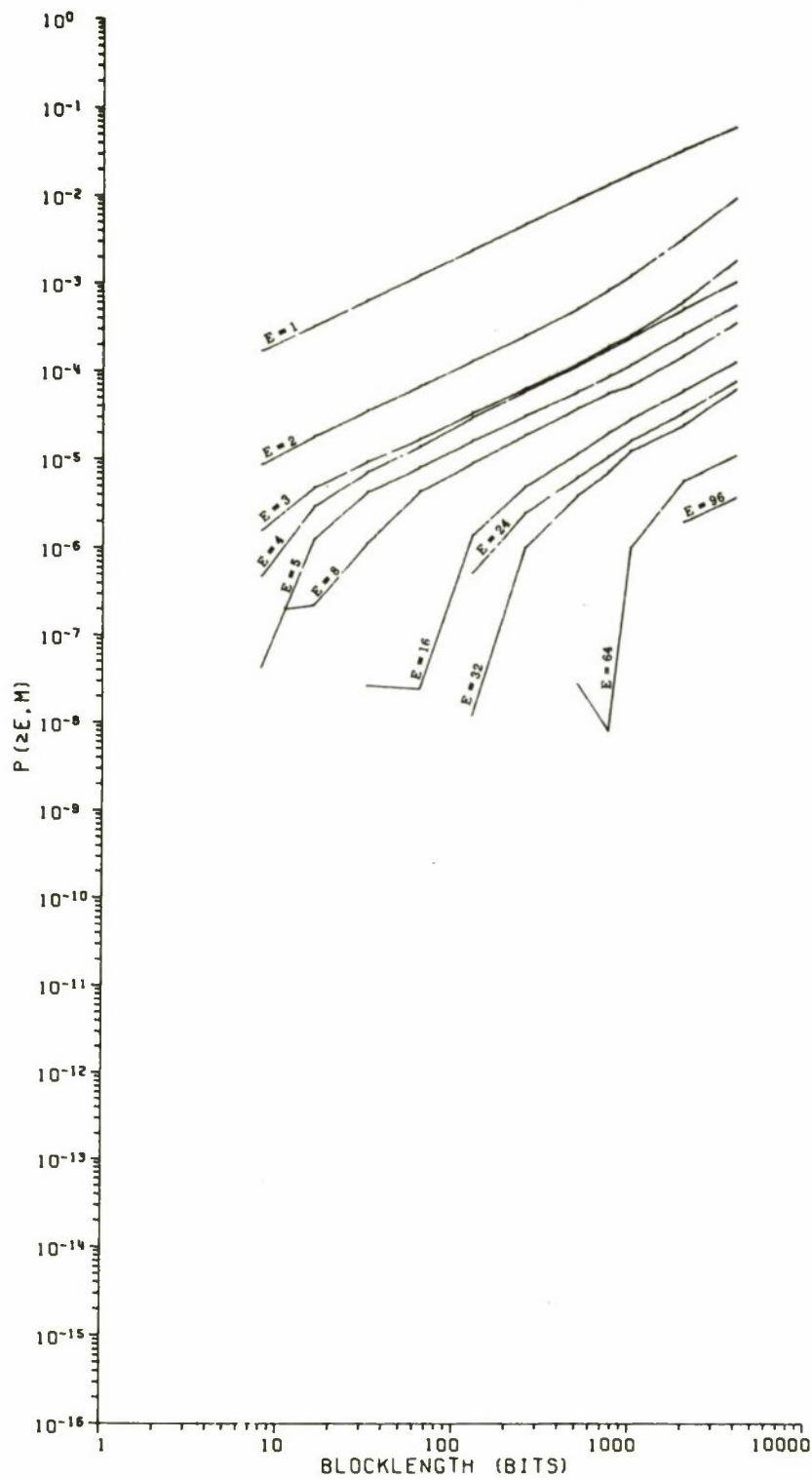


Figure 37. Probability of at Least E Errors in an M Bit Block — Circuit ≤ 1000 MI/4800 b/s

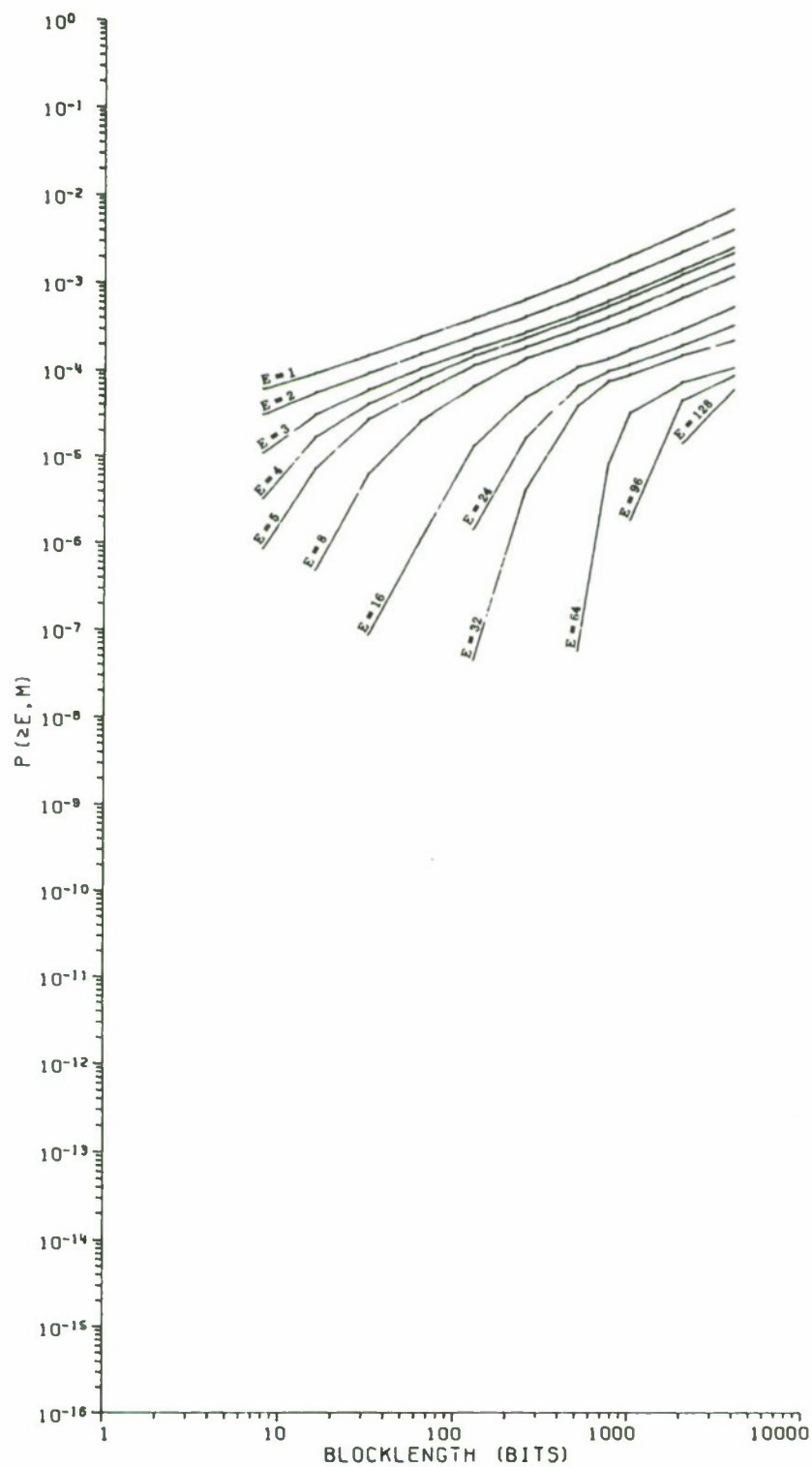


Figure 38. Probability of at Least E Errors in an M Bit Block — 1000 MI < Circuit < 3000 MI/4800 b/s

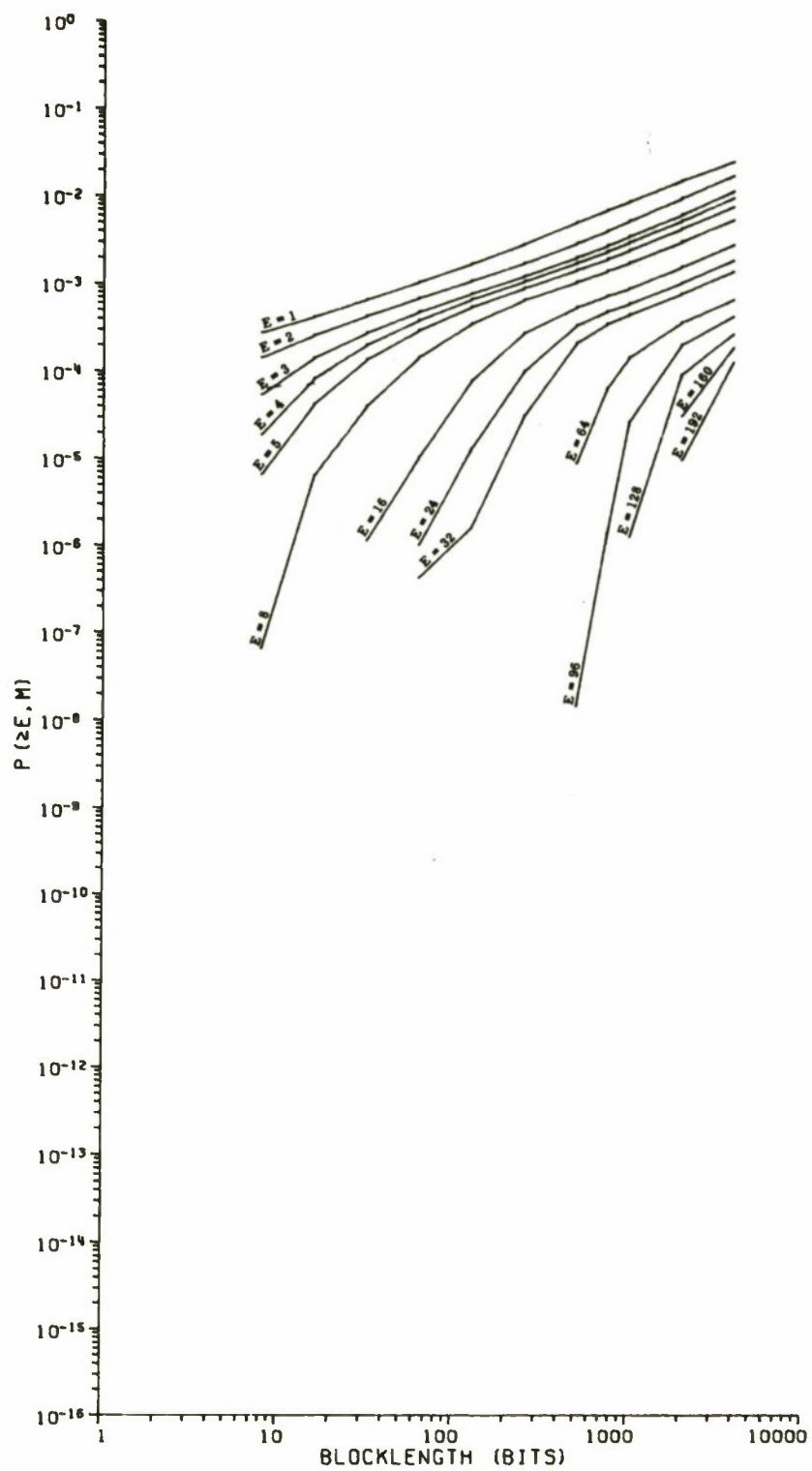


Figure 39. Probability of at Least E Errors in an M Bit Block — Circuit ≥ 3000 MI/4800 b/s

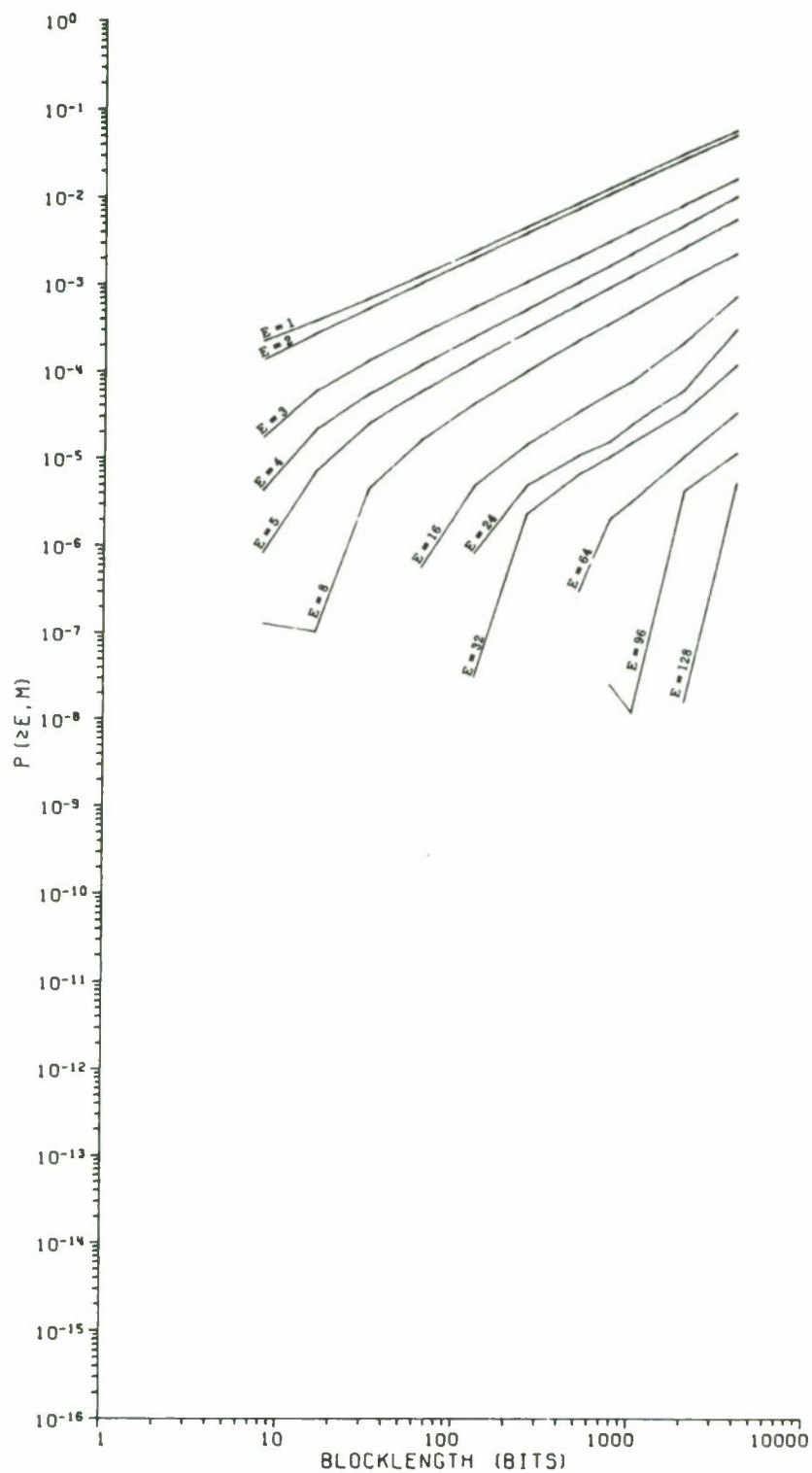


Figure 40. Probability of at Least E Errors in an M Bit Block — Circuit ≤ 1000 MI/9600 b/s

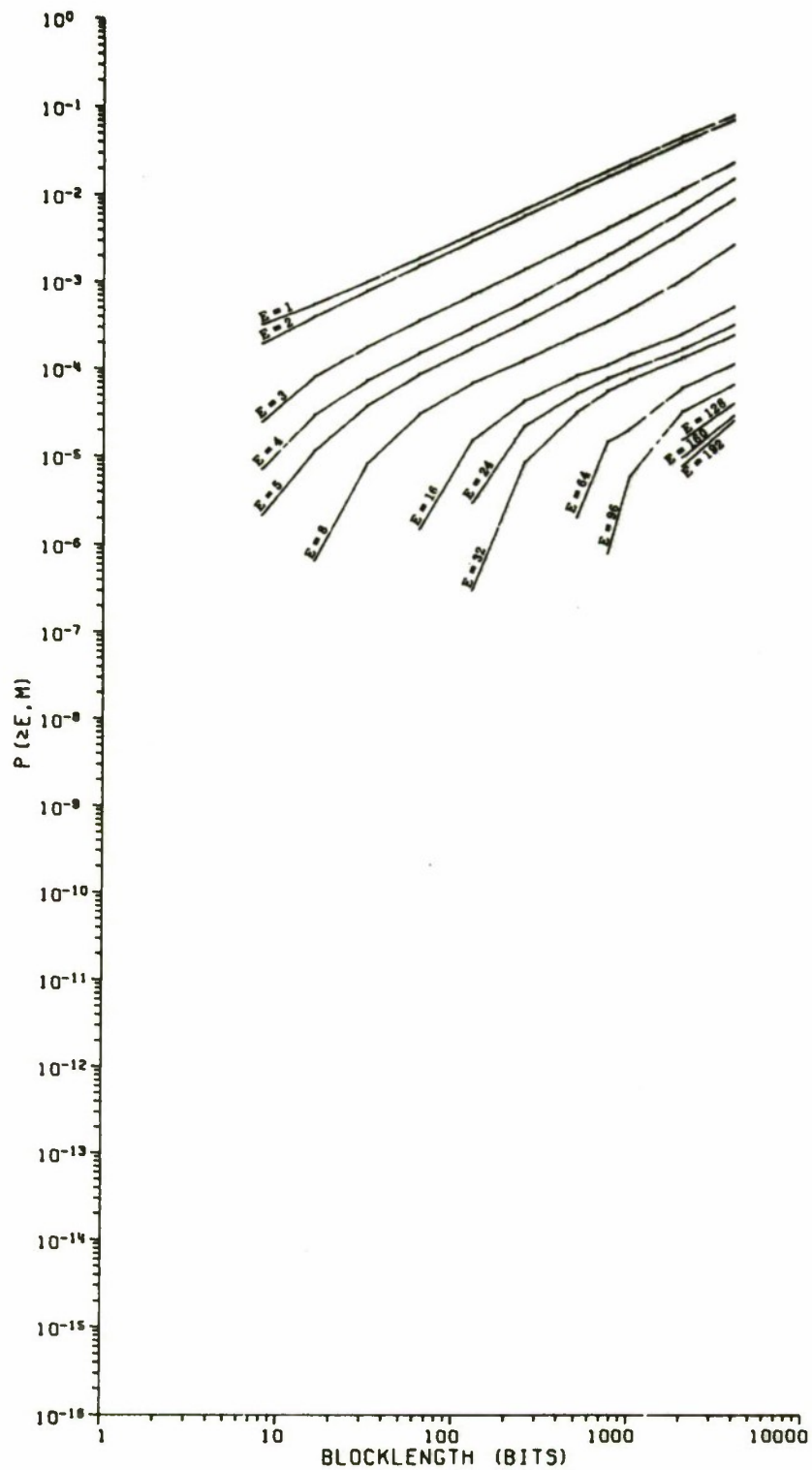


Figure 41. Probability of at Least E Errors in an M Bit Block — 1000 MI < Circuit < 3000 MI/9600 b/s

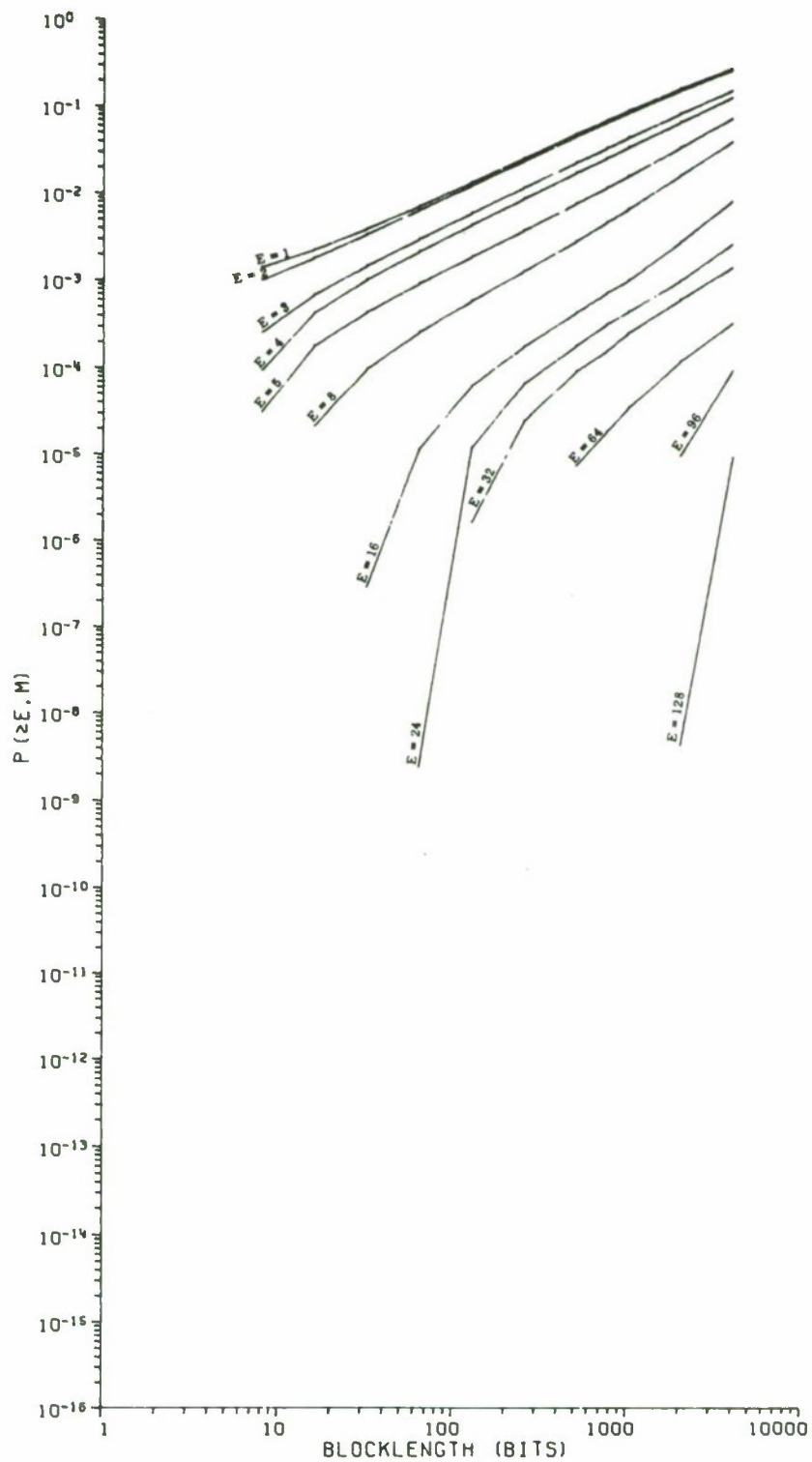


Figure 42. Probability of at Least E Errors in an M Bit Block — Circuit ≥ 3000 MI/9600 b/s

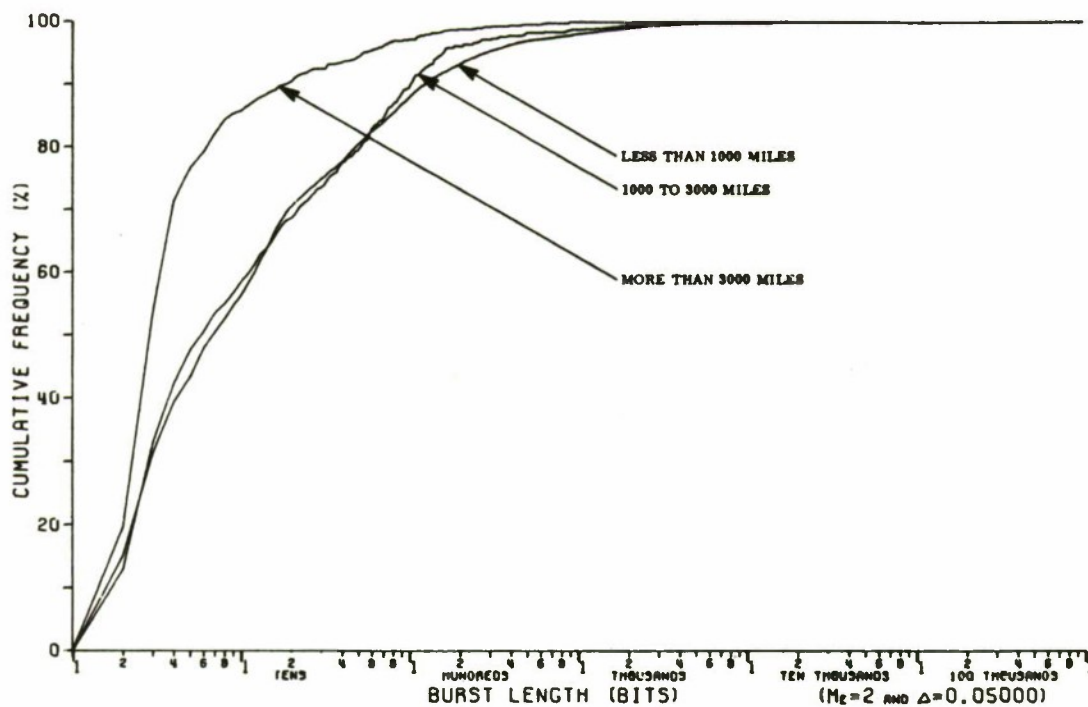


Figure 43. Cumulative Distribution on Lengths of Bursts — 4800 b/s Data

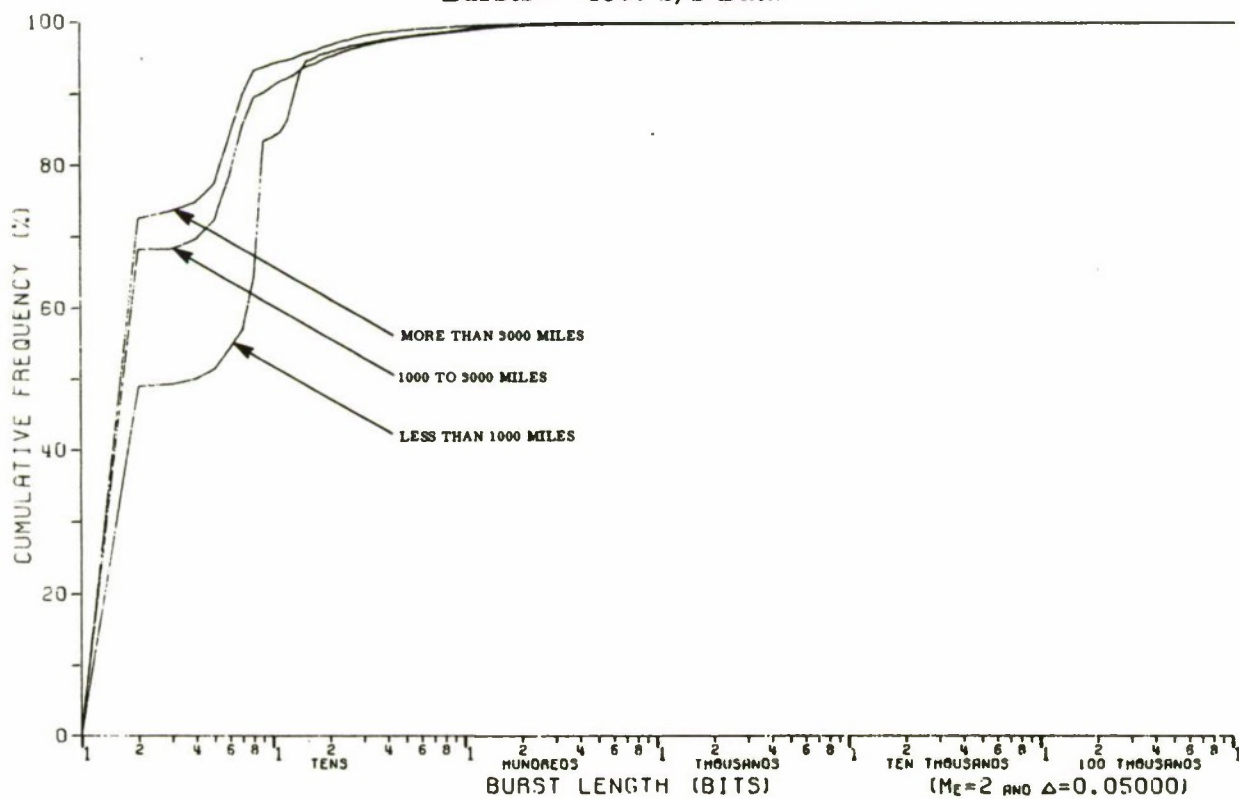


Figure 44. Cumulative Distribution on Lengths of Bursts — 9600 b/s Data

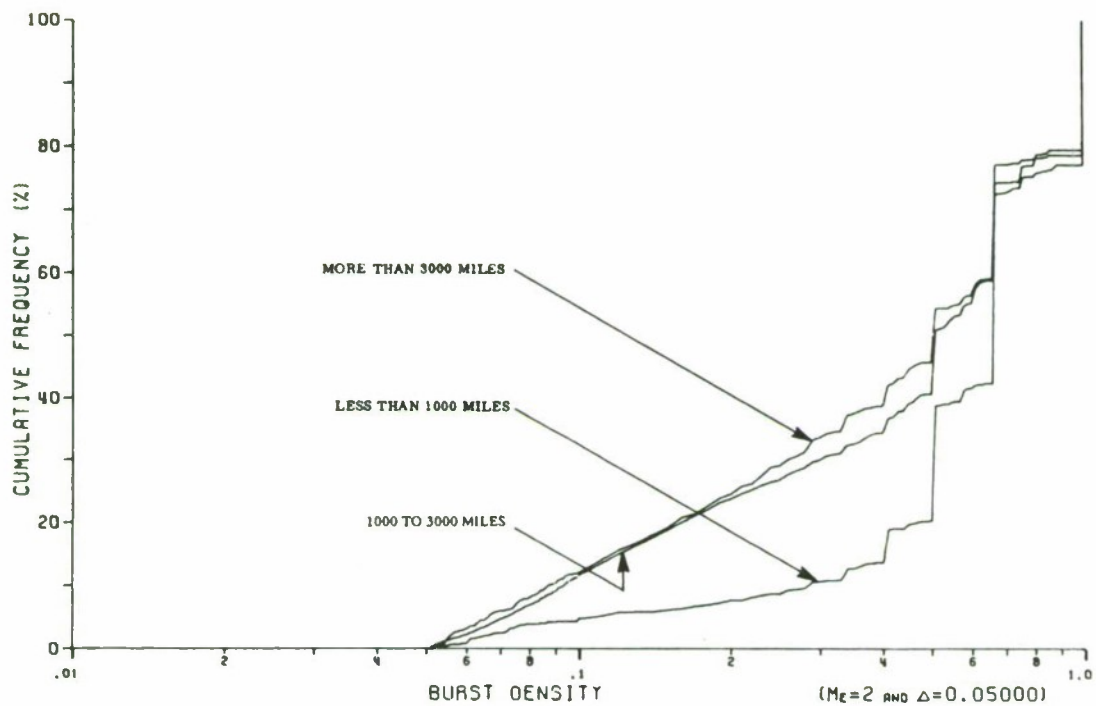


Figure 45. Cumulative Distribution on Burst Densities — 4800 b/s Data

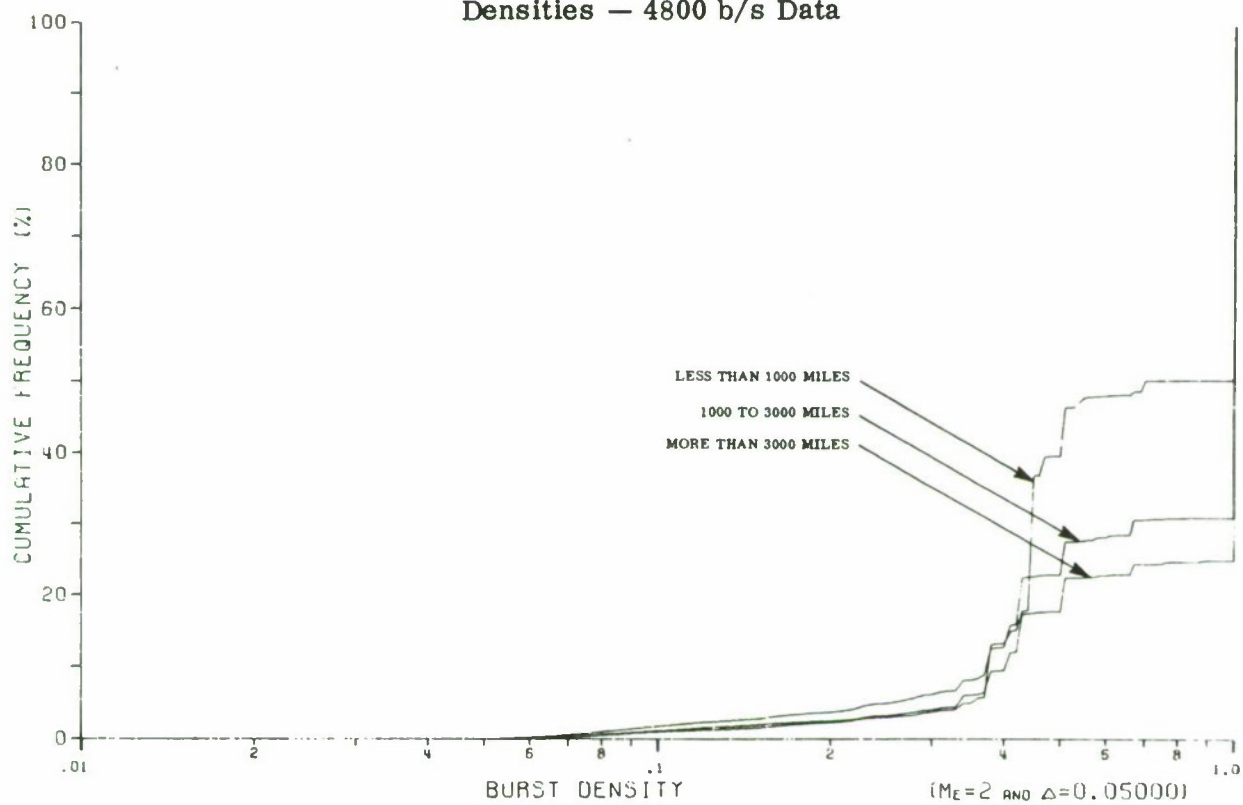


Figure 46. Cumulative Distribution on Burst Densities — 9600 b/s Data

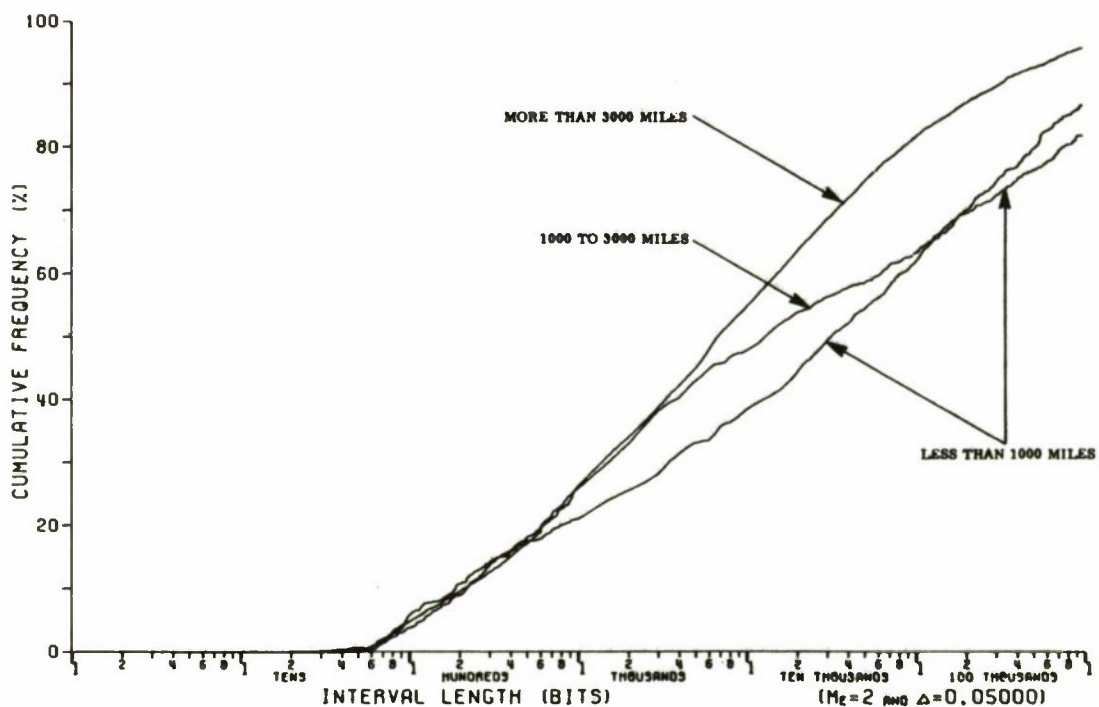


Figure 47. Cumulative Distribution on Lengths of Intervals — 4800 b/s Data

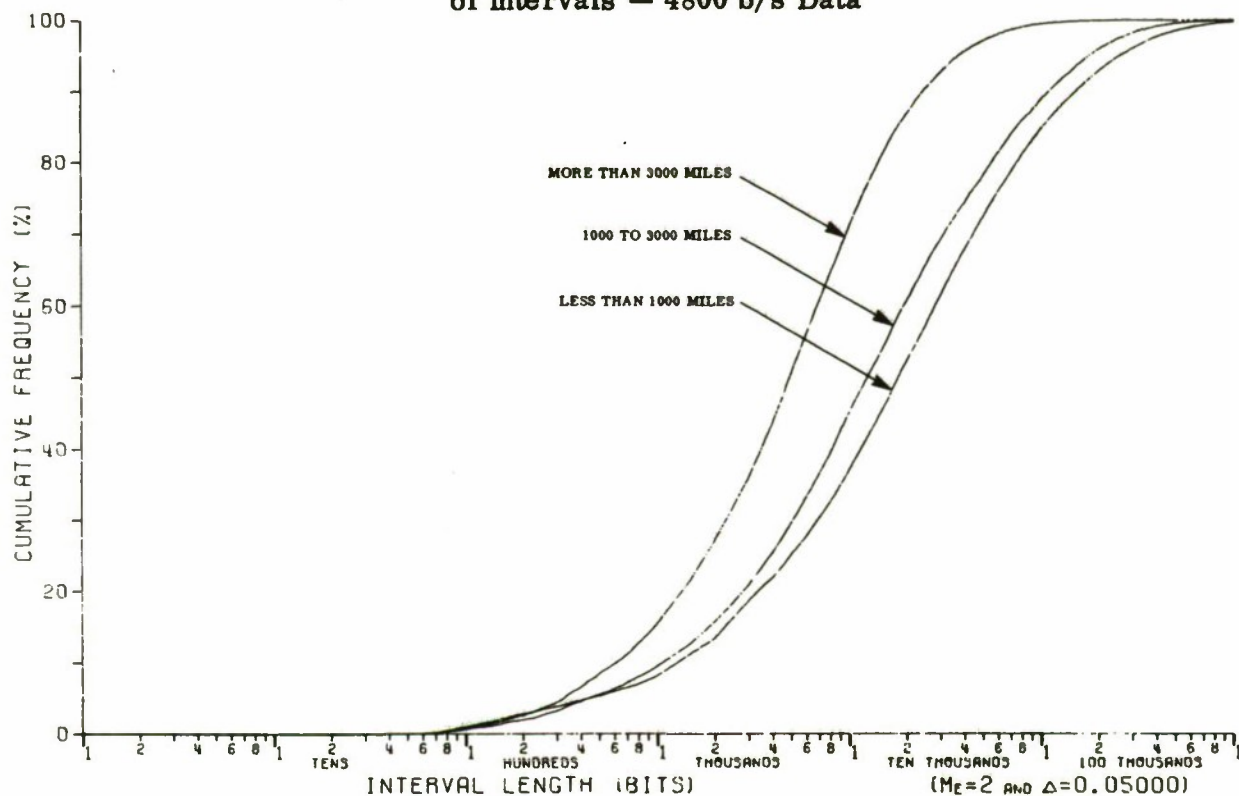


Figure 48. Cumulative Distribution on Lengths of Intervals — 9600 b/s Data

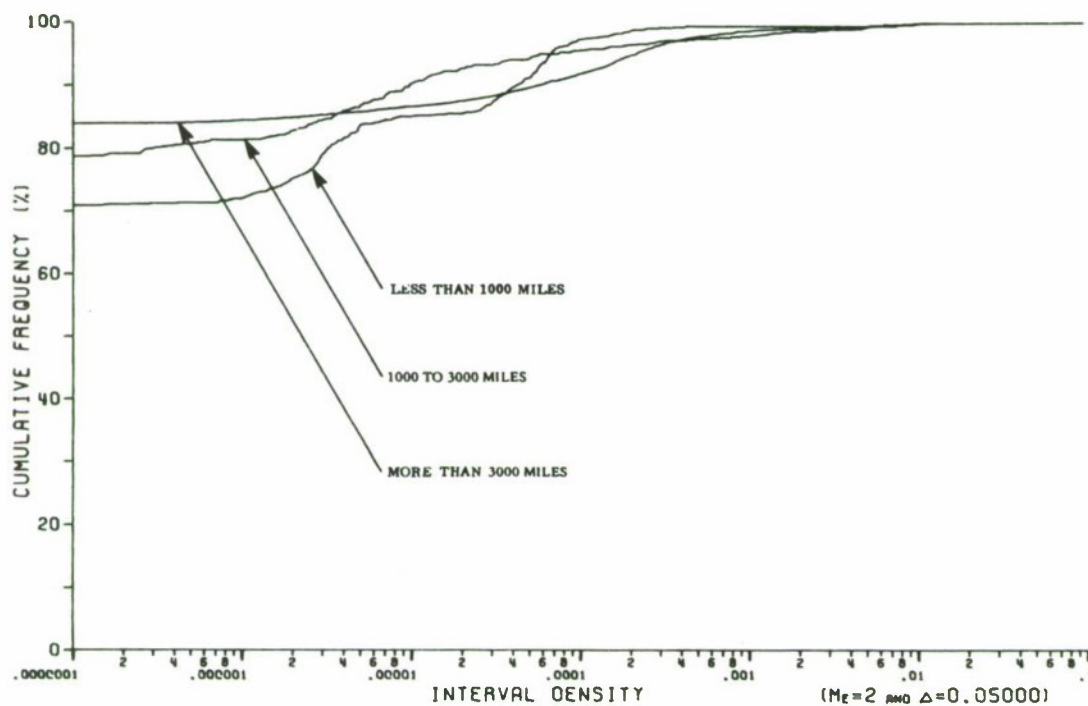


Figure 49. Cumulative Distribution on Interval Densities — 4800 b/s Data

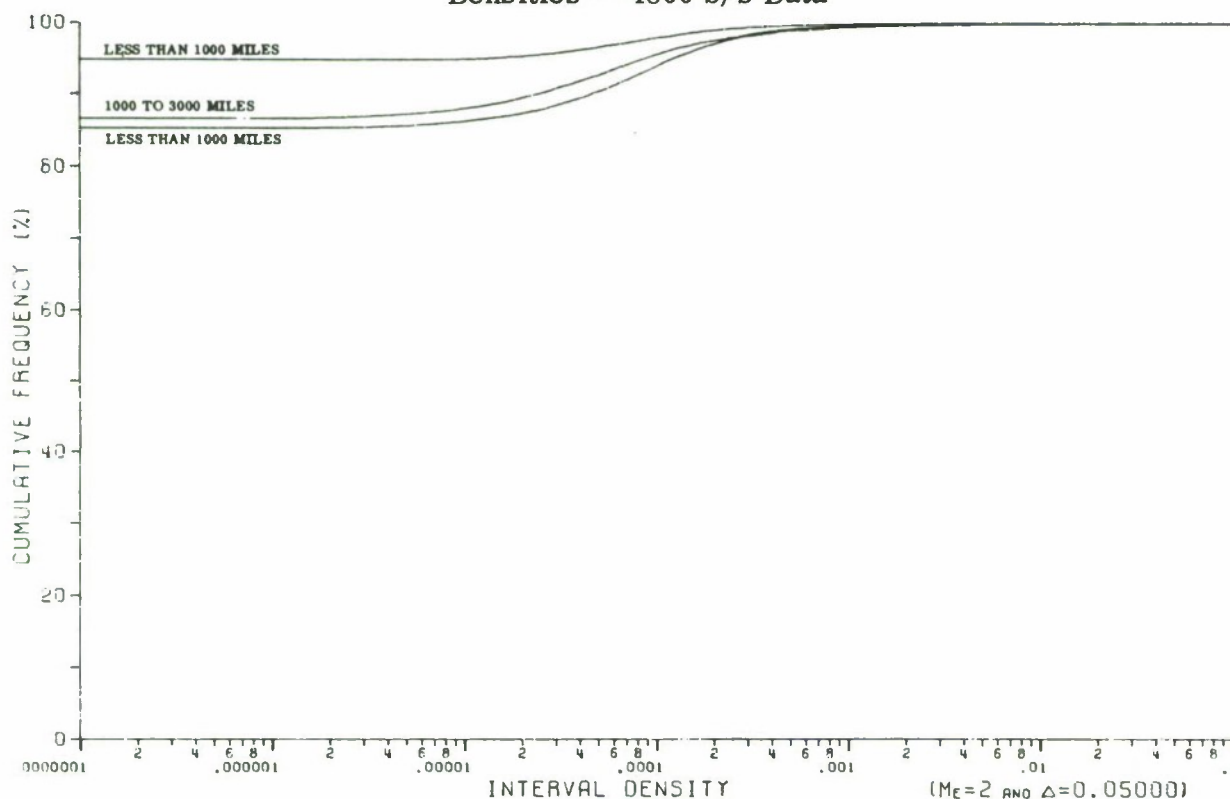


Figure 50. Cumulative Distribution on Interval Densities — 9600 b/s Data

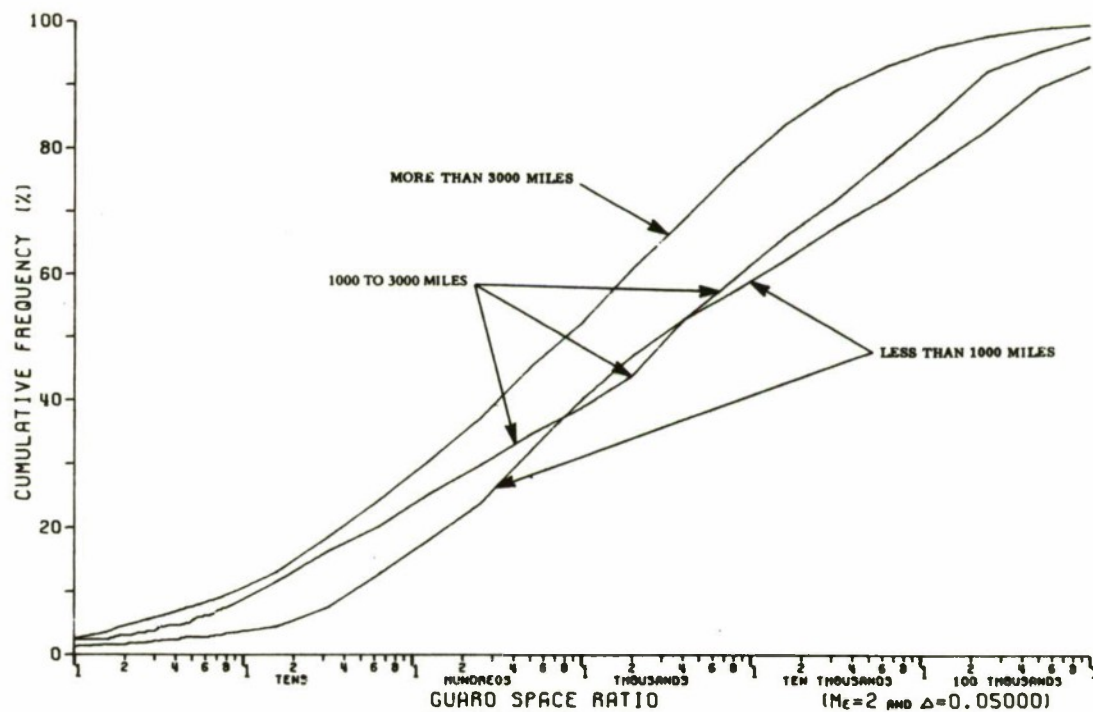


Figure 51. Interval to Burst Ratios — 4800 b/s Data

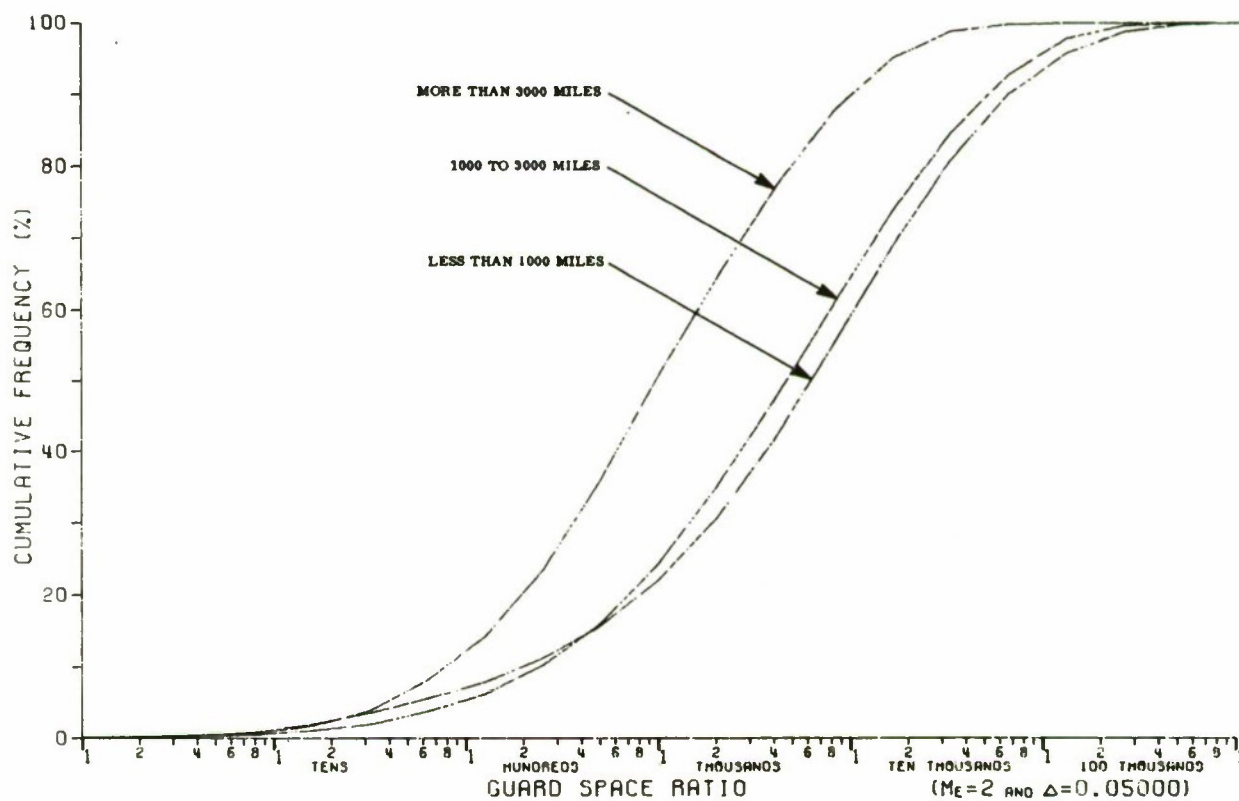


Figure 52. Interval to Burst Ratios — 9600 b/s Data

SECTION V

ANALYSIS ACCORDING TO NUMBERS OF TRUNKS

The AUTOVON data can be organized in various ways. In previous sections, the data has been examined from the point of view of how many switches were dialed through (to determine the impact of switches on error patterns) and the lengths of circuits in miles (to determine the impact of mileage on error patterns). Another approach to organizing the data is according to the number of trunks connected. The bit error rates clearly show (Table V) that as more trunks are connected, the relative frequency of error occurrence increases. Care should be taken to note that this is not purely a switch-dependent effect since the data sample size divides differently when considering trunks rather than switches (i.e., there are different numbers of trunks interconnecting the selected AUTOVON switches). *

INTER-ERROR DISTRIBUTIONS

The distributions of consecutive errors at 4800 b/s and 9600 b/s (Figures 53 and 54) are essentially the same as for switch connections. The error-free intervals at 4800 b/s (Figure 55) show bursts for five or more trunks, while for lesser numbers of trunks, the distribution is that of random errors set on a pedestal of short dense bursts. The 9600 b/s error-free intervals (Figure 56) show the same complexity as previously identified. This complexity appears to be a characteristic of the 9600 b/s data independent of switch connectivity, trunk connectivity, or mileage. At 4800 b/s, the error-free intervals show random

* Private communication from J. McEvoy, RADC.

Table V
Data Summary - By Trunks

Connectivity	Data Rate	Total Bits	Total Errors	Bit Error Rate
Two	4800 b/s	252,746,958	1,124	4.4 E-6
Four	4800 b/s	1,454,503,456	39,972	2.7 E-5
Five or more	4800 b/s	1,367,510,419	88,646	6.5 E-5
Two	9600 b/s	2,398,133,462	101,320	4.2 E-5
Four	9600 b/s	1,580,953,906	221,419	1.4 E-4
Six	9600 b/s	16,977,353	2,391	1.4 E-4

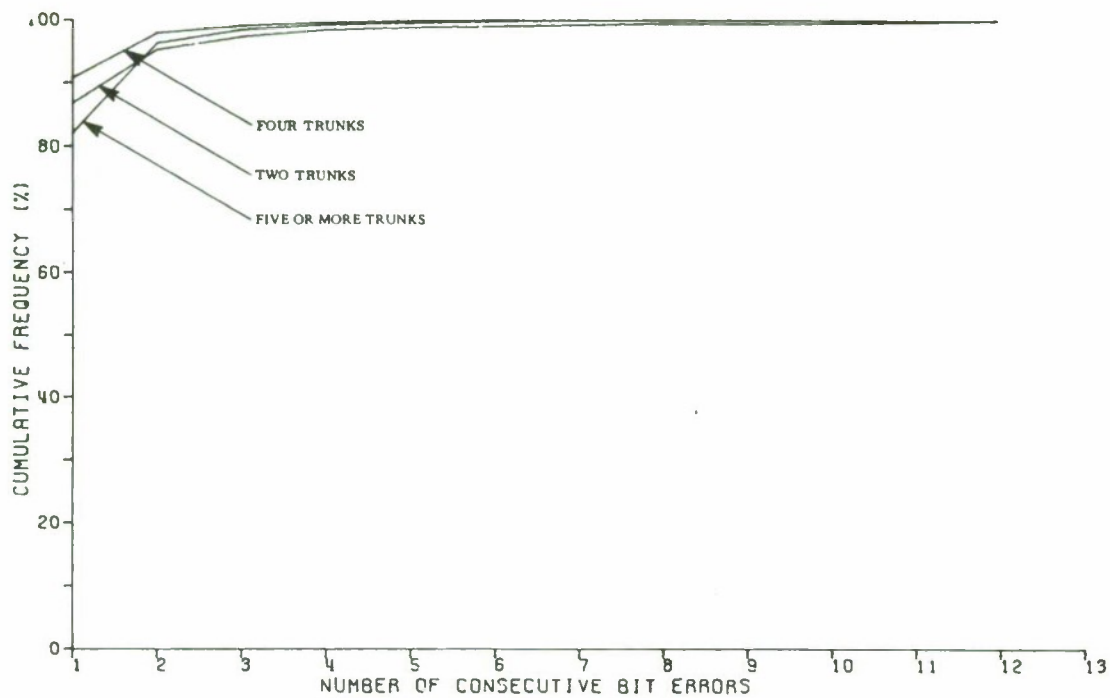


Figure 53. Cumulative Distribution of Consecutive Errors — 4800 b/s Data

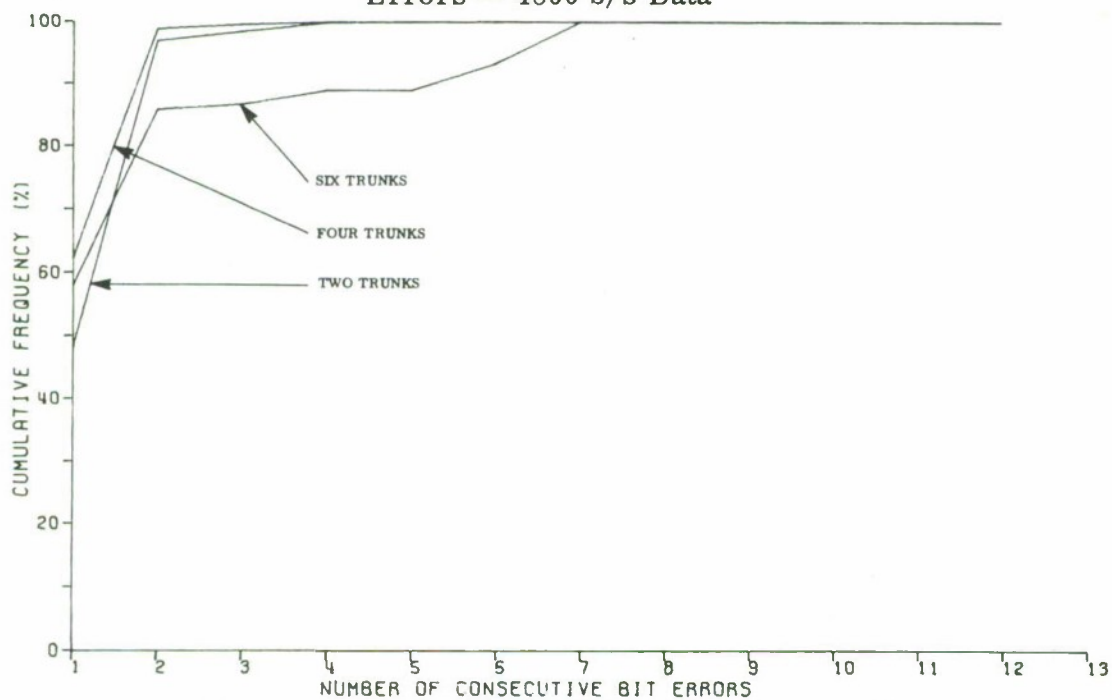


Figure 54. Cumulative Distribution of Consecutive Errors — 9600 b/s Data

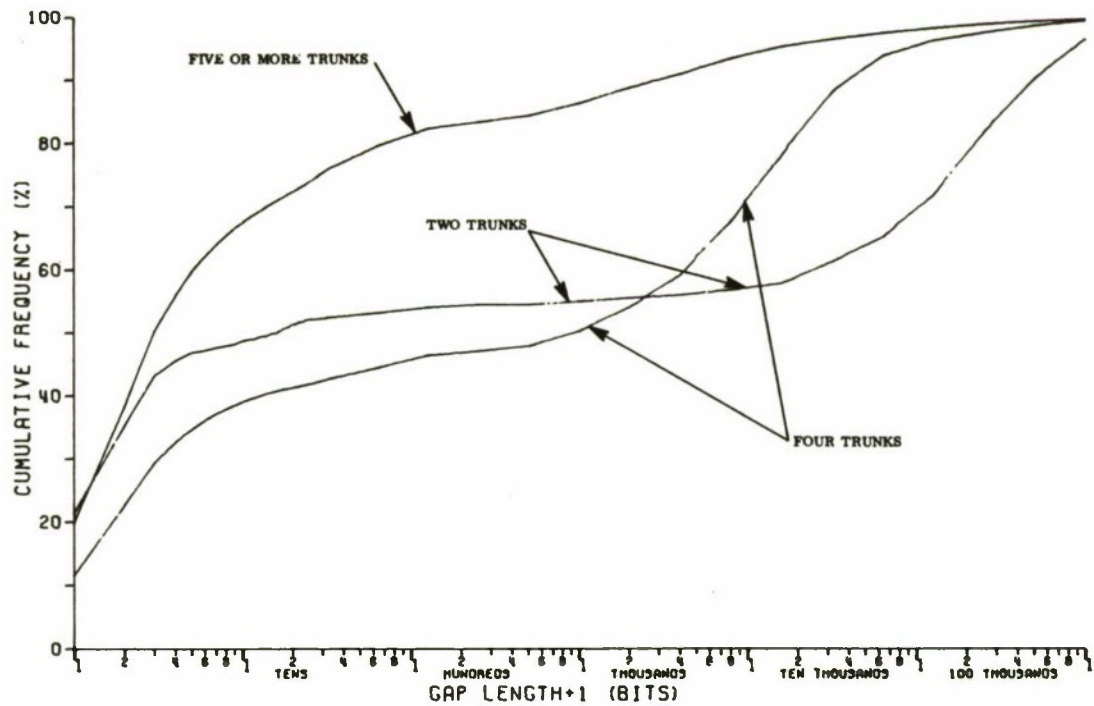


Figure 55. Cumulative Distribution of Error-Free Gaps - 4800 b/s Data

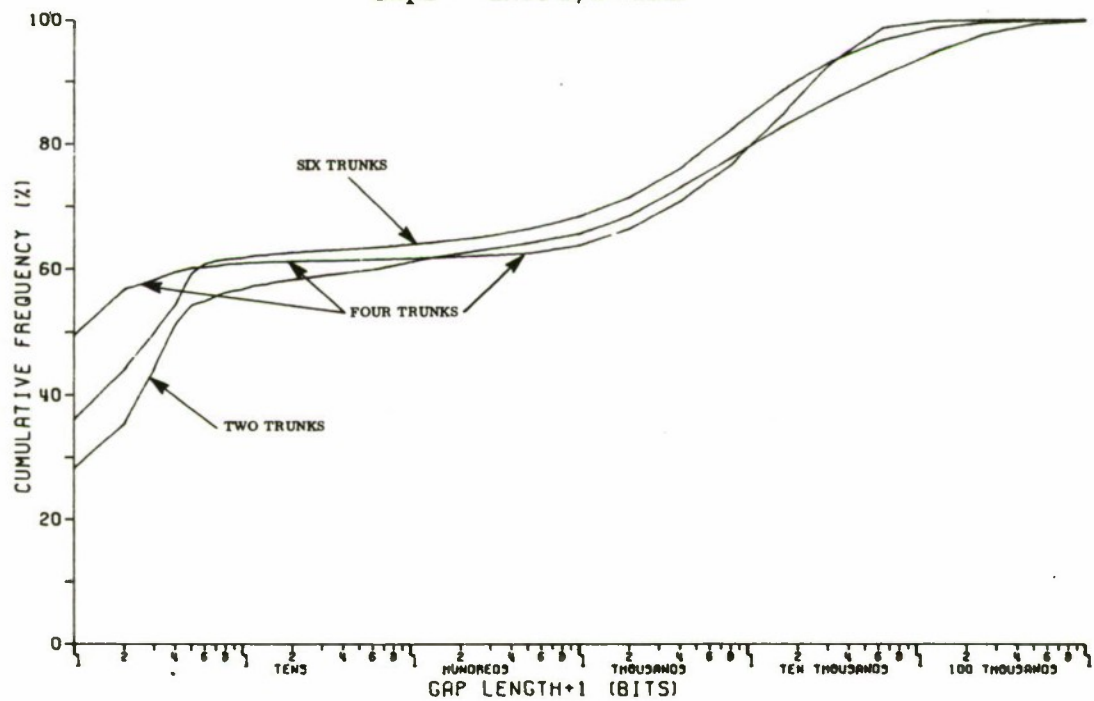


Figure 56. Cumulative Distribution of Error-Free Gaps - 9600 b/s Data

characteristics for short mileage or few trunks with burst frequency increasing as the number of switches are added.

At 4800 b/s, the $P(\geq E, M)$ curves show increasing values of both E and $P(\geq E, M)$ as a function of increasing numbers of trunks in the circuit (Figures 57 through 59). This same phenomena occurs at 9600 b/s (Figures 60 through 62), although the small amount of data collected for a six trunk connectivity has masked the increase in the range of E .

BURST DISTRIBUTIONS

The distributions of bursts (Figures 63 and 64) show very little variation with trunks as do the densities of errors in those bursts (Figures 65 and 66). Likewise, the interval distributions are similar (Figures 67 and 68) with the exception that the intervals between bursts on the 4800 b/s two trunk connection are very long. The interval densities at 4800 b/s show no variation (Figure 69), but at 9600 b/s the percentage of intervals which are error-free on six trunks (Figure 70) is less than 60%. Both data rates show bursts that are generally followed by long intervals (Figures 71 and 72).

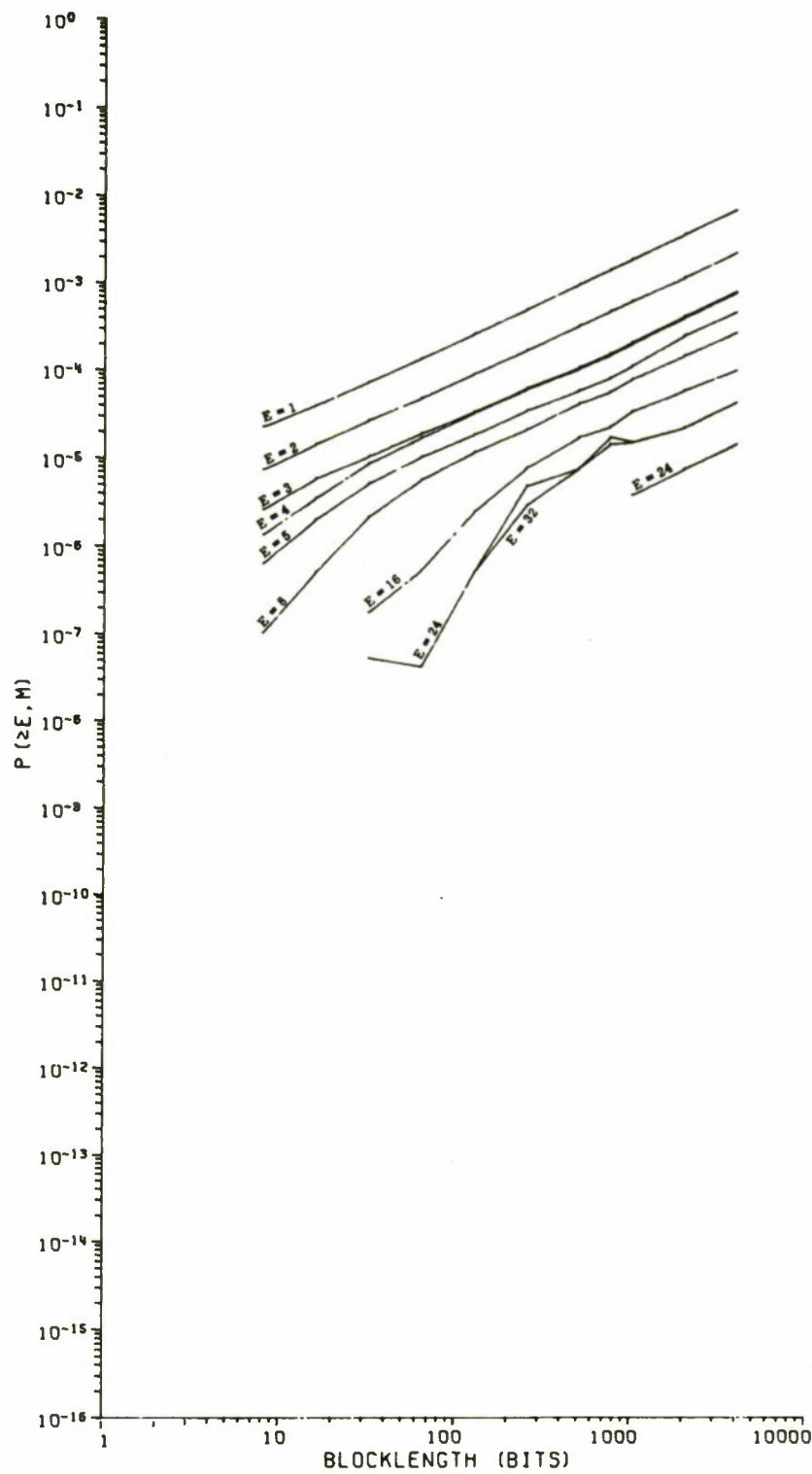


Figure 57. Probability of at Least E Errors in an M Bit Block — Loop on 2 Trunks/4800 b/s

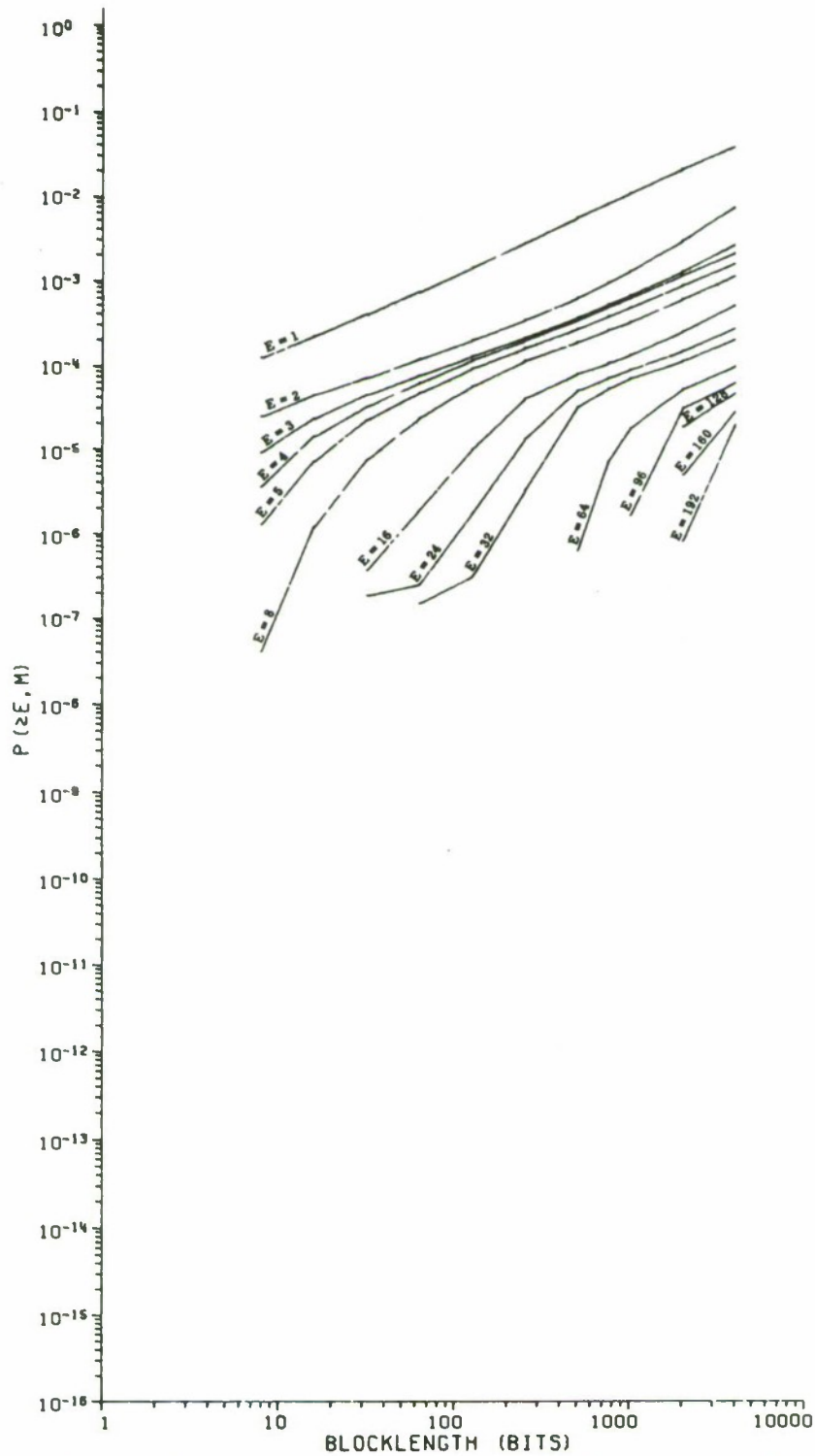


Figure 58. Probability of at Least E Errors in an M Bit Block — Loop on 4 Trunks/4800 b/s

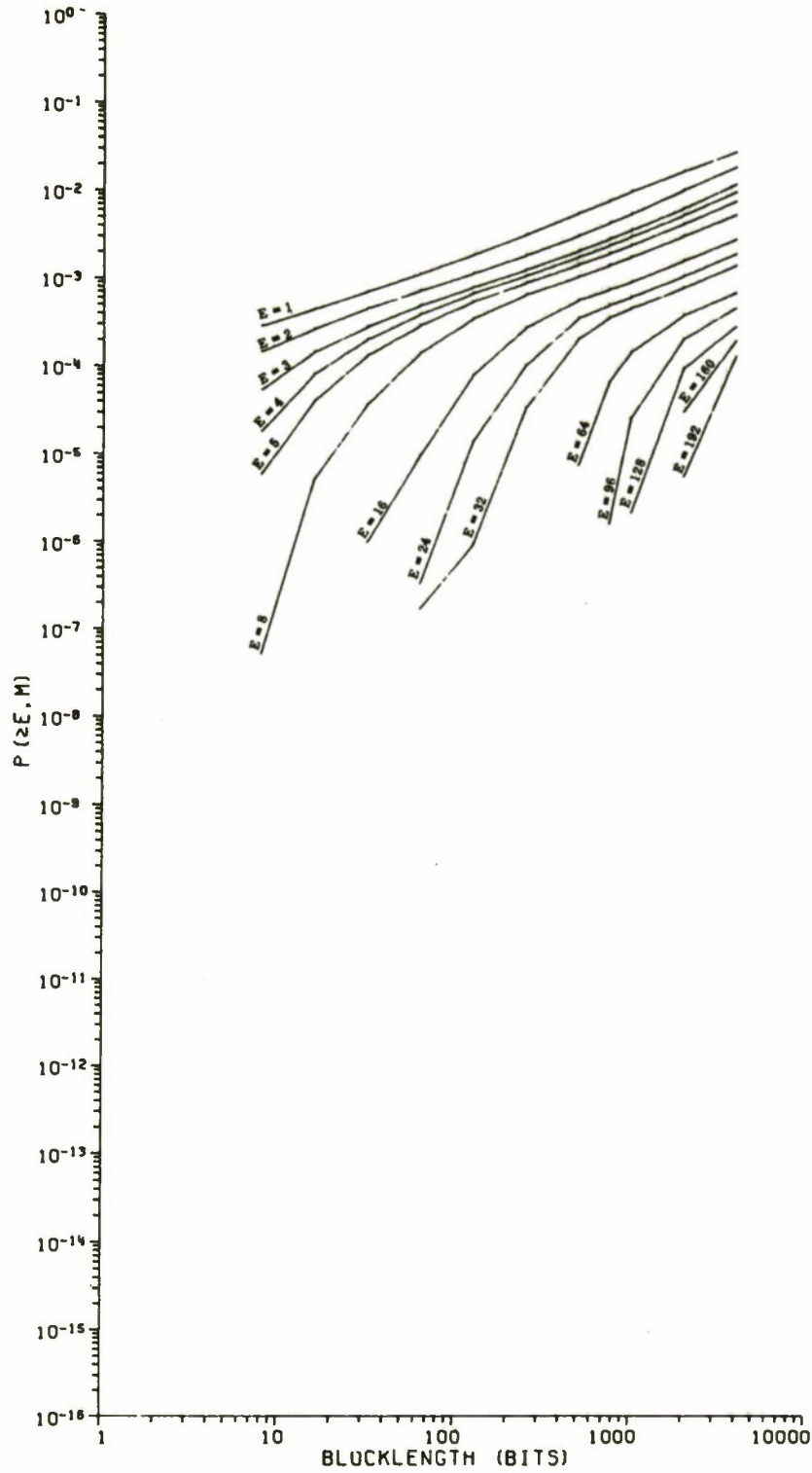


Figure 59. Probability of at Least E Errors in an M Bit Block — Loop on 5 or More Trunks/4800 b/s

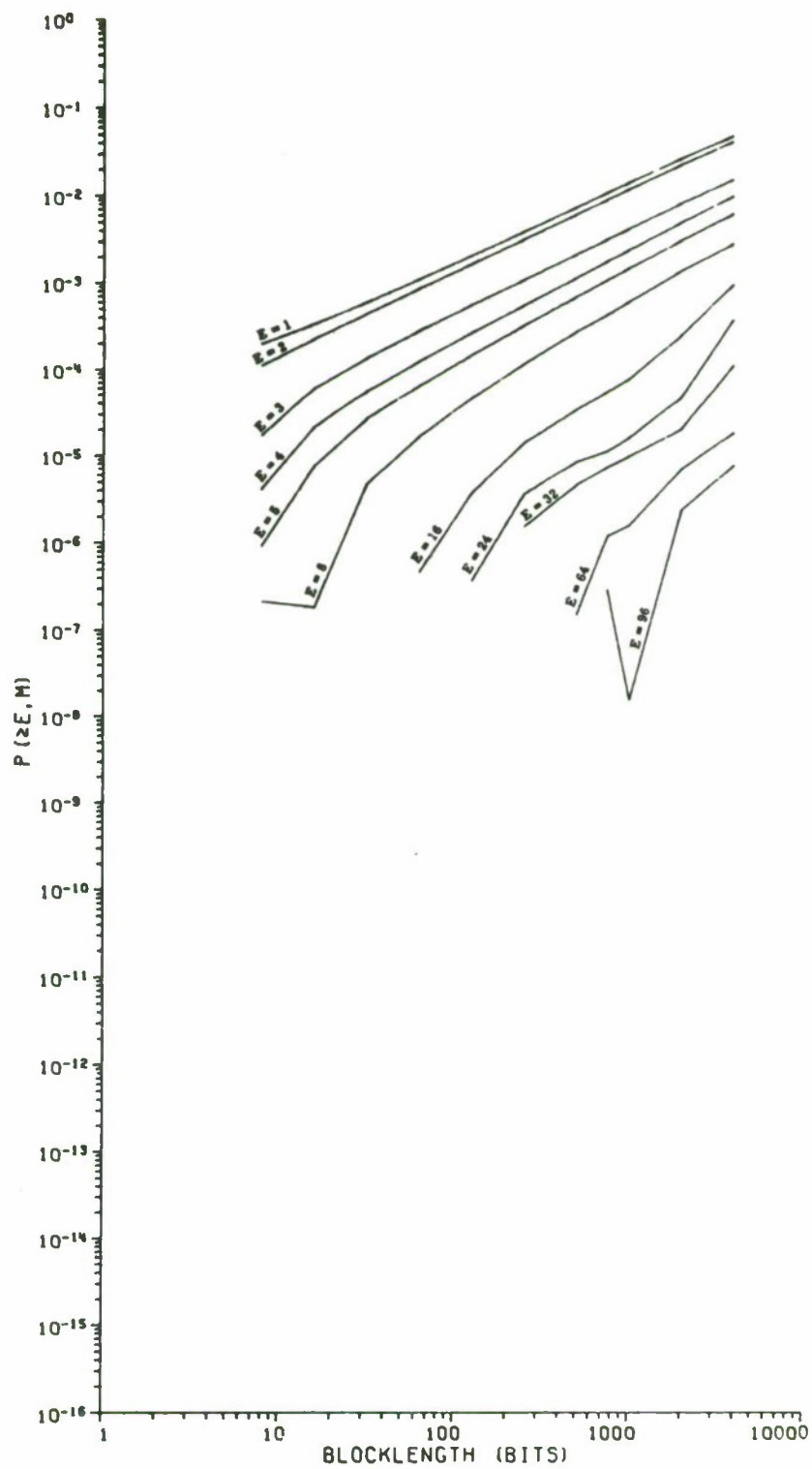


Figure 60. Probability of at Least E Errors in an M Bit Block — Loop on 2 Trunks/9600 b/s

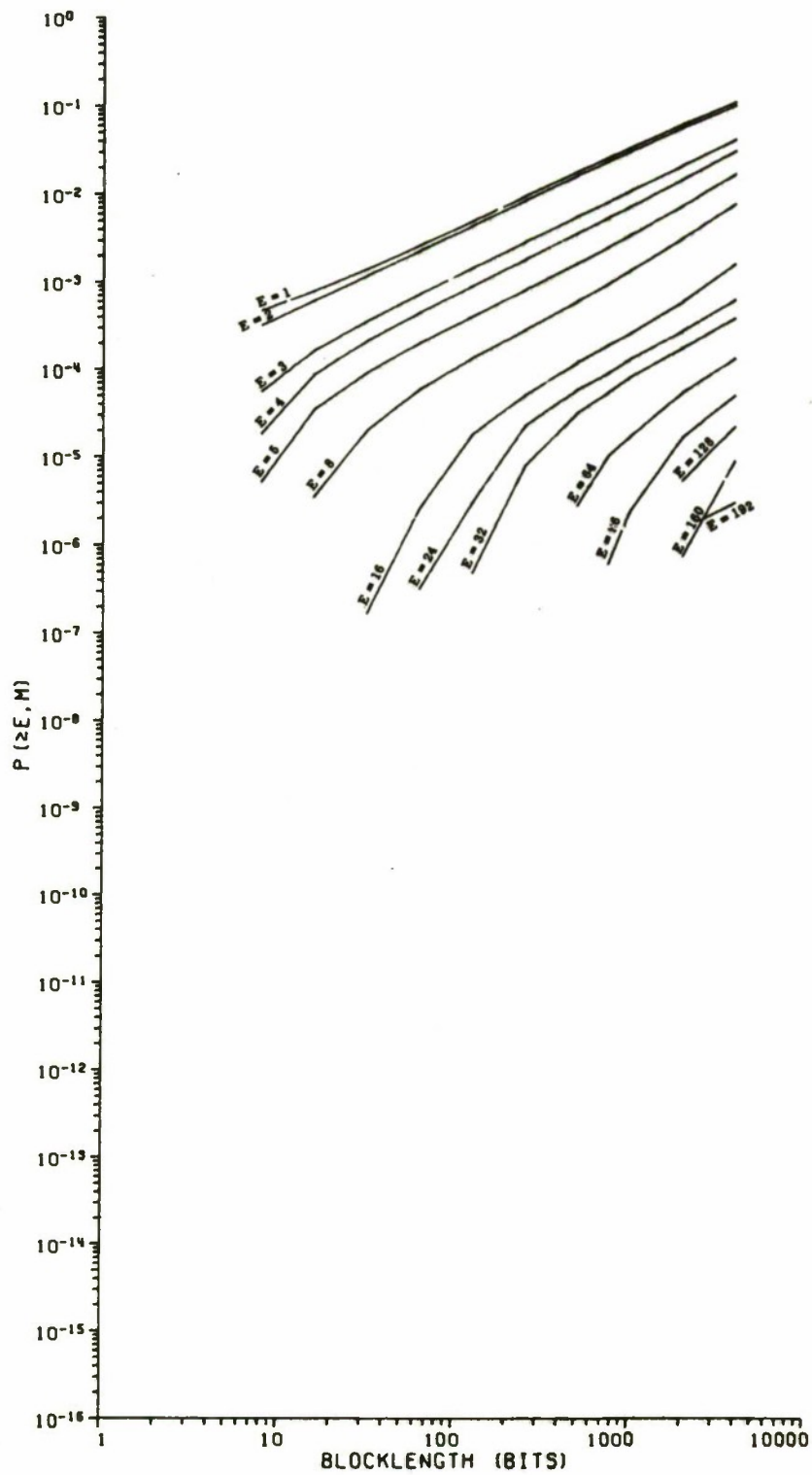


Figure 61. Probability of at Least E Errors in an M Bit Block — Loop on 4 Trunks/9600 b/s

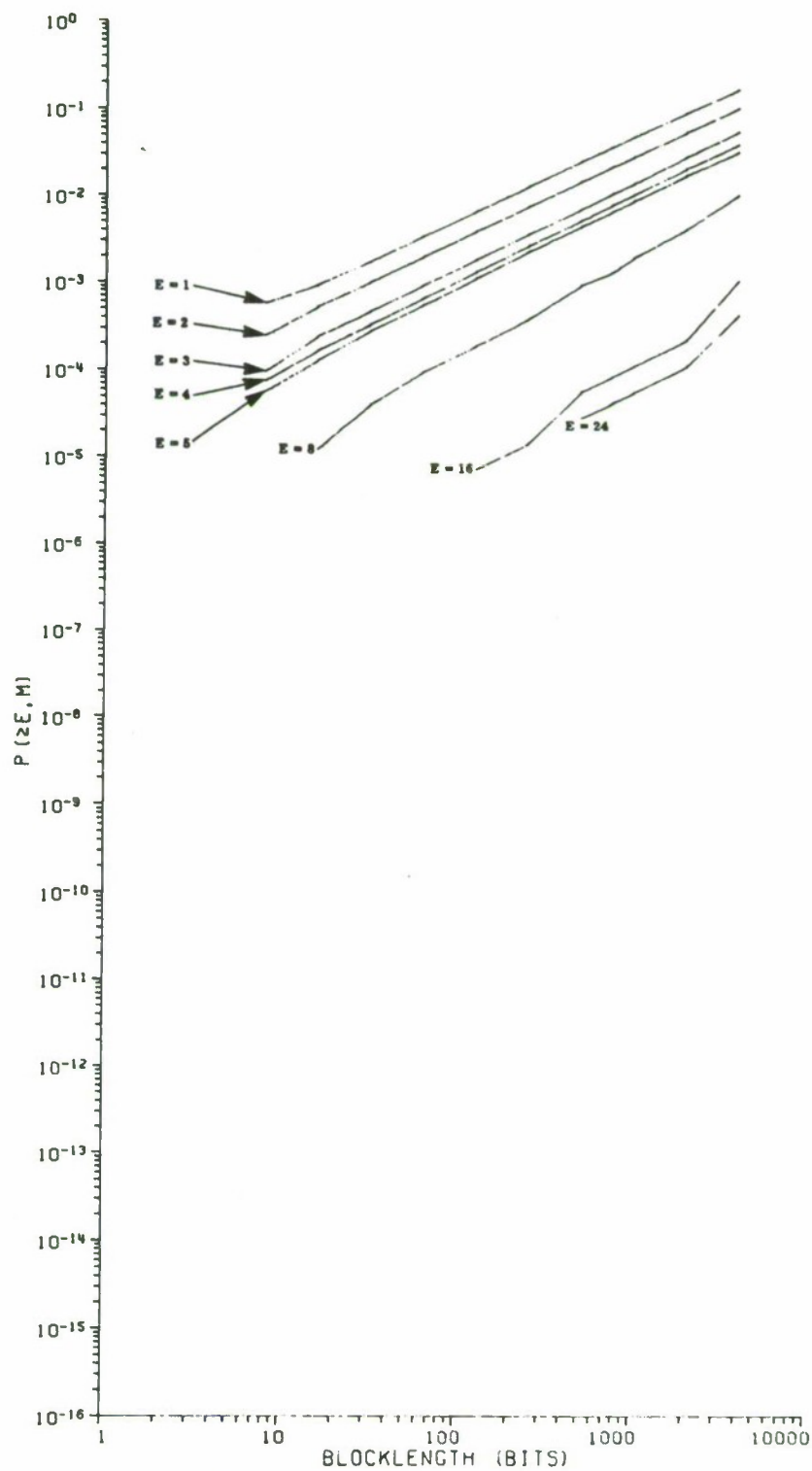


Figure 62. Probability of at Least E Errors in an M Bit Block — Loop on 6 Trunks/9600 b/s

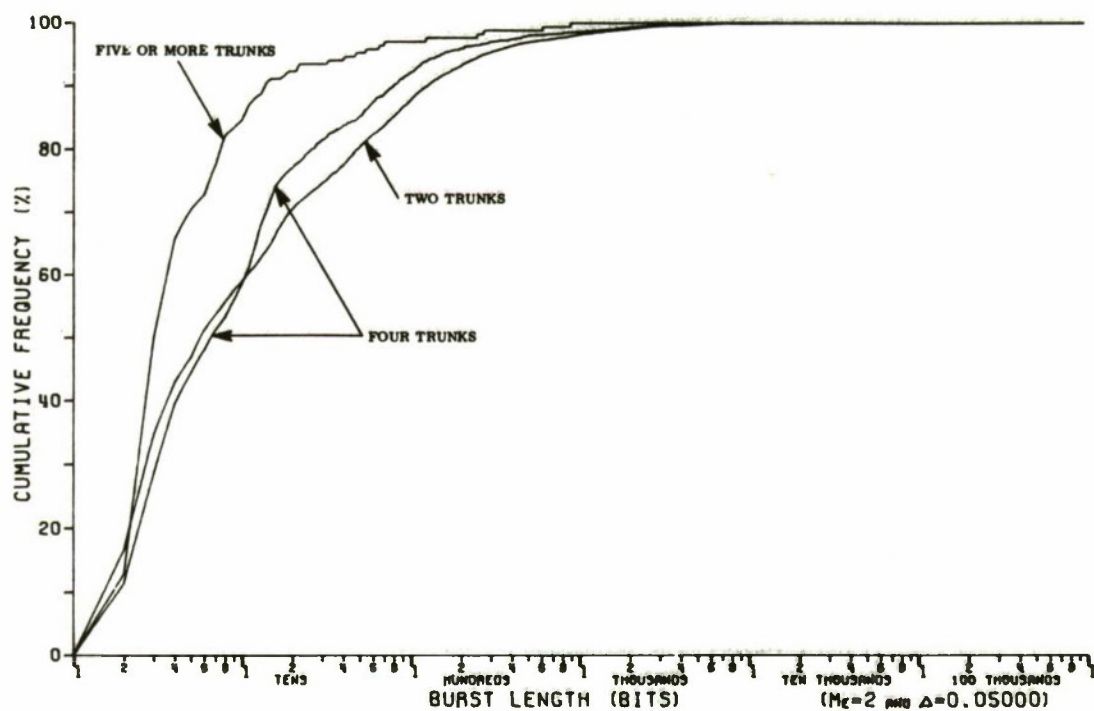


Figure 63. Cumulative Distribution on Lengths of Bursts — 4800 b/s Data

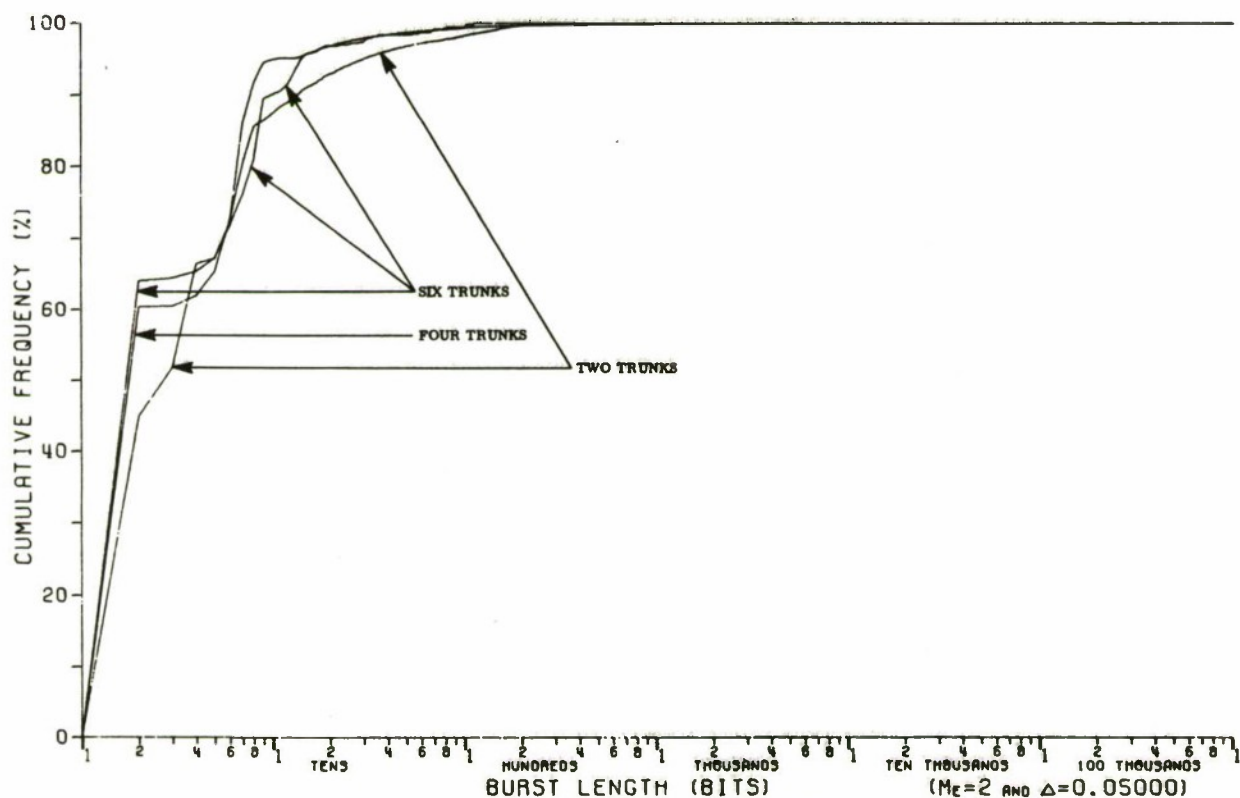


Figure 64. Cumulative Distribution on Lengths of Bursts — 9600 b/s Data

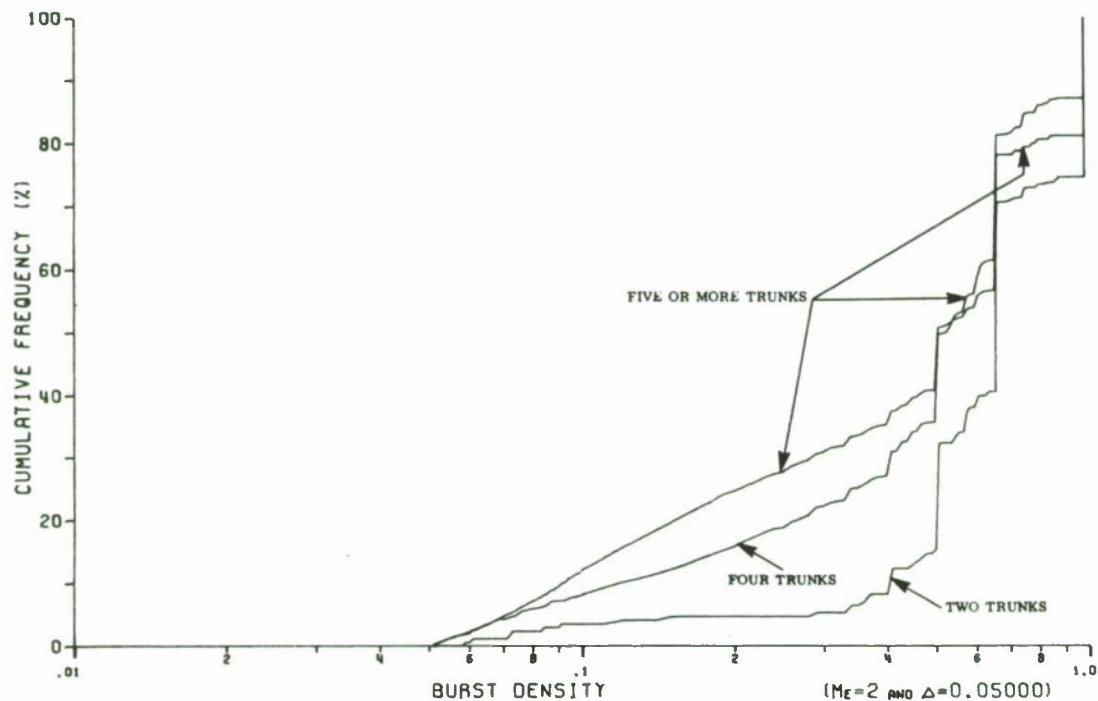


Figure 65. Cumulative Distribution on Burst Densities — 4800 b/s Data

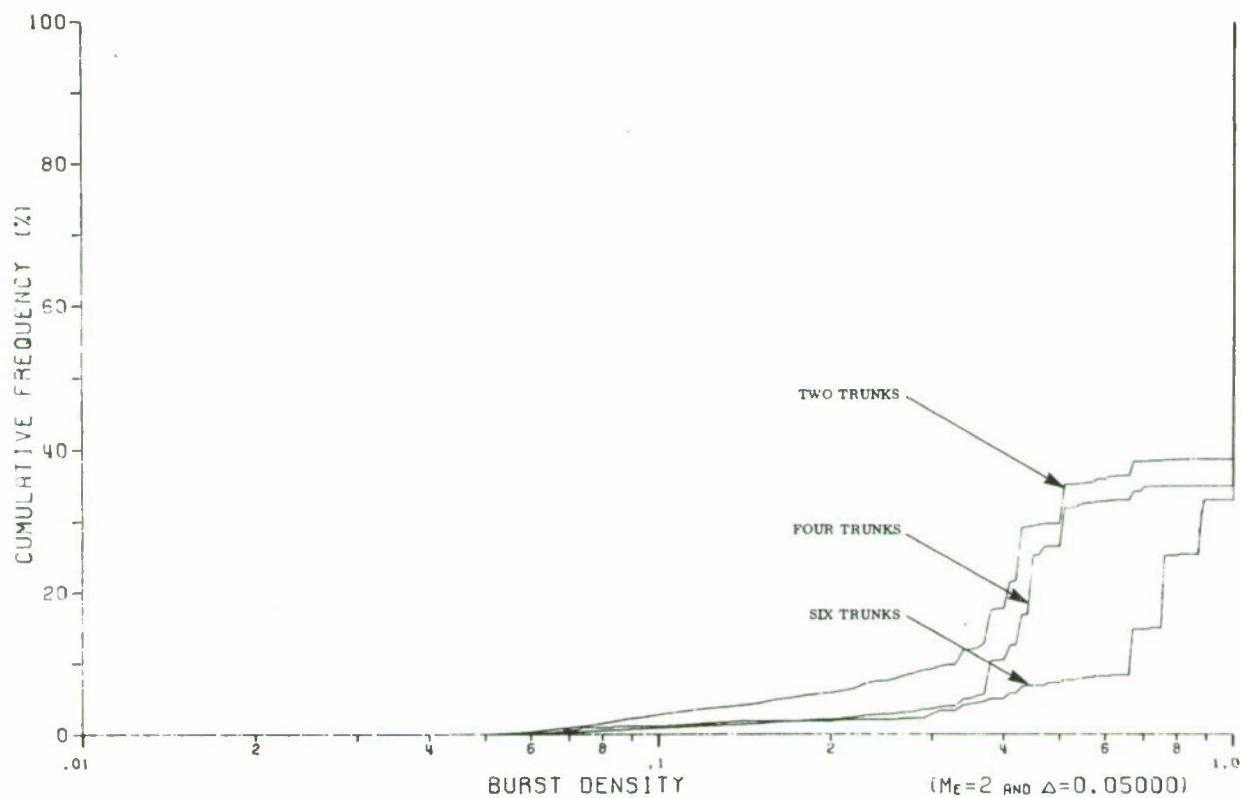


Figure 66. Cumulative Distribution on Burst Densities — 9600 b/s Data

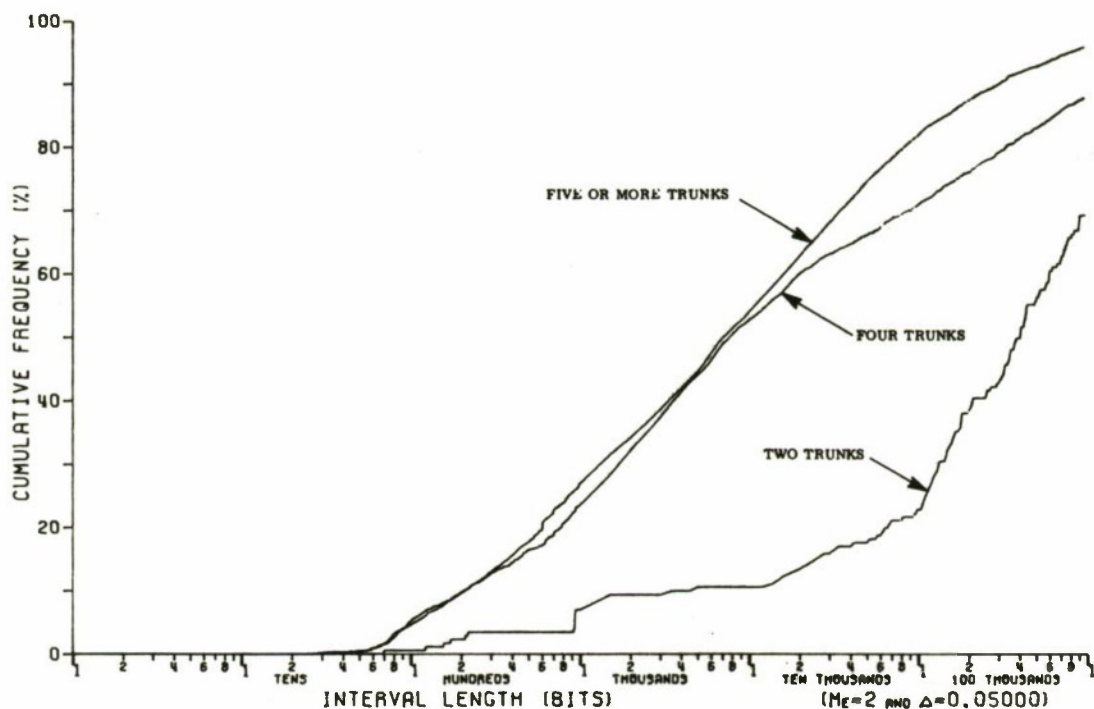


Figure 67. Cumulative Distribution on Lengths of Intervals — 4800 b/s Data

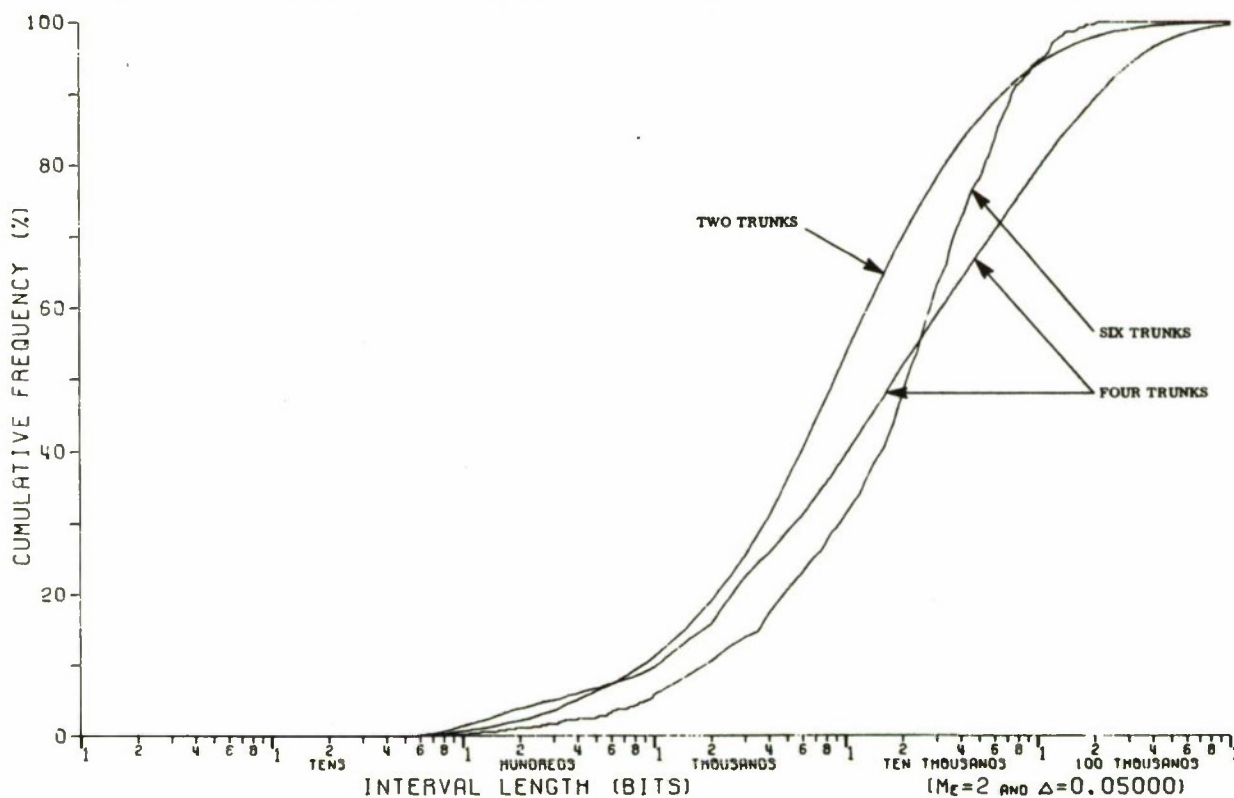


Figure 68. Cumulative Distribution on Lengths of Intervals — 9600 b/s Data

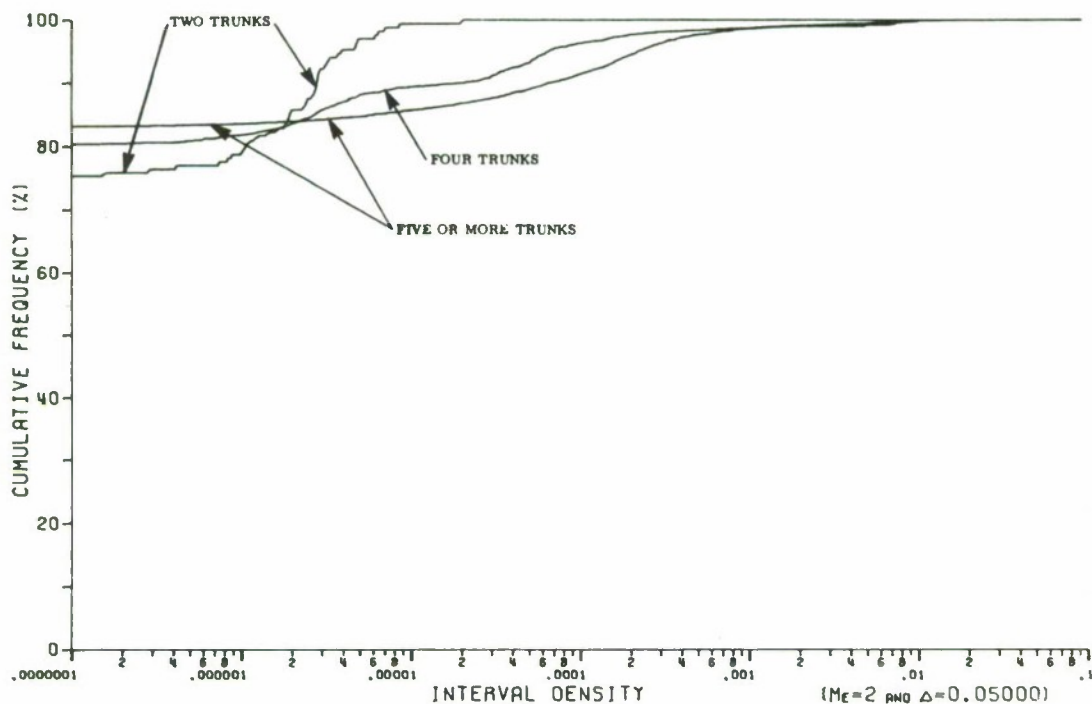


Figure 69. Cumulative Distribution on Interval Densities — 4800 b/s Data

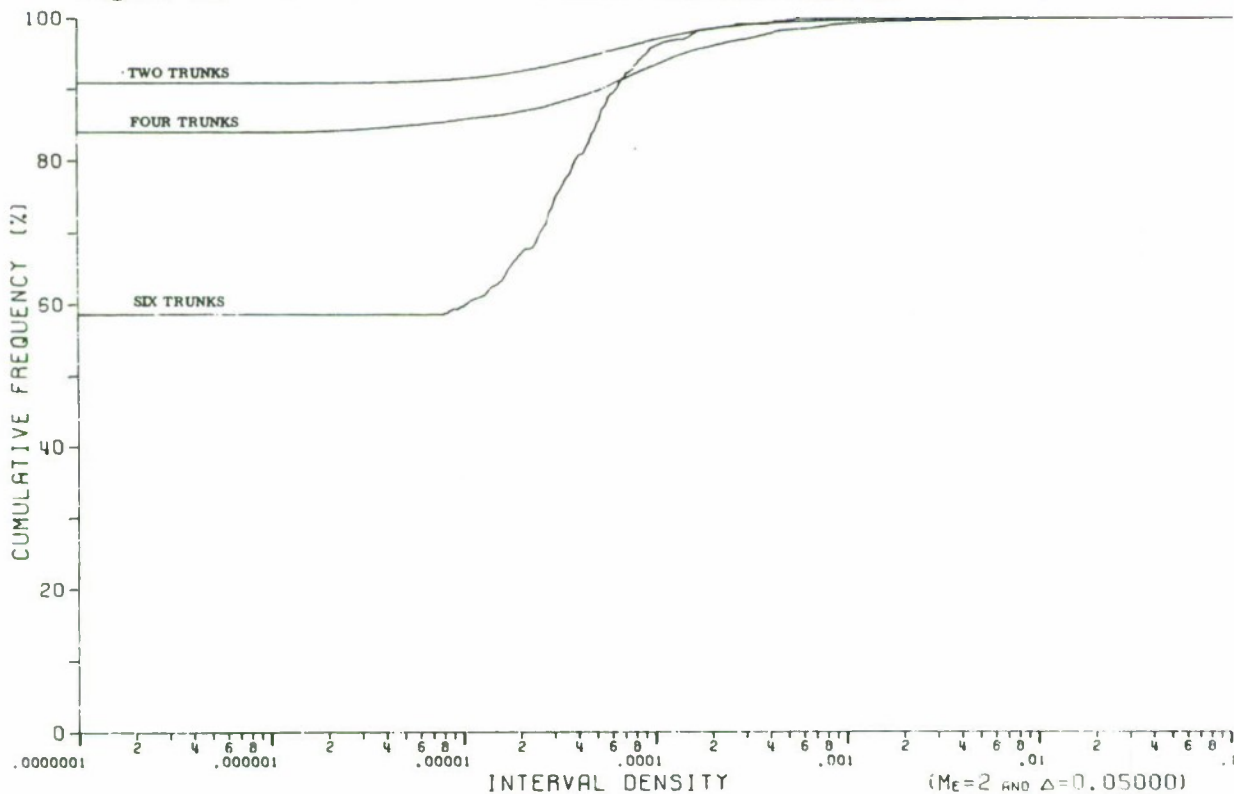


Figure 70. Cumulative Distribution on Interval Densities — 9600 b/s Data

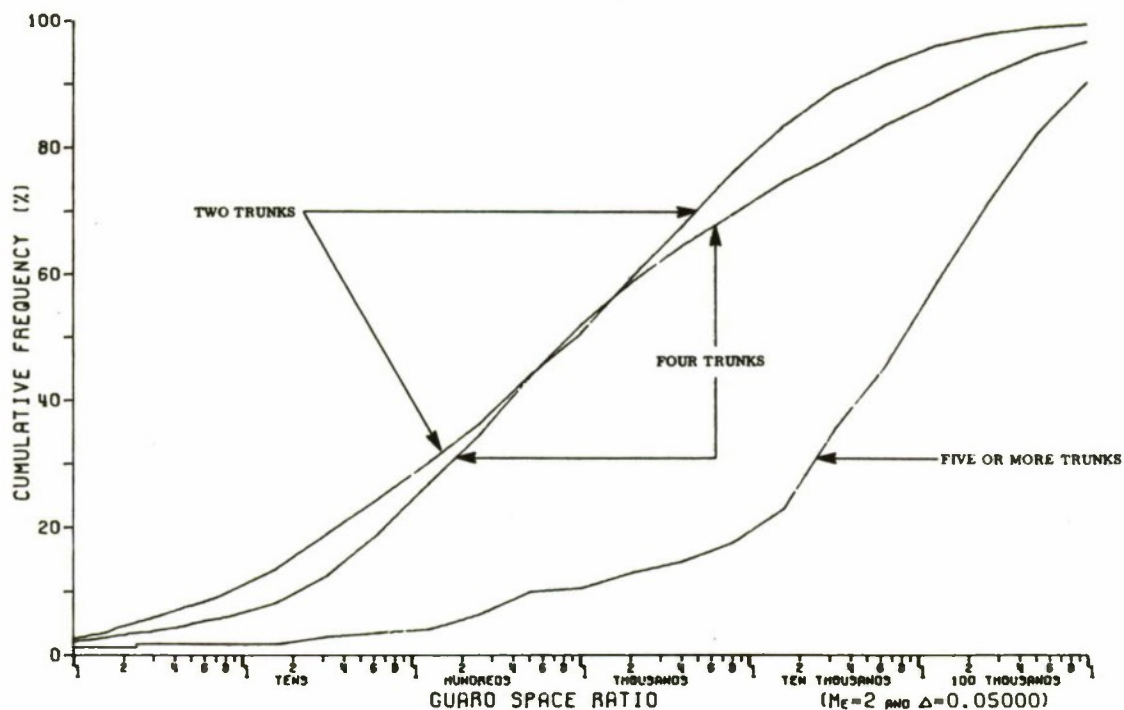


Figure 71. Interval to Burst Ratios — 4800 b/s Data

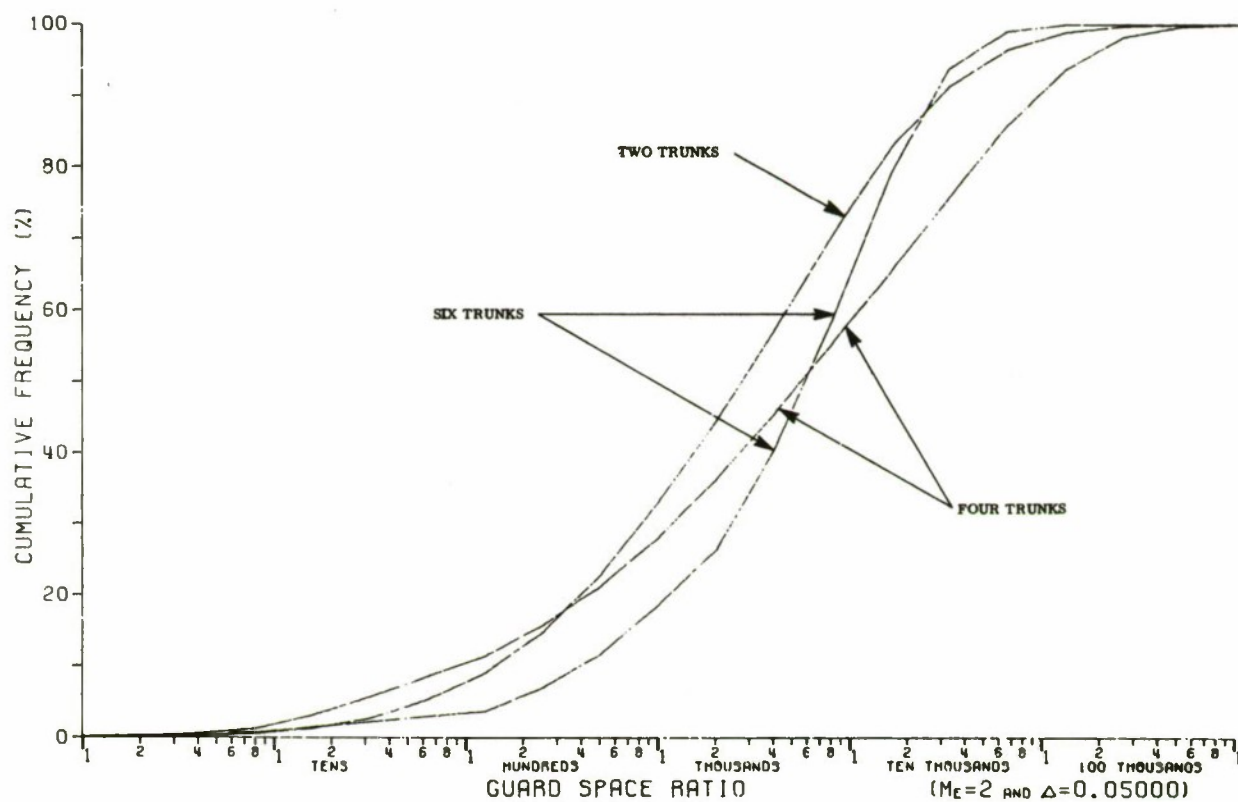


Figure 72. Interval to Burst Ratios — 9600 b/s Data

SECTION VI

CONCLUSIONS

The objective of this paper has been to examine the characteristics of the error patterns that occur in digital data transmission at 4800 b/s and 9600 b/s on the AUTOVON telephone network.

At 4800 b/s, the error patterns are generally random on simple circuits with few switches, over short distances, on a few trunks. As the number of switches are increased from one to four, the burstiness of the data increases. Similarly, as the circuit distance exceeds 3,000 miles or more than four trunks are incorporated, the burstiness increases.

At 9600 b/s, the error patterns are a complicated combination of bursts and random errors for the full range of switches, miles, or trunks. This leads to the possible conclusion that while 4800 b/s data transmission is most likely circuit limited, 9600 b/s data transmission, at least with the Codex 9600 modem, is modem limited.

APPENDIX I

TULLY ACCESS LINE ERROR PATTERNS

All of the circuits tested were accessed from the Rome Air Development Center through the Tully, N.Y. AUTOVON switch. Since the tests were loop tests, the access line appeared twice in every tested circuit. It was felt that it would be of interest to evaluate the error patterns on the simple circuit from RADC to Tully and back. Most of the time this circuit was error-free; therefore, it was difficult to obtain error pattern data on this circuit. The total data collected on the RADC to Tully circuit is indicated in Table VI. The error rate was an order of magnitude higher (10^{-5} versus 10^{-6}) at 9600 b/s than at 4800 b/s and one-half to one order of magnitude lower than on AUTOVON plus the access line. Generally, the errors occurred singly (Figure 73) and both circuits exhibited the error-free gap distribution typical of random errors set on a plateau of short bursts (Figure 74). The block error probabilities (Figure 75 and 76, $E = 1$) are one-half order of magnitude higher at 9600 b/s than at 4800 b/s. There are a few blocks with large numbers of errors on the access line and any code that detects or corrects errors on AUTOVON plus the access line will do the same on the access line alone.

Table VI
Data Summary - Tully Access Line

Data Rate	Total Bits	Total Errors	Bit Error Rate
4800 b/s	15, 294, 560	63	4.0 E-6
9600 b/s	96, 441, 088	2, 963	3.1 E-5

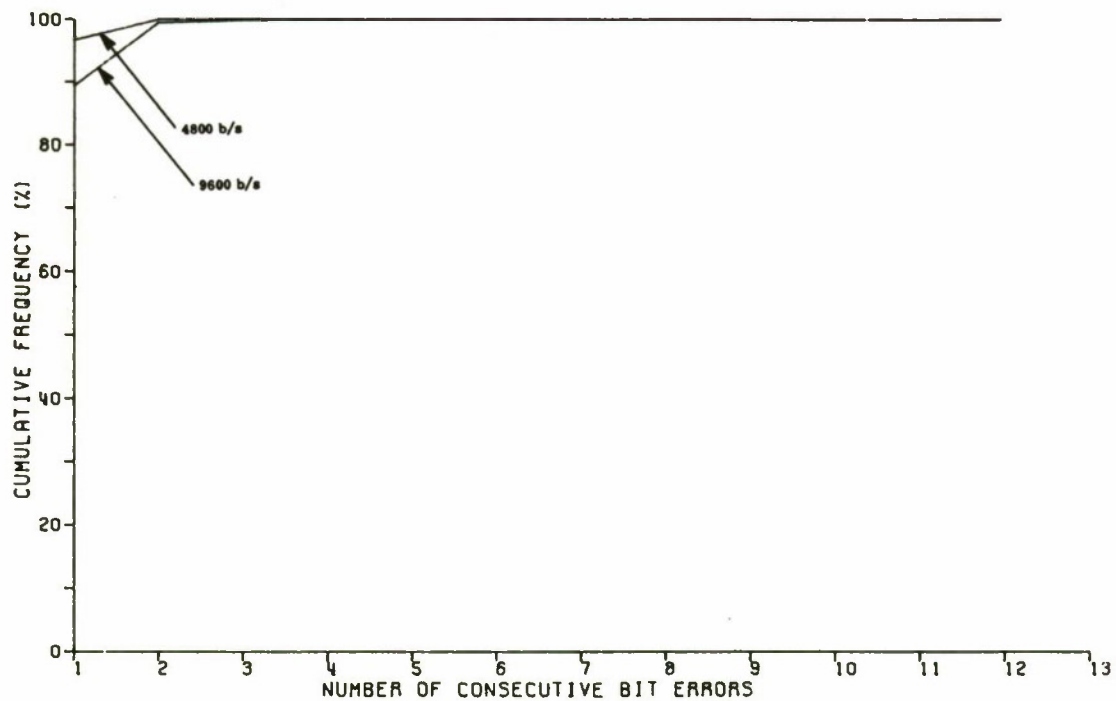


Figure 73. Cumulative Distribution of Consecutive Errors — DICEF to Tully Access Line

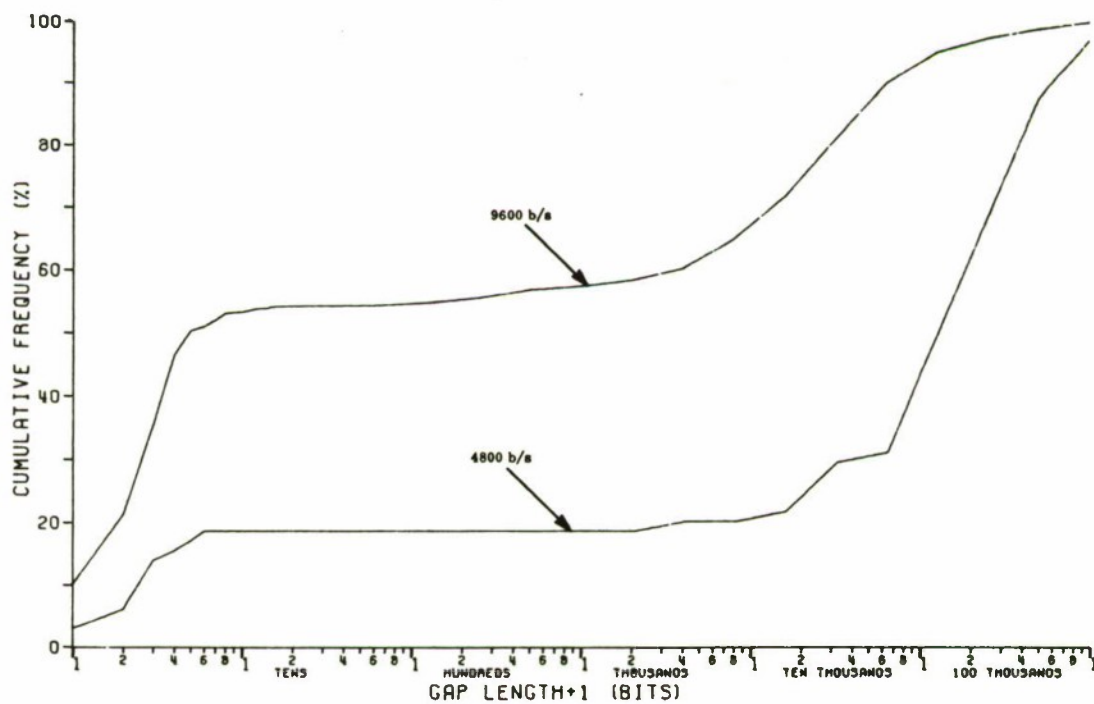


Figure 74. Cumulative Distribution of Error-Free Gaps — DICEF to Tully Access Line

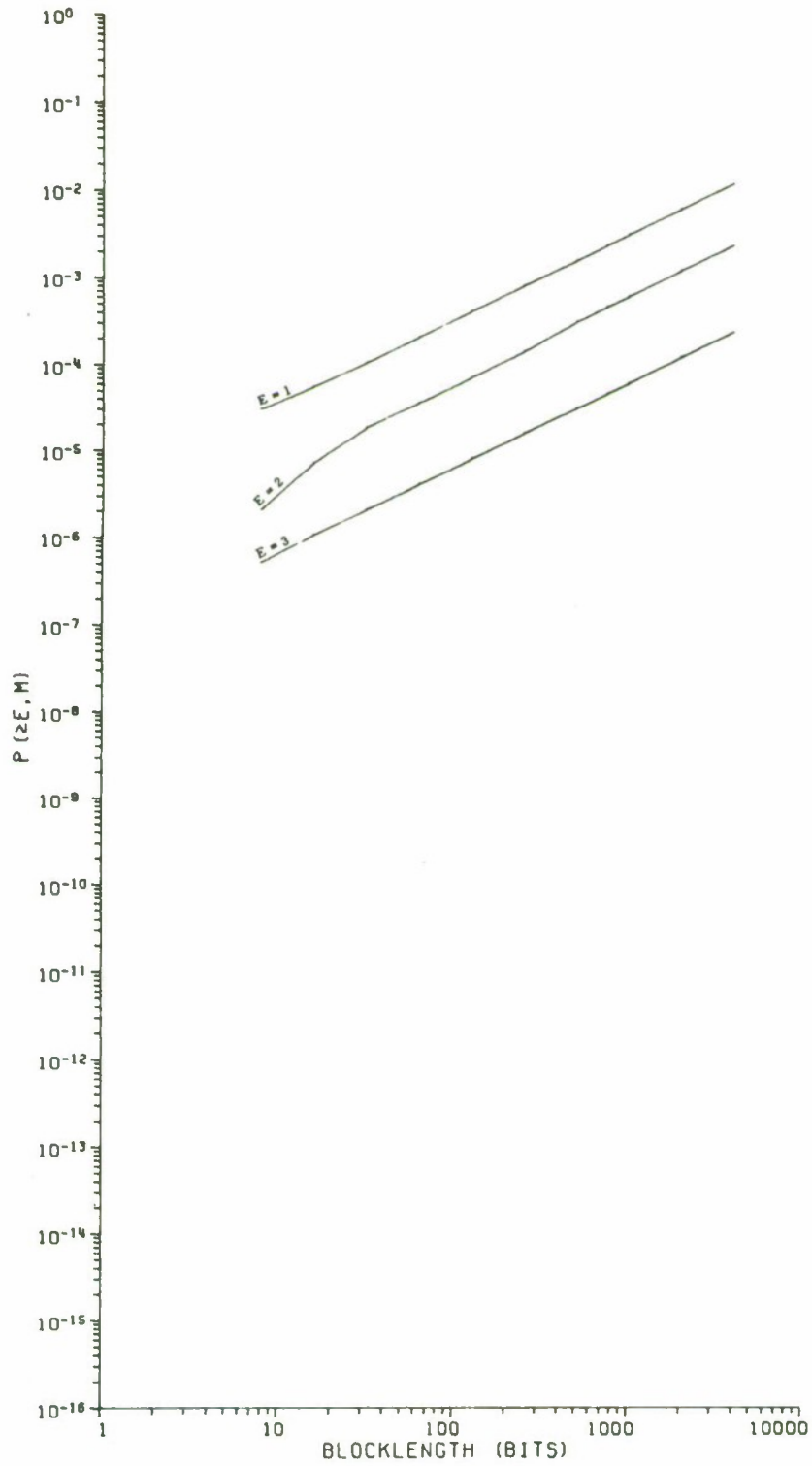


Figure 75. Probability of at Least E Errors in an M Bit Block — DICEF to Tully Access Line 4800 b/s

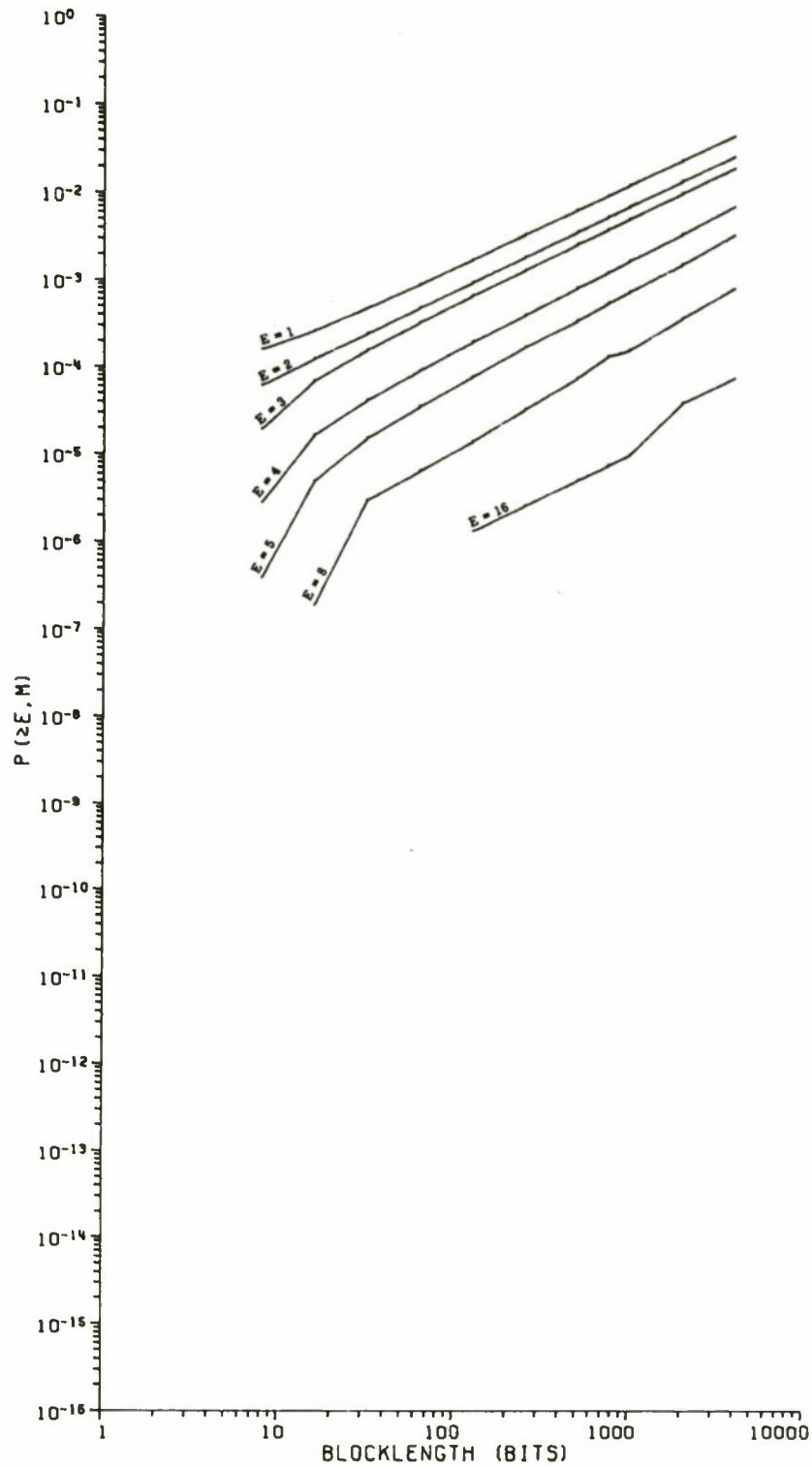


Figure 76. Probability of at Least E Errors in an M Bit Block — DICEF to Tully Access Line 9600 b/s

The distributions of bursts and burst densities (Figures 77 and 78) are the same at either data rate and show very short, dense bursts. The intervals between bursts are much longer at 4800 b/s than at 9600 b/s (Figure 79), but less than 10% are error-free at 4800 b/s as compared to almost 60% at 9600 b/s (Figure 80). Virtually all bursts are followed by long intervals (Figure 81).

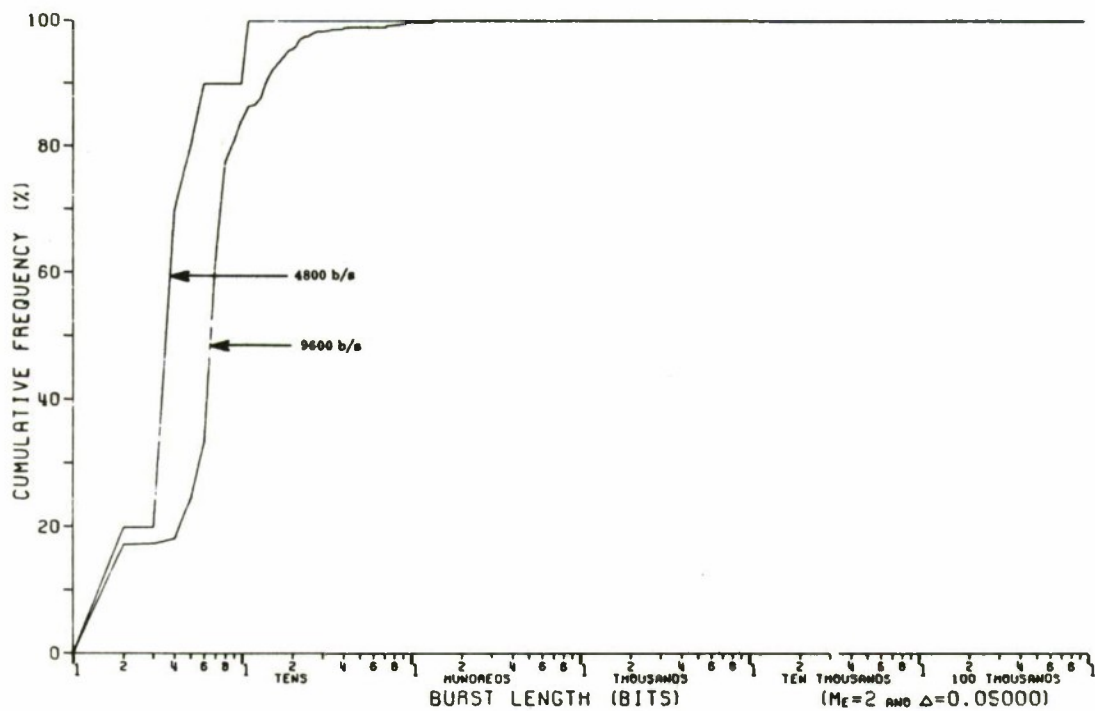


Figure 77. Cumulative Distribution on Lengths of Bursts — DICEF to Tully Access Line

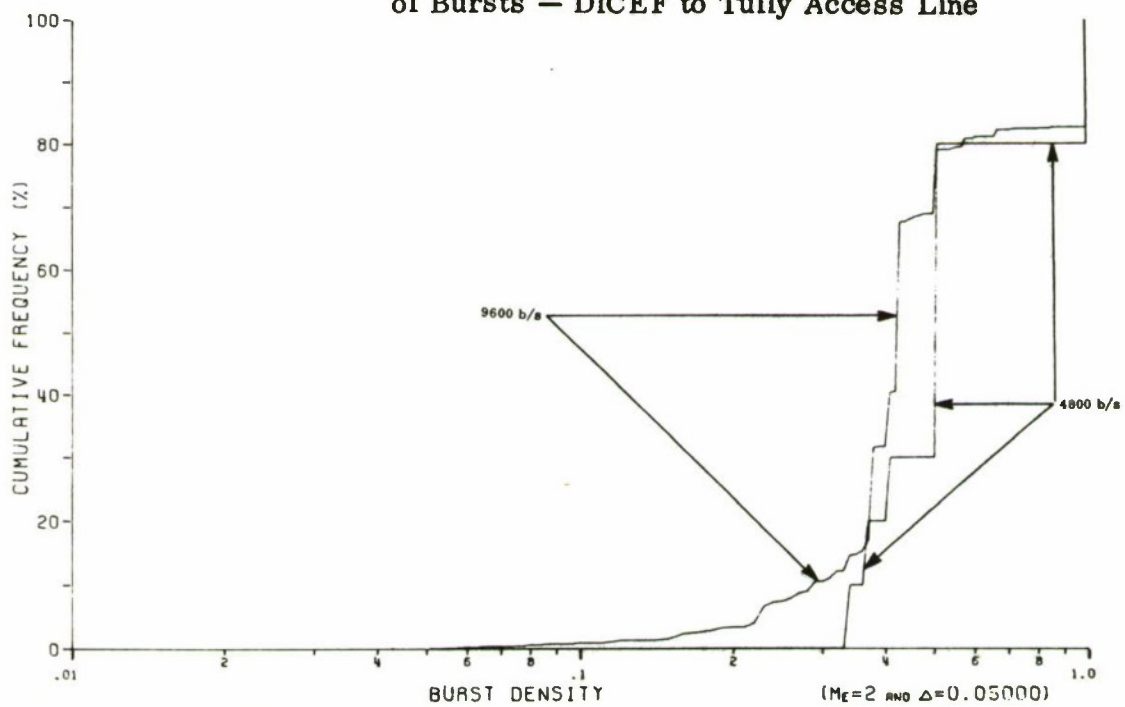


Figure 78. Cumulative Distribution on Burst Densities — DICEF to Tully Access Line

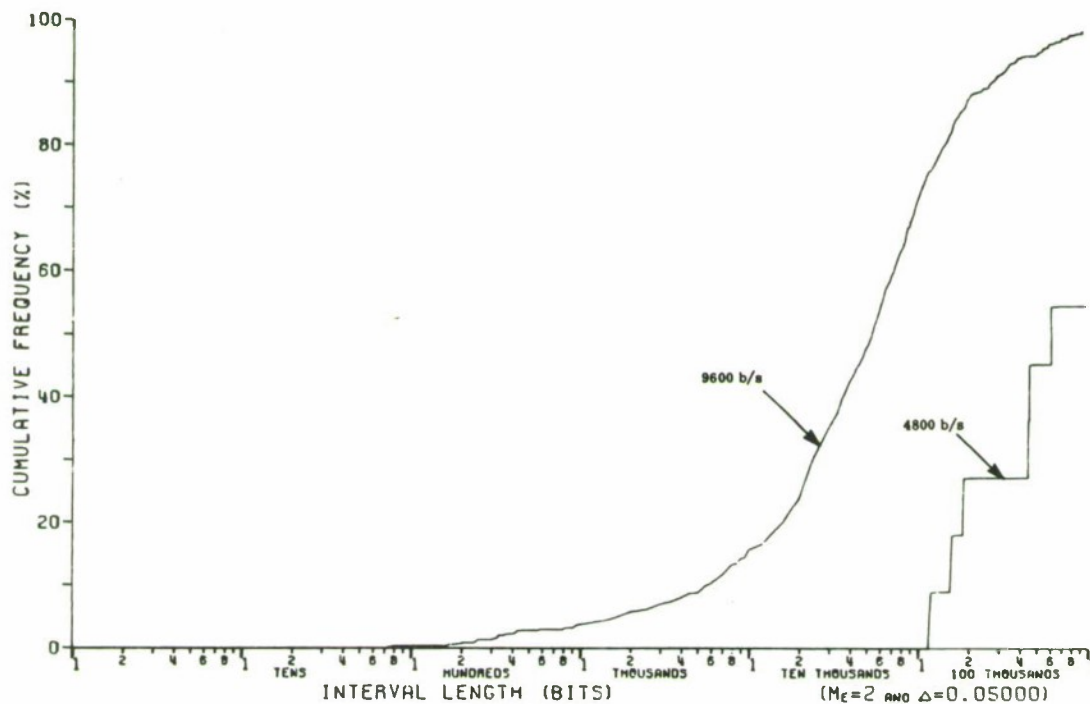


Figure 79. Cumulative Distribution on Lengths of Intervals — DICEF to Tully Access Line

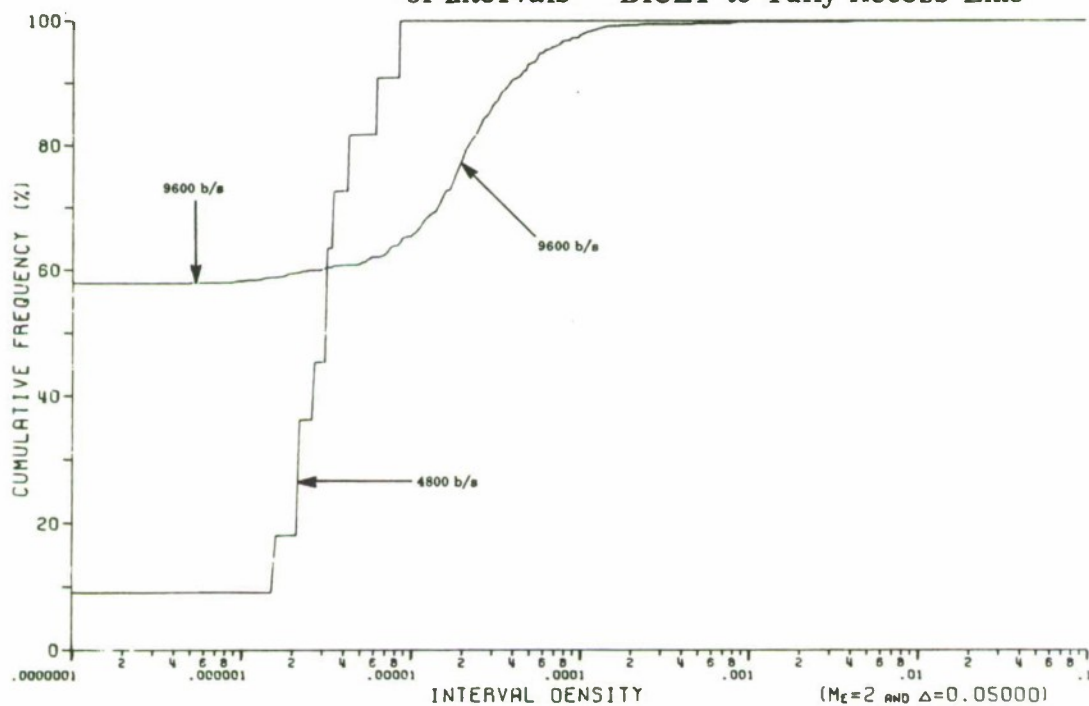


Figure 80. Cumulative Distribution on Interval Densities — DICEF to Tully Access Line

APPENDIX II

COMPARATIVE ERROR PATTERNS OF BELL AND CODEX MODEMS

In addition to the data collected with the Codex 9600 modem, RADC was able to obtain a limited sample of data with the BELL 208A modem* at 4800 b/s. This modem is designed for 4800 b/s synchronous operation on an unconditioned 4-wire 3002-type channel. The modem uses phase shift-keying and an adaptive equalizer with a 50 ms training time. The design objective of the modem is to provide a block error rate no higher than 10^{-2} for a 1000 bit block^[5]. In this appendix, the error patterns of the two modems shall be compared. The data sample, while limited, is similar in magnitude to some of the circuit configurations collected with the Codex modem and should, therefore, be as significant as that data. As is evidenced in Table VII, the error rate of the BELL modem is slightly less than that of the Codex modem. Analysis shall be by circuit and only circuit-independent conclusions, if any, shall be drawn.

LOOP TO ARLINGTON, VIRGINIA

As can be determined from the consecutive error distributions (Figure 82) and the error-free gap distributions (Figure 83), the errors themselves appear more random with the Codex modem than with the BELL. There are fewer occurrences of consecutive errors, and the error-free gap distribution has a greater appearance of randomness with the Codex modem. This is an interesting case since it is somewhat deceiving. On examination of the burst distributions (Figure 84), it can be seen that when all data is forced to be in either a burst or an interval, the Codex data is constructed of short bursts (under 100 bits), while the BELL data is

* Referred to within the Bell System as the Data Set 208A. ^[5]

Table VII
Data Summary - BELL Modem vs. Codex Modem

Connectivity	Data Rate	Total Bits	Total Errors	Bit Error Rate
Loop to Arlington, VA. BELL Modem	4800 b/s	52, 816, 209	929	1.8 E-5
Loop to Arlington, VA. Codex Modem	4800 b/s	653, 676, 879	20, 826	3.2 E-5
Loop to Santa Rosa, CA. BELL Modem	4800 b/s	94, 399, 277	1, 184	1.3 E-5
Loop to Santa Rosa, CA. Codex Modem	4800 b/s	322, 684, 013	16, 167	5.0 E-5
Loop to Rockdale, GA. BELL Modem	4800 b/s	13, 466, 412	541	4.0 E-5
Loop to Rockdale, GA. Codex Modem	4800 b/s	945, 024, 659	65, 216	6.9 E-5

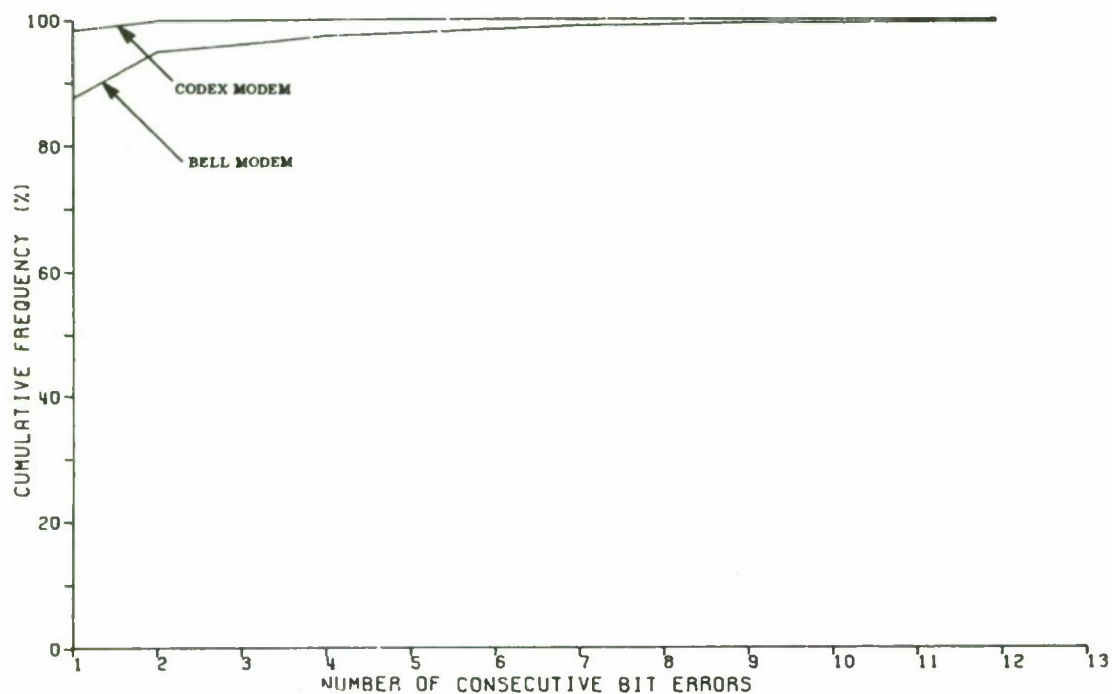


Figure 82. Cumulative Distribution of Consecutive Errors — Loop to Arlington 4800 b/s

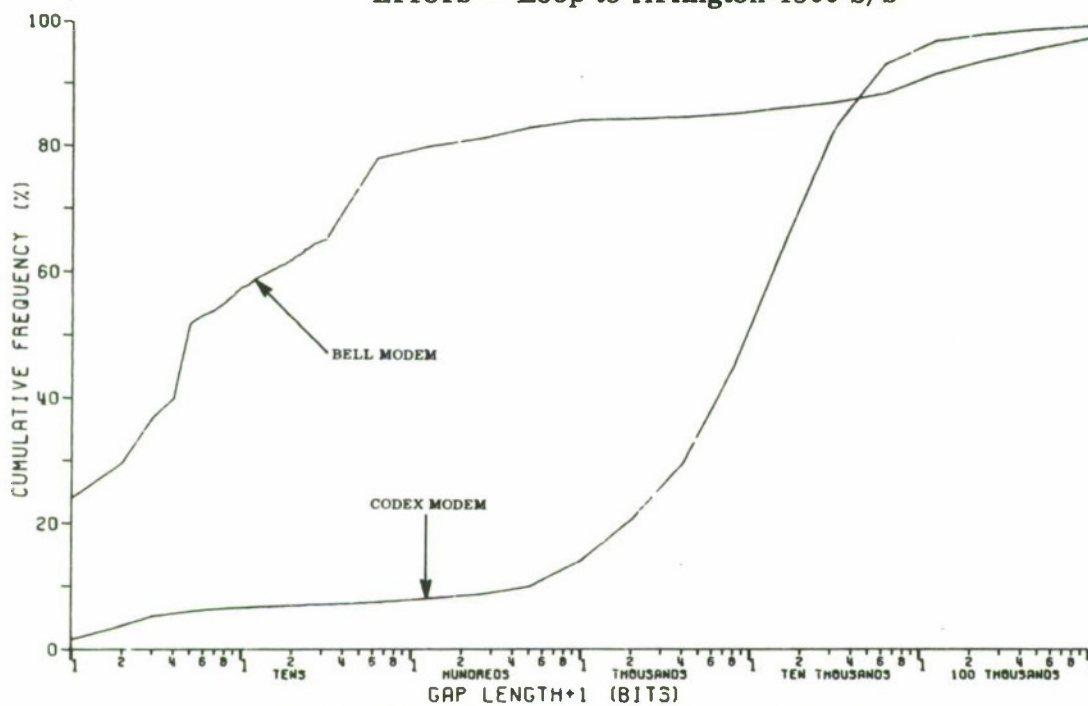


Figure 83. Cumulative Distribution of Error-Free Gaps — Loop to Arlington 4800 b/s

composed primarily of bursts in the 100 to 1,000 bit range. In both cases, the burst densities vary widely (Figure 85), and while a high percentage of the Codex bursts are very dense (over 70%), these are the short runs of consecutive errors. The remaining Codex bursts are low-density and, as a result, the earlier distributions (consecutive error and error-free gap) give the impression of randomness. In both cases, the bursts are separated by long intervals (Figure 86) containing similar densities of errors (Figure 87). The bursts are followed by longer intervals (Figure 88) with the Codex modem making these bursts better candidates for error detection and correction in systems employing interleaving or retransmission. This interval-to-burst ratio advantage is to be expected since the Codex modem bursts are very short. The probabilities of at least E errors in a block (Figures 89 and 90) are somewhat mixed. The block error-rate ($E = 1$) is higher for the Codex modem, but the probabilities of larger numbers of errors in a block are higher for the BELL modem. This is consistent with the high frequency of single errors in the Codex modem data and the block error-rate design objective of the BELL modem is satisfied.

LOOP TO SANTA ROSA, CALIFORNIA

The differences in the Codex and BELL data on the circuit to Santa Rosa, CA. are relatively slight. The Codex modem shows a slightly higher occurrence of double errors (Figure 91) and of short bursts (Figure 92). In Figure 92, neither modem shows any random error characteristic. Here again the error-free characteristic is not a precise gauge of burst length as evidenced in Figure 93. The BELL modem displays more bursts under 100 bits, while the Codex modem bursts are over 100 bits long. As on the Arlington, VA. circuit, the Codex bursts are denser (Figure 94) and

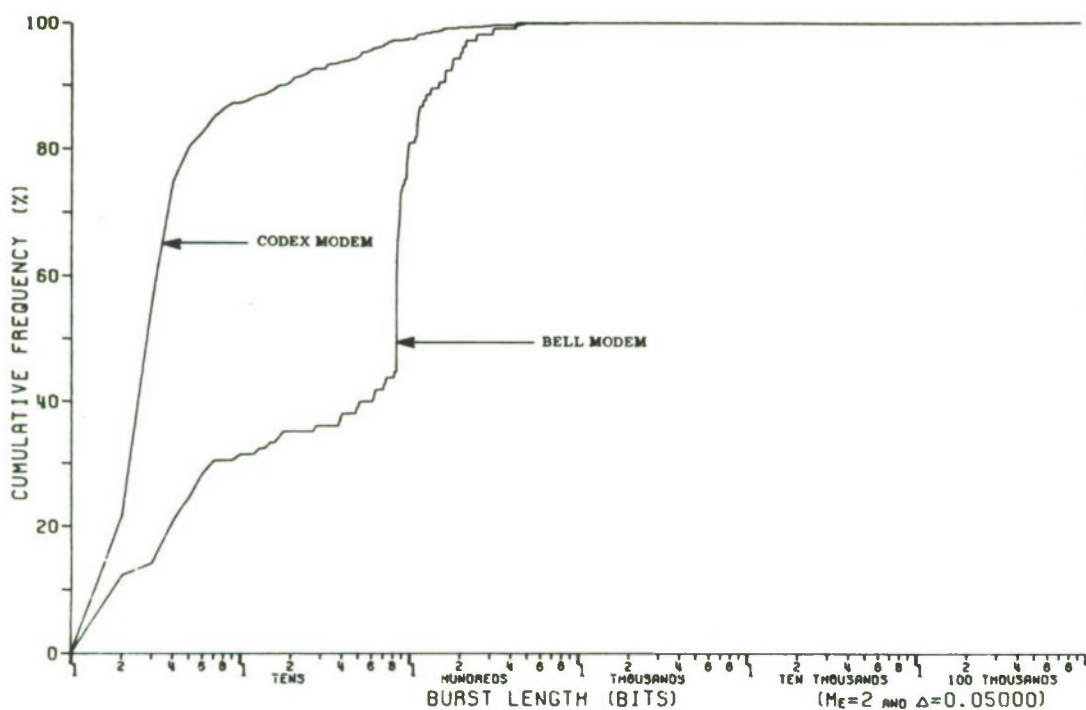


Figure 84. Cumulative Distribution on Lengths of Bursts — Loop to Arlington 4800 b/s

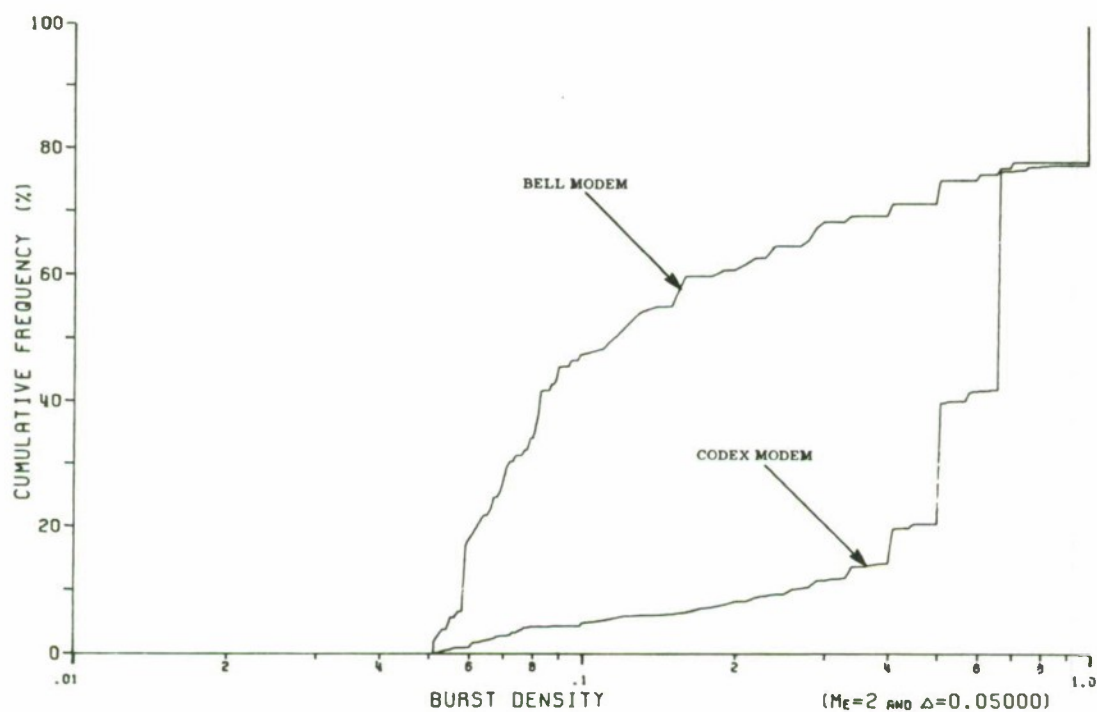


Figure 85. Cumulative Distribution on Burst Densities — Loop to Arlington 4800 b/s

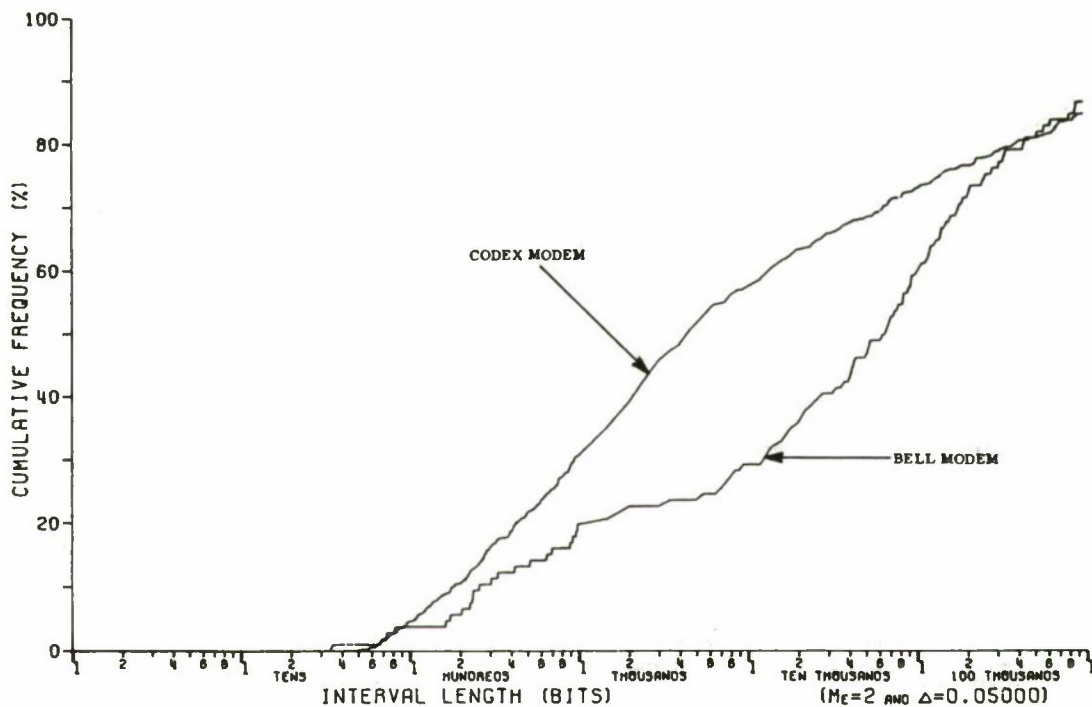


Figure 86. Cumulative Distribution on Lengths of Intervals — Loop to Arlington 4800 b/s

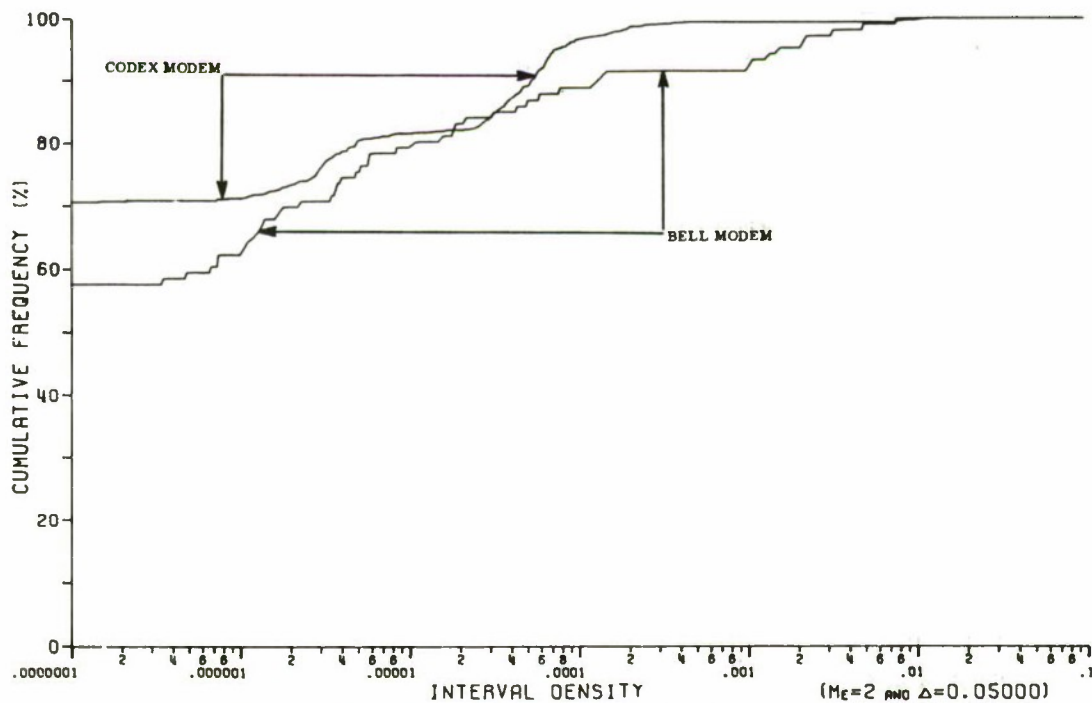


Figure 87. Cumulative Distribution on Interval Densities — Loop to Arlington 4800 b/s

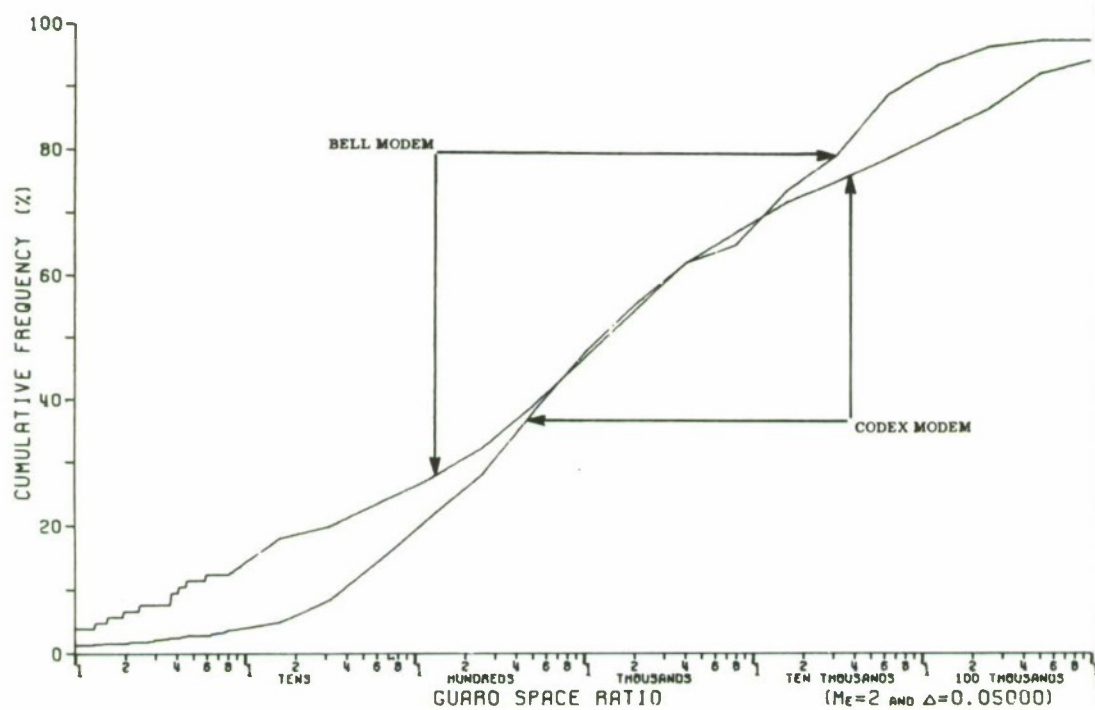


Figure 88. Interval to Burst Ratios — Loop to Arlington 4800 b/s

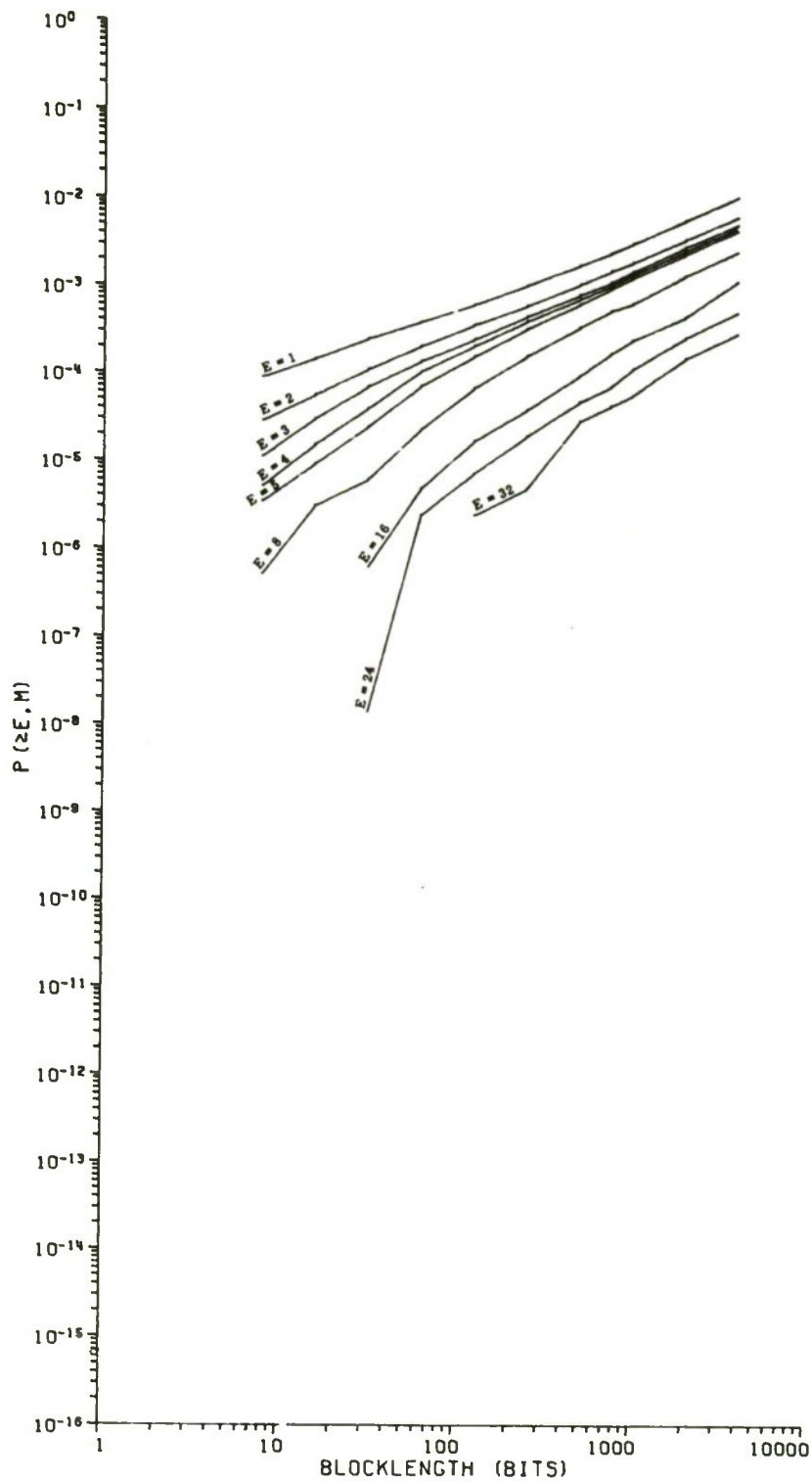


Figure 89. Probability of at Least E Errors in an M Bit Block — Loop to Arlington/Bell 4800 b/s

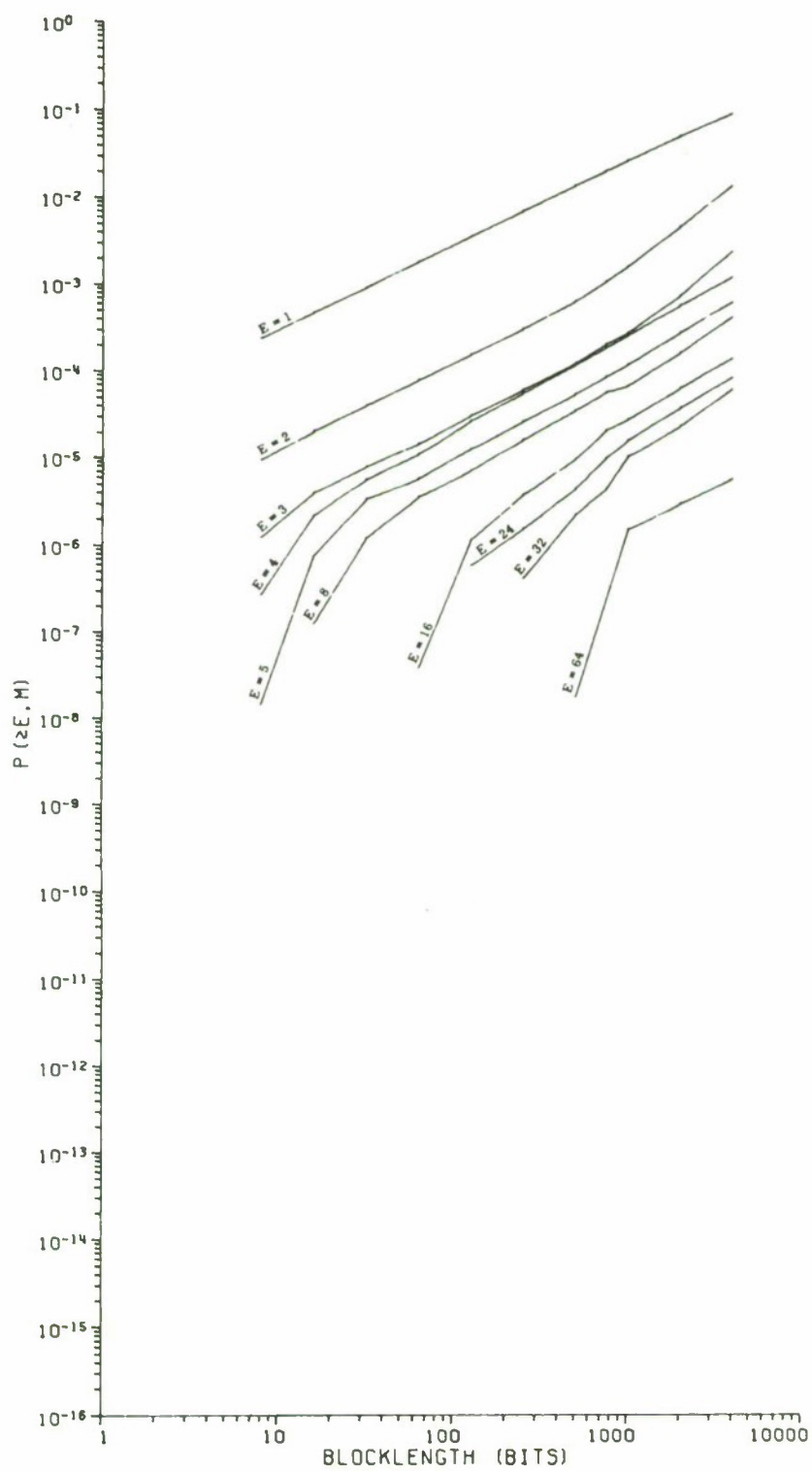


Figure 90. Probability of at Least E Errors in an M Bit Block — Loop to Arlington/Codex 4800 b/s

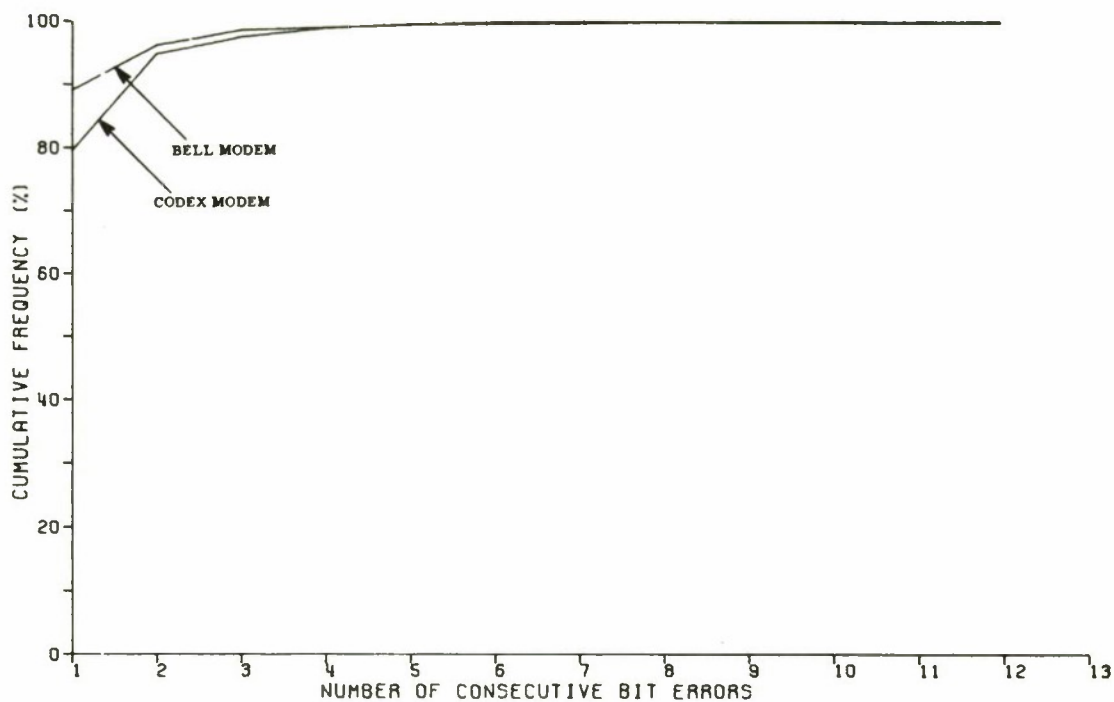


Figure 91. Cumulative Distribution of Consecutive Errors —
Loop to Santa Rosa 4800 b/s

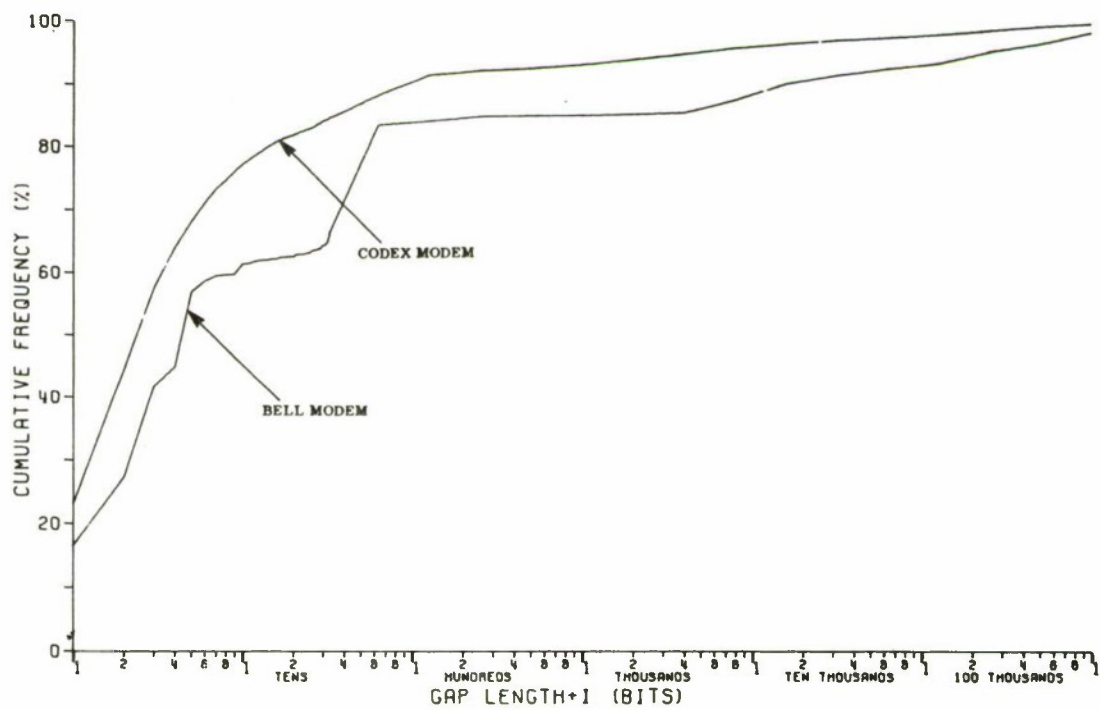


Figure 92. Cumulative Distribution of Error-Free Gaps —
Loop to Santa Rosa 4800 b/s

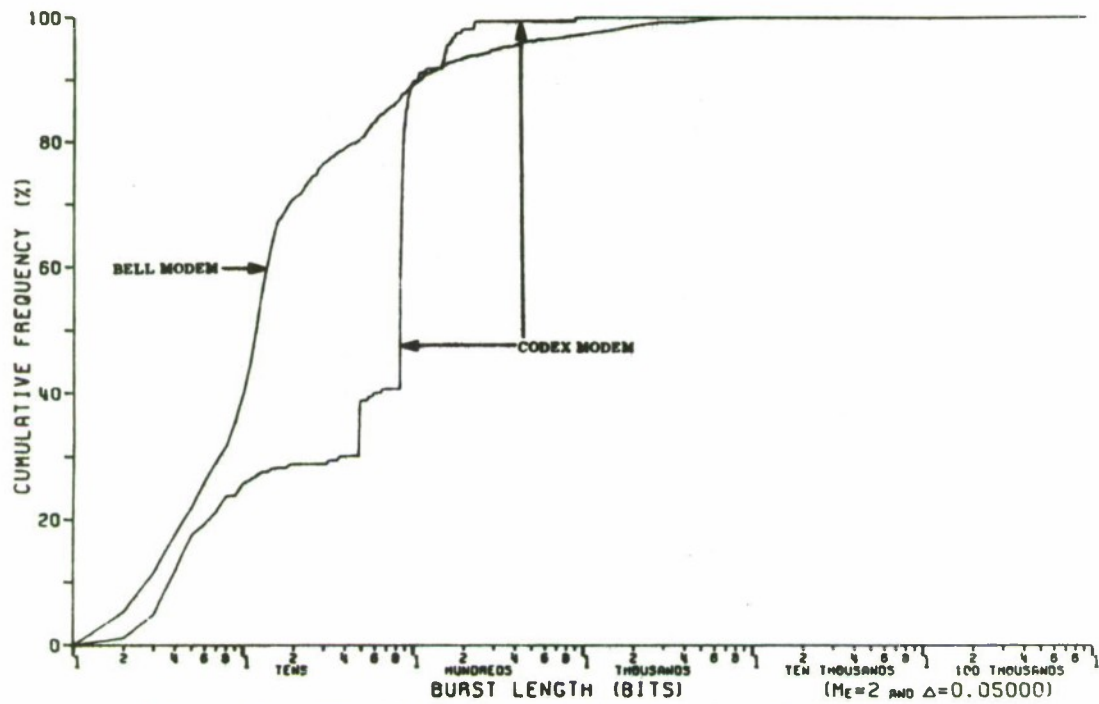


Figure 93. Cumulative Distribution on Lengths of Bursts —
Loop to Santa Rosa 4800 b/s

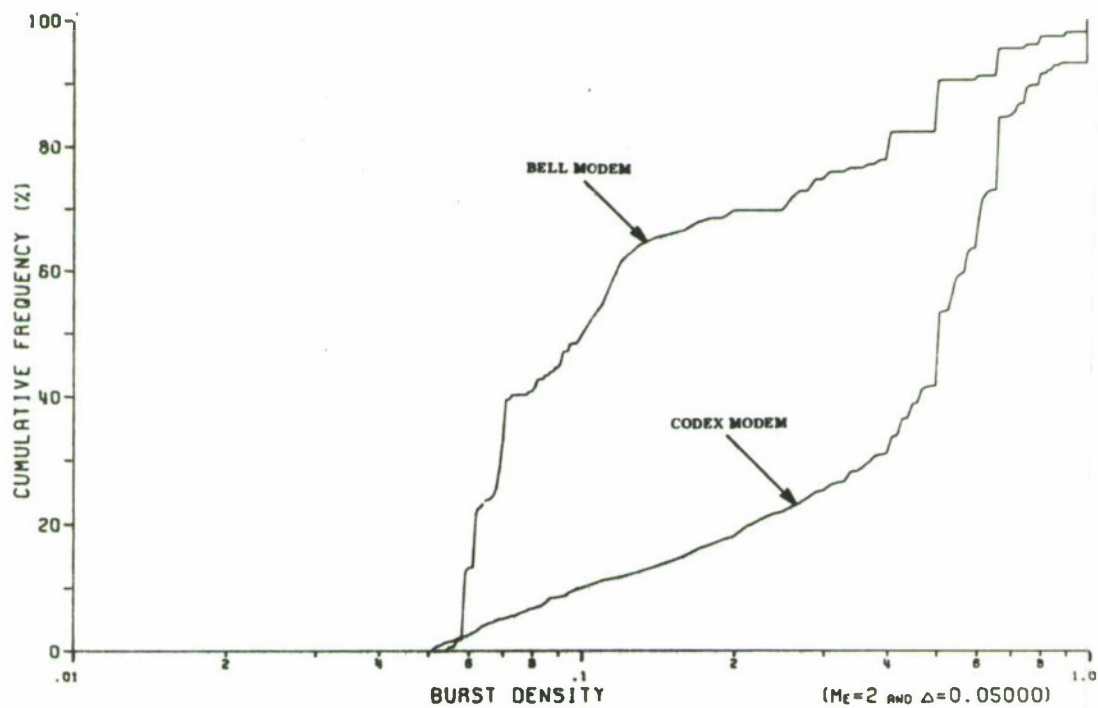


Figure 94. Cumulative Distribution on Burst Densities —
Loop to Santa Rosa 4800 b/s

the interval lengths (Figure 95) are larger for both modems with intervals of similar low density of errors (Figure 96). Both modems show a good distribution of long intervals following short bursts, although the Codex modem is somewhat poorer in this respect (Figure 97). The Codex modem exhibits higher probabilities of having large numbers of errors in a block for all block sizes (Figures 98 and 99), and the BELL modem meets its block error-rate design objective.

LOOP TO ROCKDALE, GEORGIA

The comparative data to Rockdale, GA. is essentially the same as that to Santa Rosa, CA. and is presented only for completeness (Figures 100 through 108). Any differences can probably be ascribed to the small amount of BELL data in this sample. This is the probable reason for the BELL modem slightly exceeding its block error-rate design objective.

CONCLUSIONS

Based on the relatively small sample of data, there seems to be little difference between the two modems in error distribution on the circuits considered. The only real differences are highlighted in Figures 109 and 110, from which it is evident, that for large block lengths (over 300 bits), there will be fewer errors in a block with the BELL modem than with the Codex modem. This could be advantageous for an error control system using random error detection and/or correction.

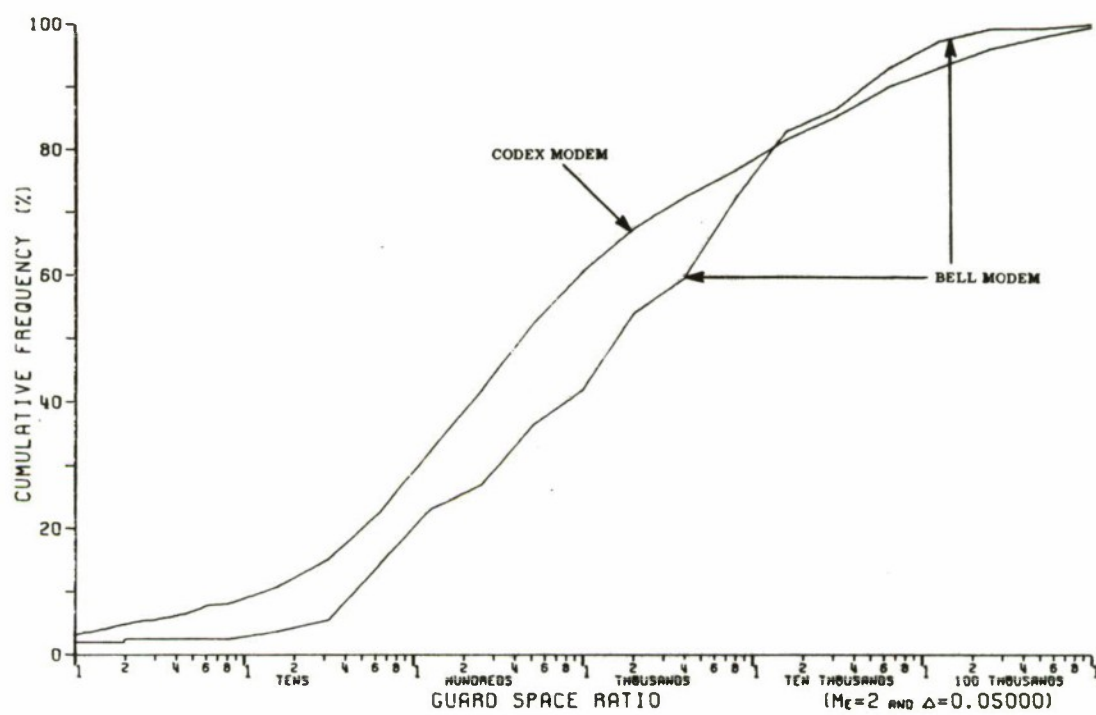


Figure 97. Interval to Burst Ratios — Loop to Santa Rosa 4800 b/s

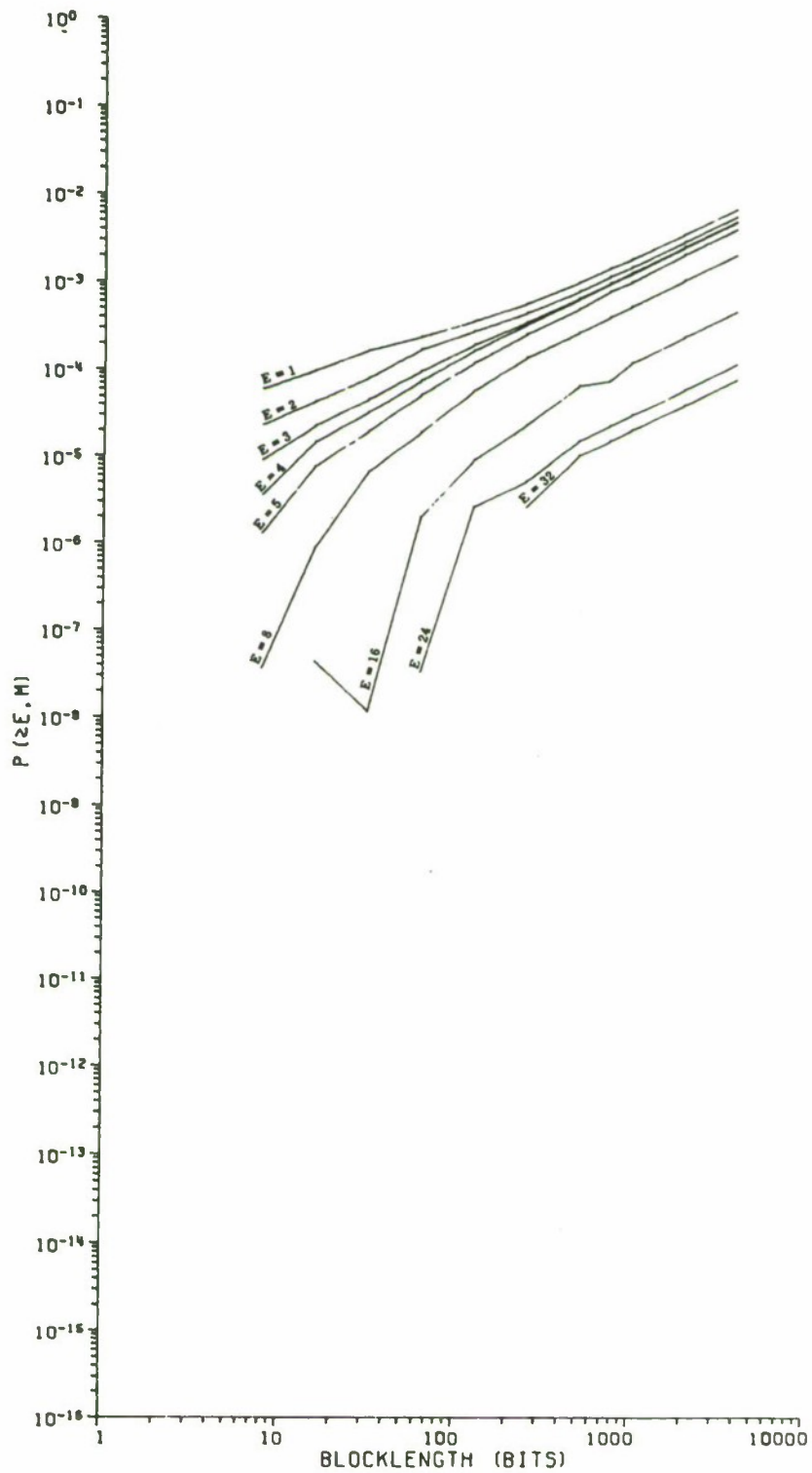


Figure 98. Probability of at Least E Errors in an M Bit Block — Loop to Santa Rosa/Bell/4800 b/s

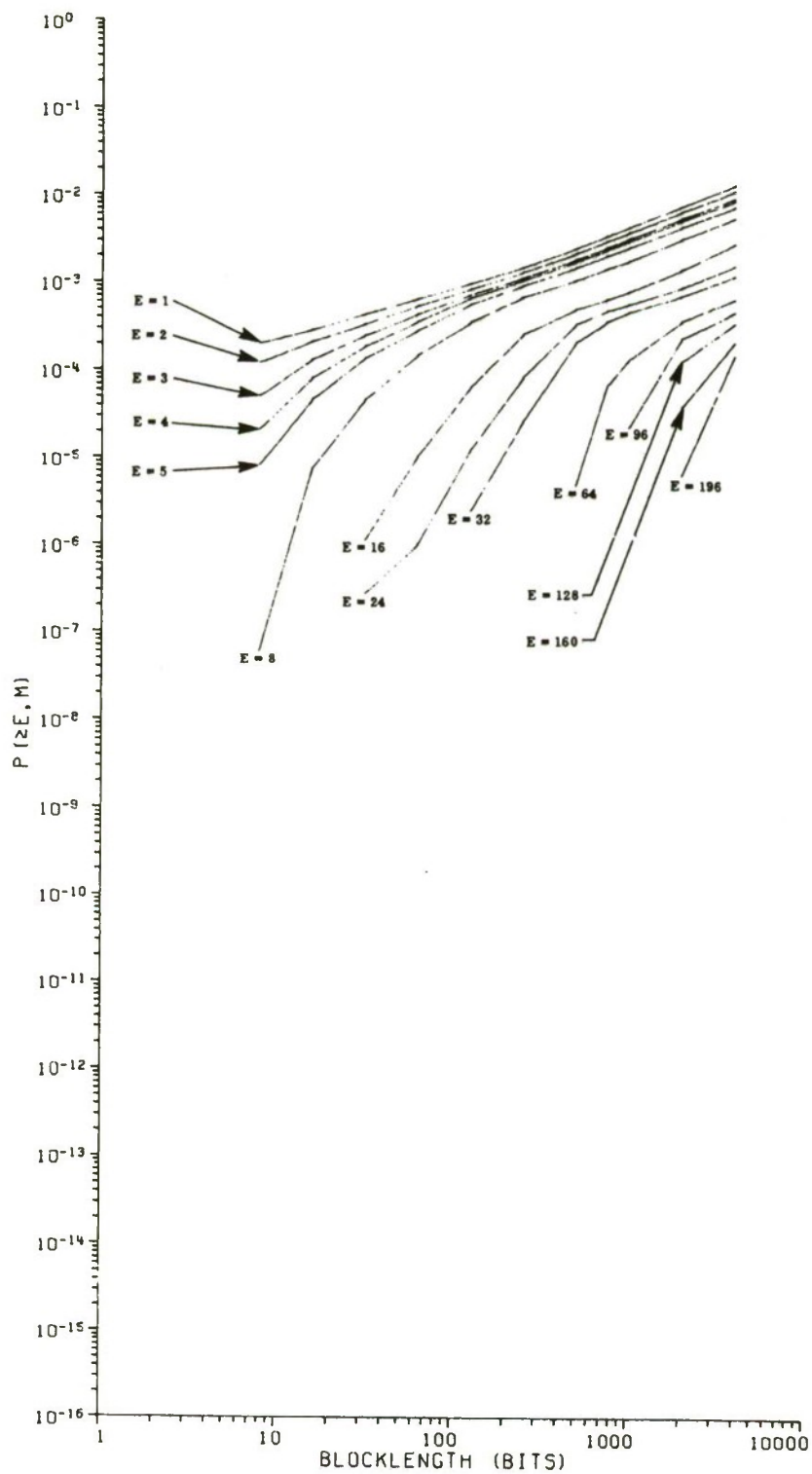


Figure 99. Probability of at Least E Errors in an M Bit Block — Loop to Santa Rosa/Codex/4800 b/s

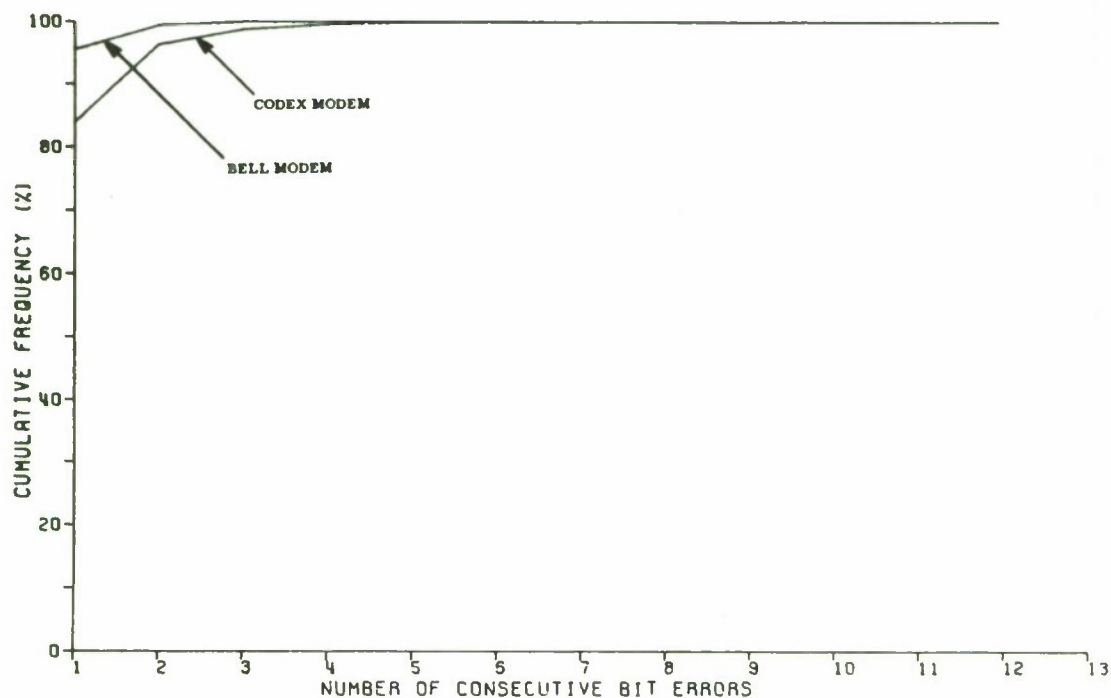


Figure 100. Cumulative Distribution of Consecutive Errors —
Loop to Rockdale/4800 b/s

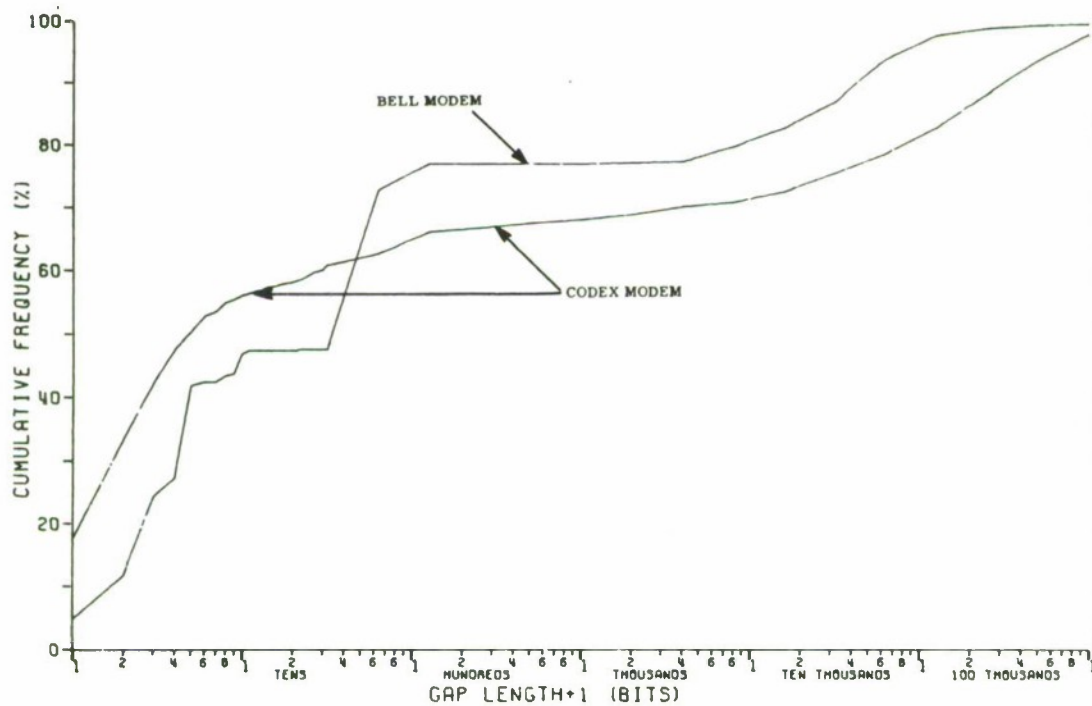


Figure 101. Cumulative Distribution of Error-Free Gaps —
Loop to Rockdale/4800 b/s

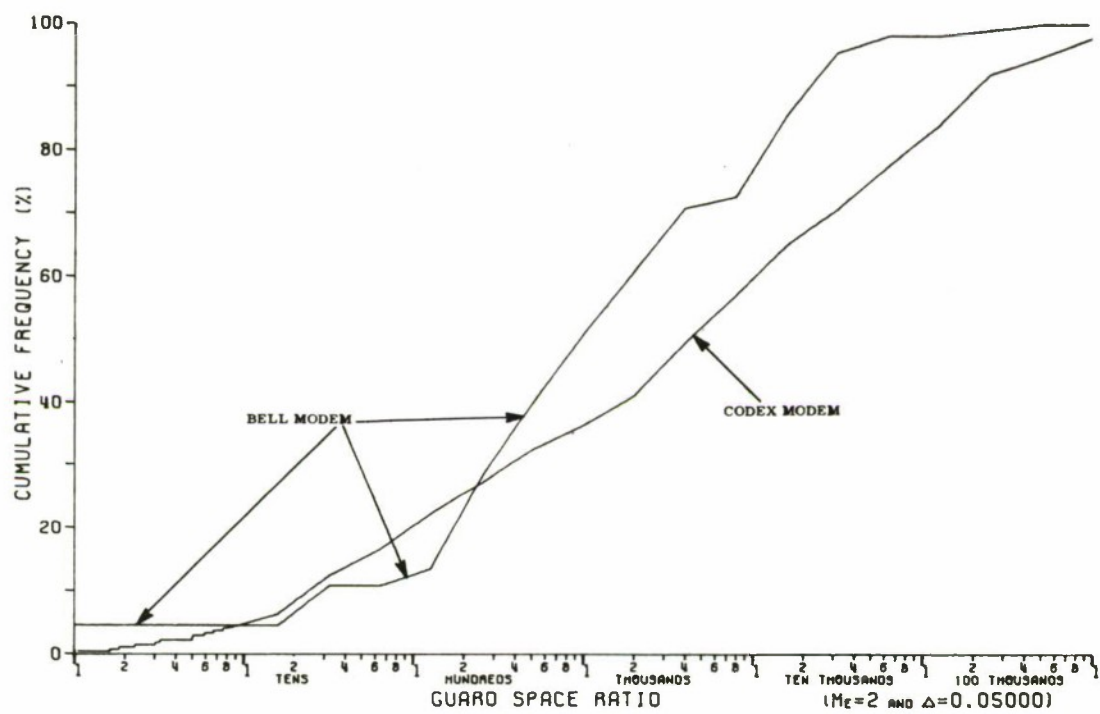


Figure 106. Interval to Burst Ratios — Loop to Rockdale 4800 b/s

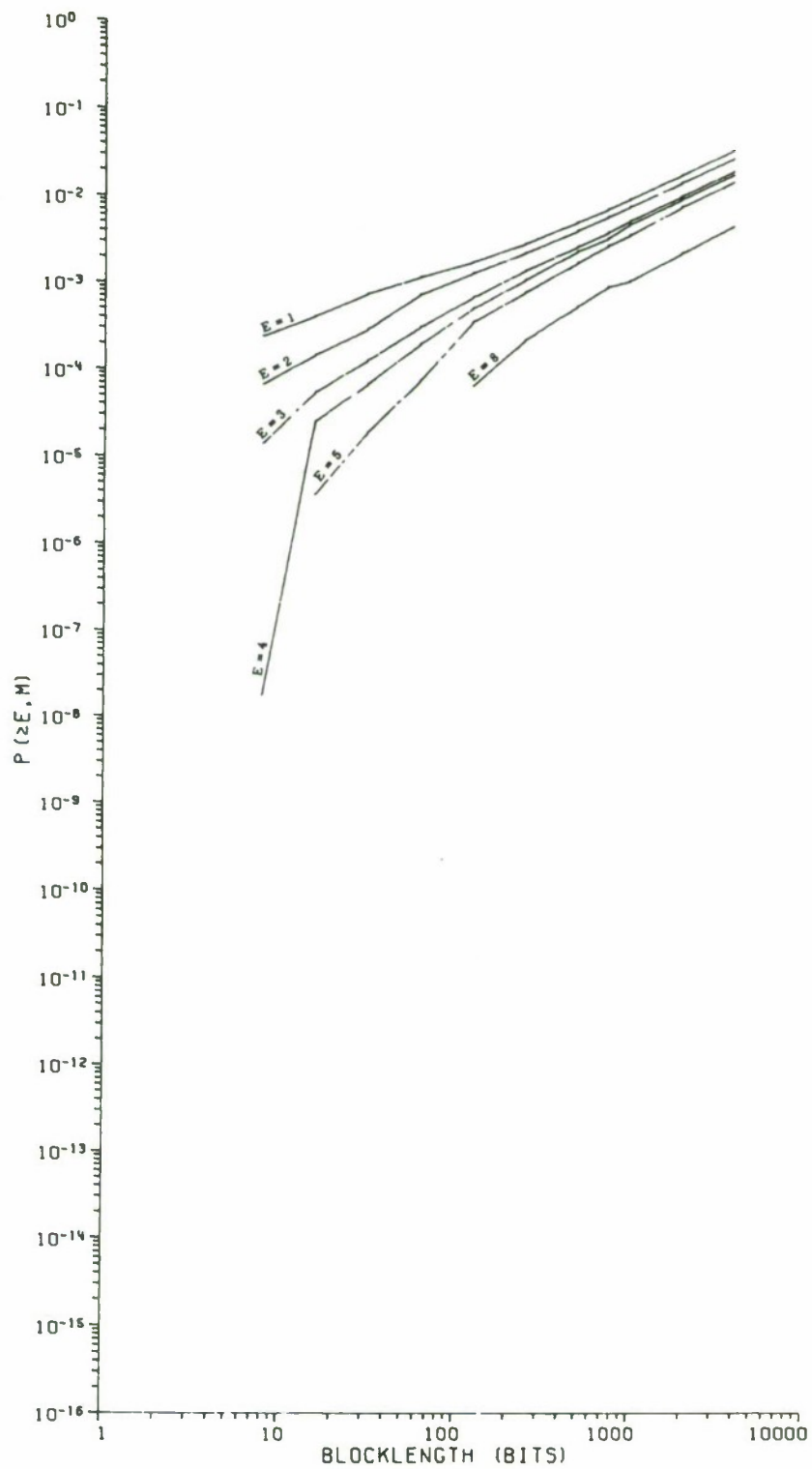


Figure 107. Probability of at Least E Errors in an M Bit Block — Loop to Rockdale/Bell 4800 b/s

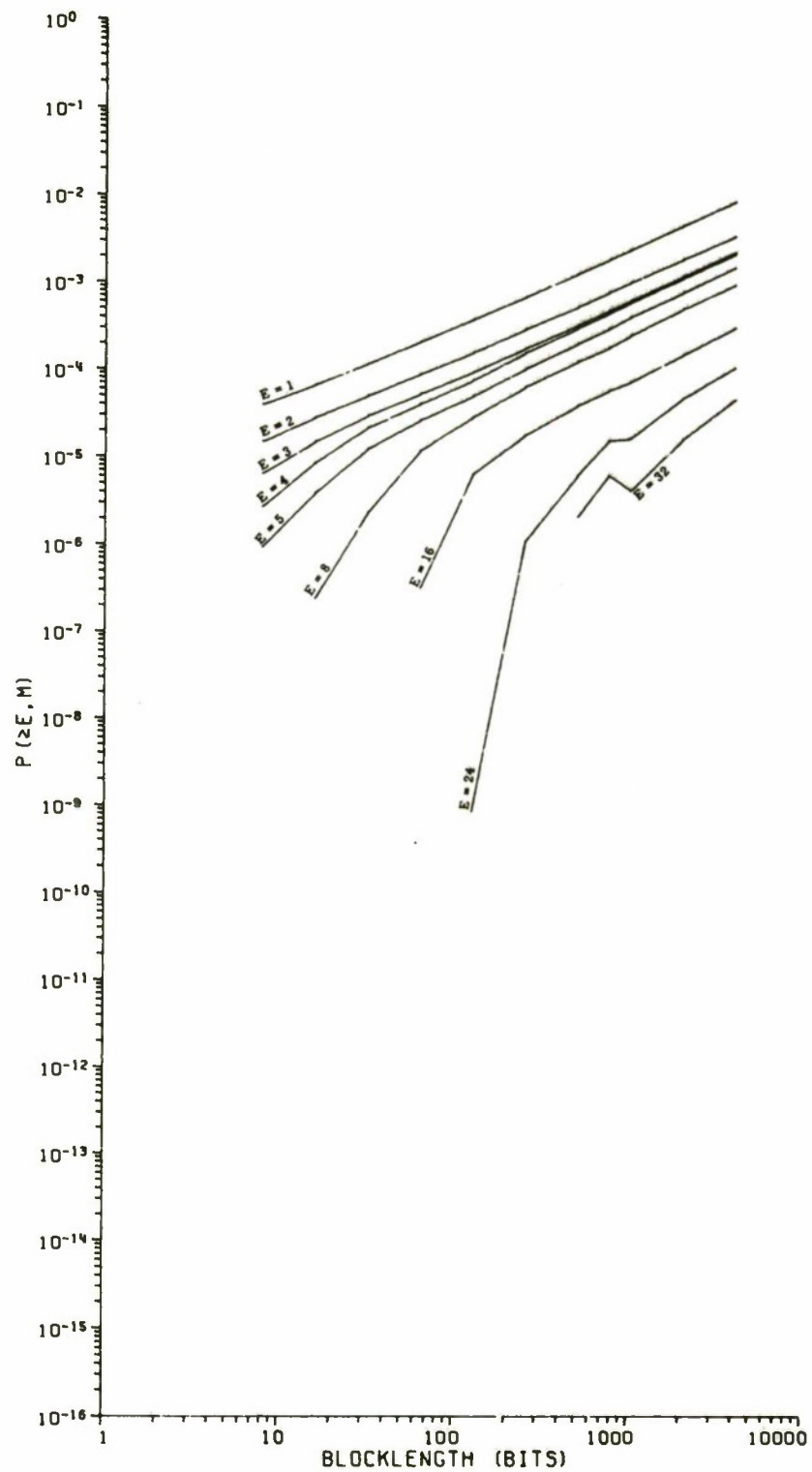


Figure 108. Probability of at Least E Errors in an M Bit Block — Loop to Rockdale/Codex 4800 b/s

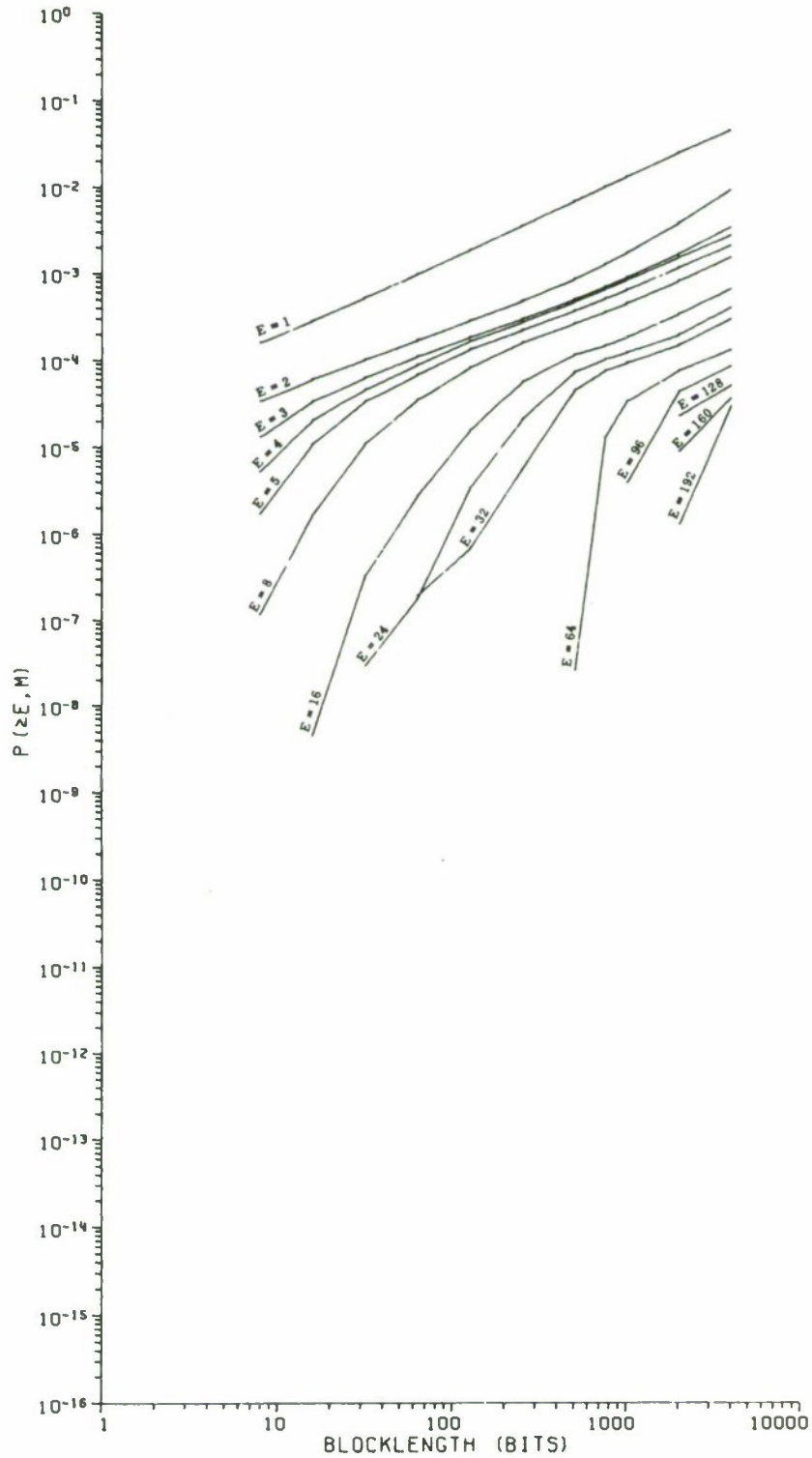


Figure 109. Probability of at Least E Errors in an M Bit Block — Loop to 1 Switch/Codex 4800 b/s

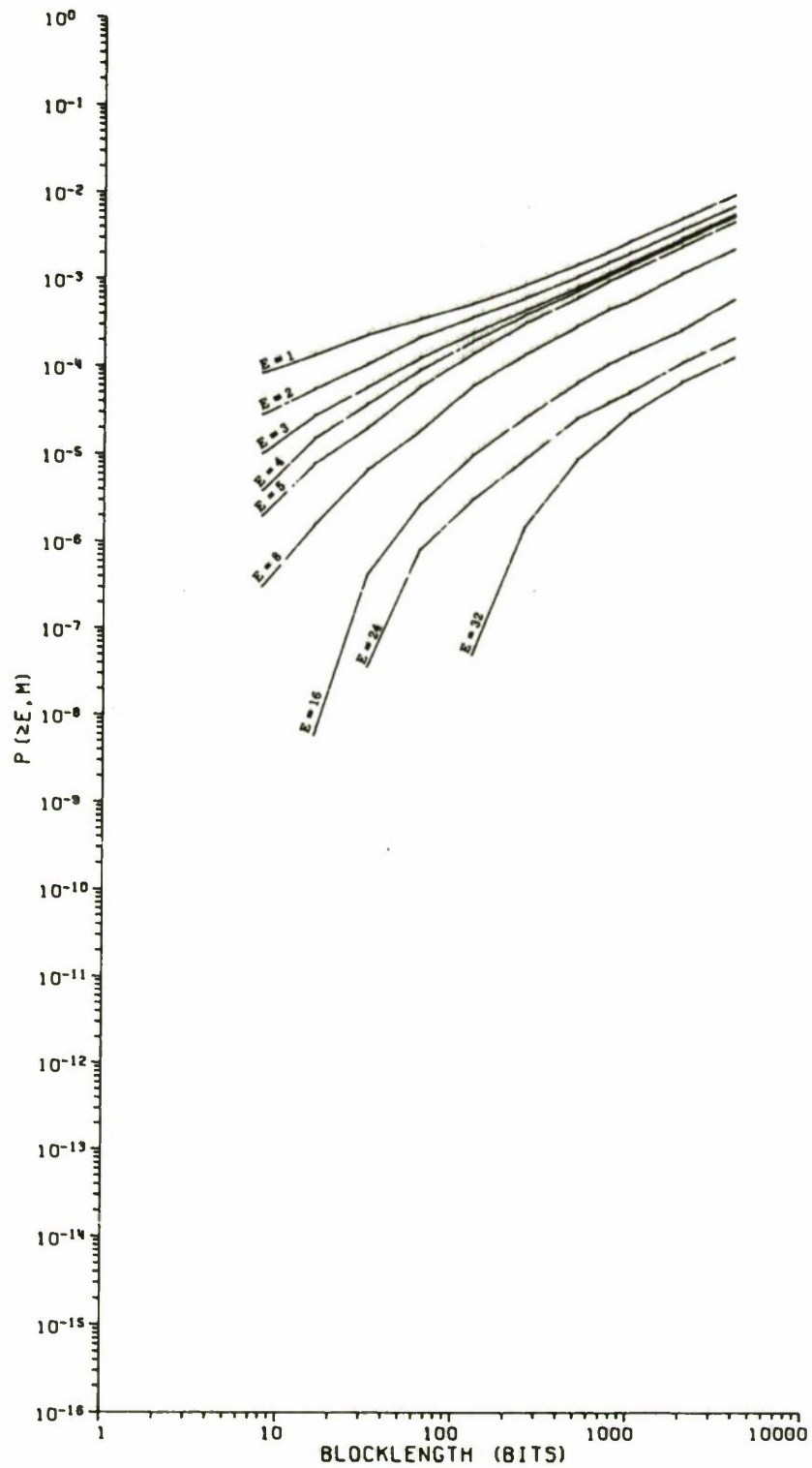


Figure 110. Probability of at Least E Errors in an M Bit Block — Loop to 1 Switch/Bell 4800 b/s

APPENDIX III

CODEX SCRAMBLER MODE VS. CODEX SELF-SYNC MODE

The main body of the error-pattern data collected with the Codex modem was collected with the modem in its scrambler (SCR) mode. This mode has the advantage of randomizing the transmitted bit-pattern so as to minimize any data dependent error pattern characteristics. A small amount of data was collected (Table VIII) with the modem in its self-sync (SS) or nonscrambler mode. The error rate was not appreciably different although the data sample sizes were radically different.

Comparative Error Distributions

The distributions of consecutive errors (Figure 111) showed no mode dependencies although the error-free gaps (Figure 112) imply more short bursts in the self-sync mode. This is not confirmed by the burst distributions, Figure 113, although in all cases the majority of bursts are well under 100 bits long. The remaining burst related distributions, Figures 114 through 117, showed no great variations between modes. The block error rates were generally lower at 4800 b/s in the self-sync versus scrambler modes (Figures 118 and 119), but higher at 9600 b/s (Figures 120 and 121).

It would appear from this limited sample of data, that the differences in error performance of the two Codex modem modes is minimal, when the source data is pseudo random.

Table VIII
Data Summary -- Codex Scrambler vs. Self-Sync

Connectivity	Data Rate	Total Bits	Total Errors	Bit Error Rate
Loop to Two Switches Scrambler	4800 b/s	838, 324, 834	34, 840	4.2 E-5
Loop to Two Switches Self-Sync	4800 b/s	49, 492, 546	600	1.2 E-5
Loop to Two Switches Scrambler	9600 b/s	100, 240, 103	13, 551	1.4 E-4
Loop to Two Switches Self-Sync	9600 b/s	17, 156, 907	6, 384	3.7 E-4

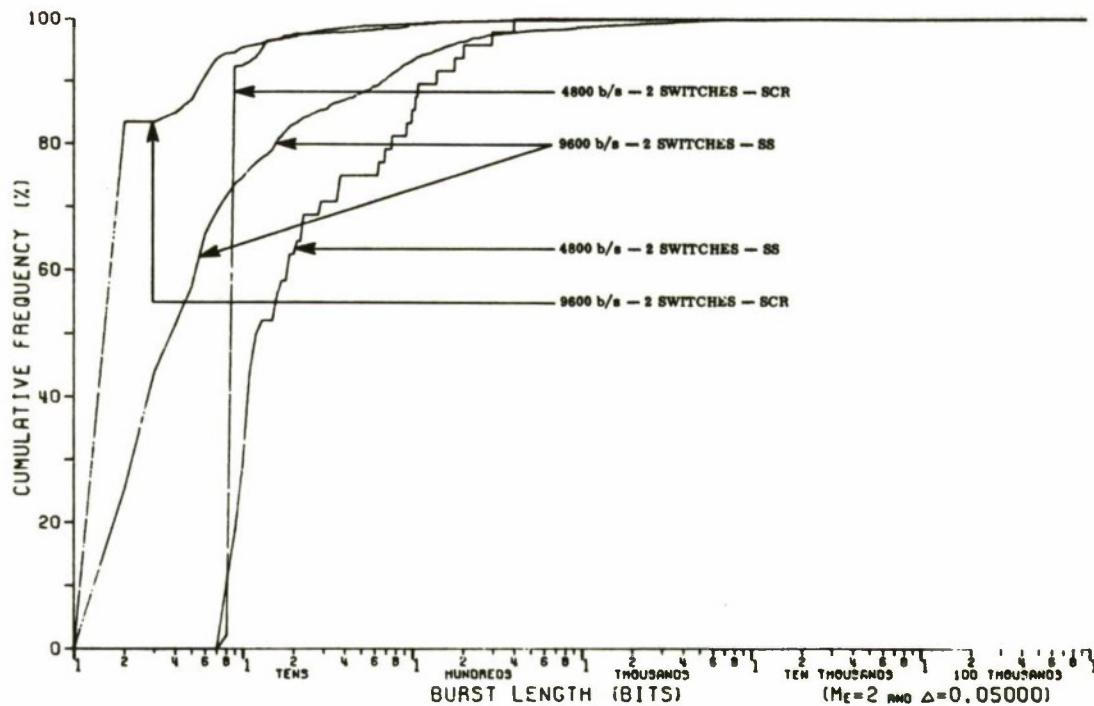


Figure 113. Cumulative Distribution on Lengths of Bursts — Codex SS vs. Codex SCR Data

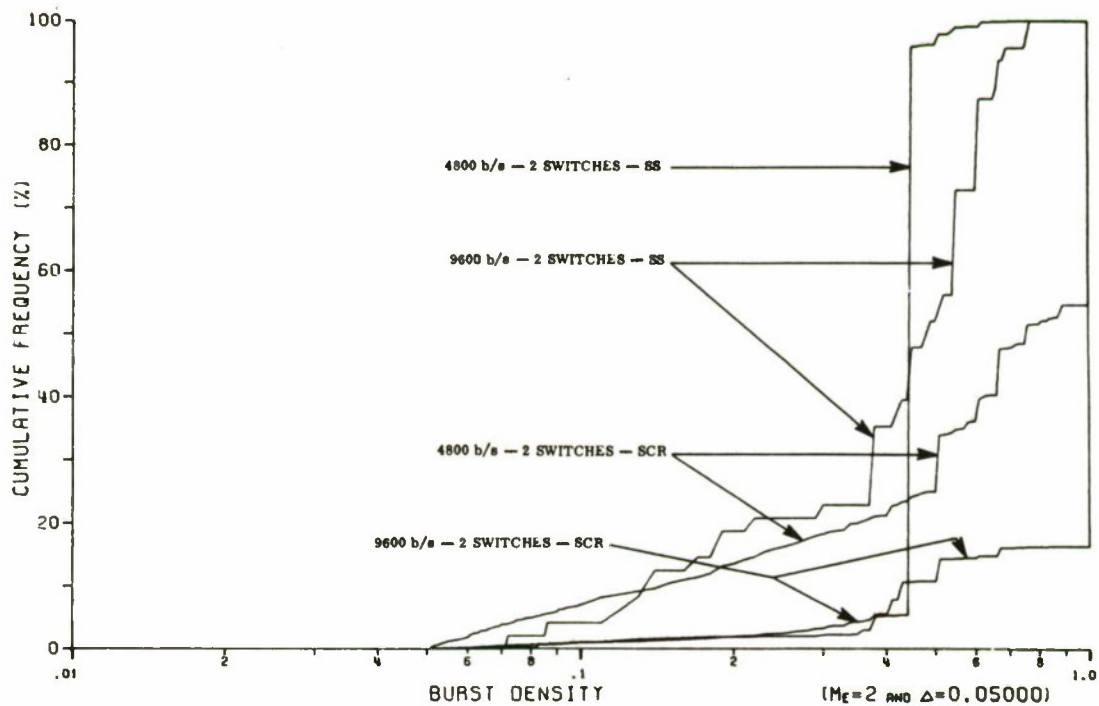


Figure 114. Cumulative Distribution on Burst Densities — Codex SS vs. Codex SCR Data

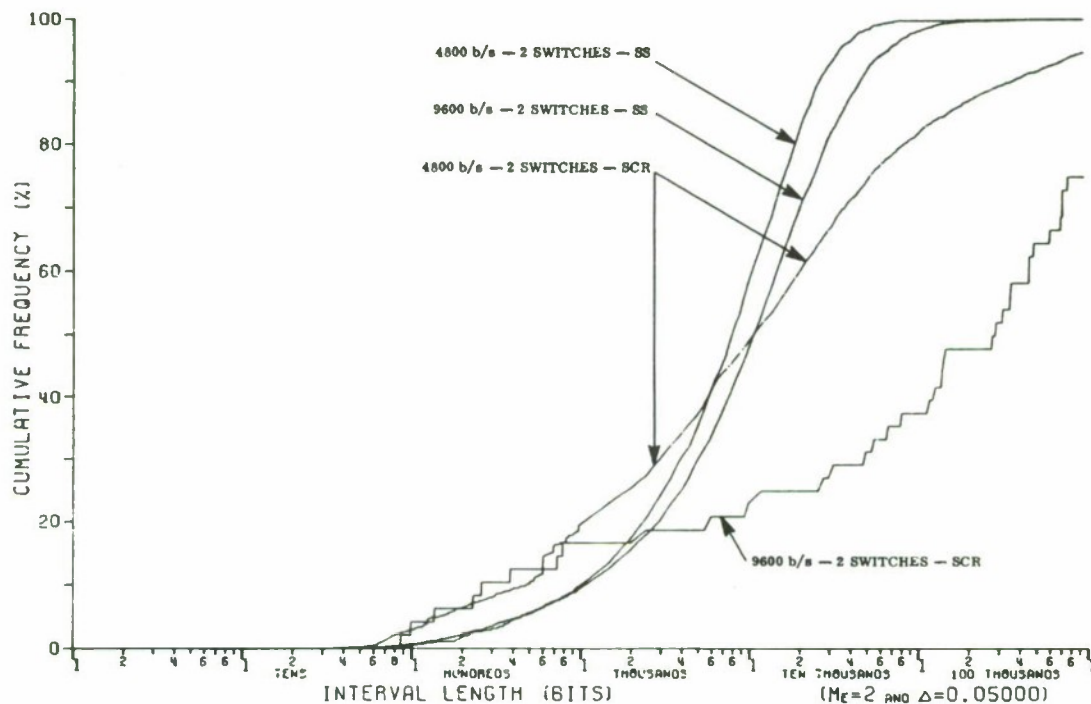


Figure 115. Cumulative Distribution on Lengths of Intervals - Codex SS vs. Codex SCR Data

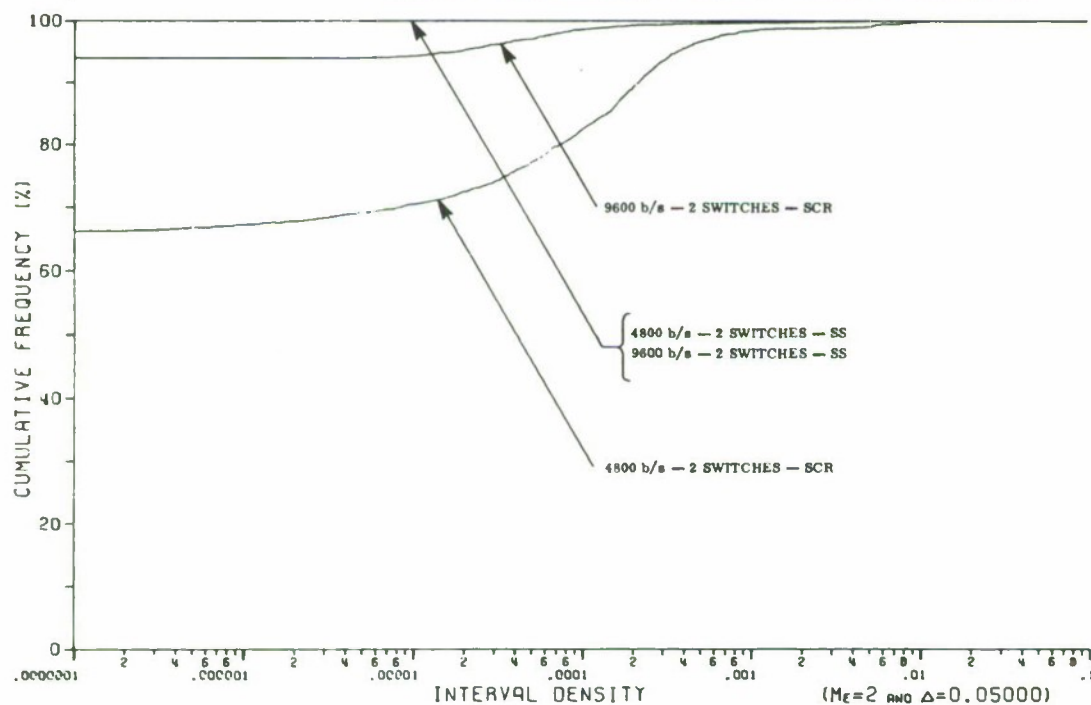


Figure 116. Cumulative Distribution on Interval Densities - Codex SS vs. Codex SCR Data

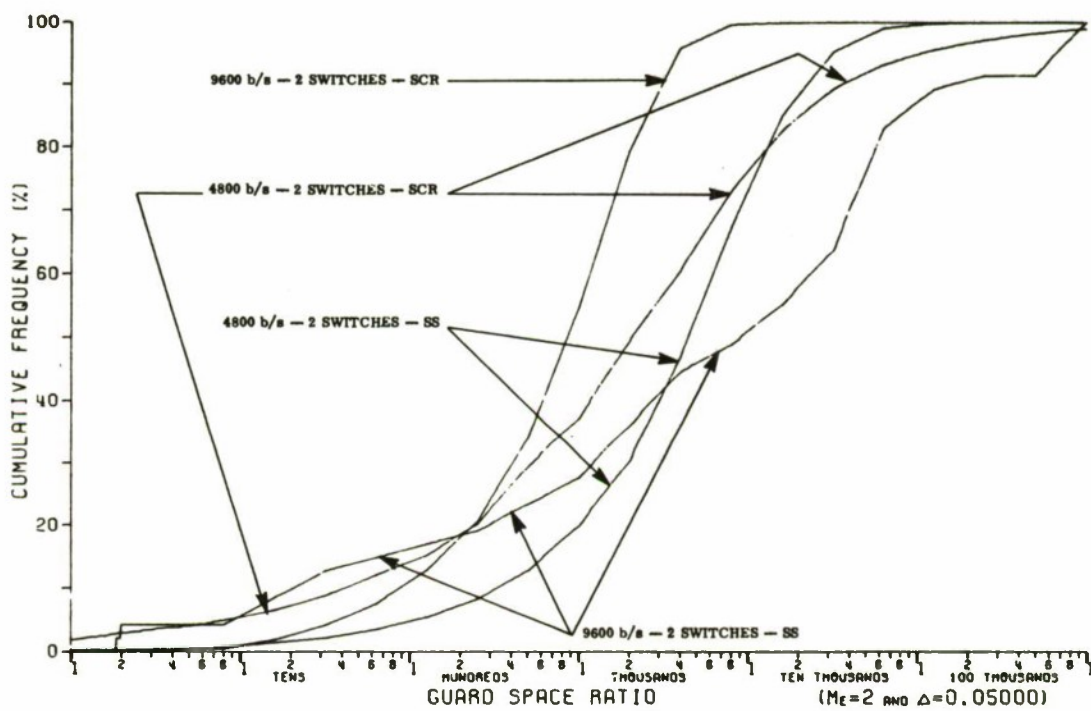


Figure 117. Interval to Burst Ratios — Codex SS vs. Codex SCR Data

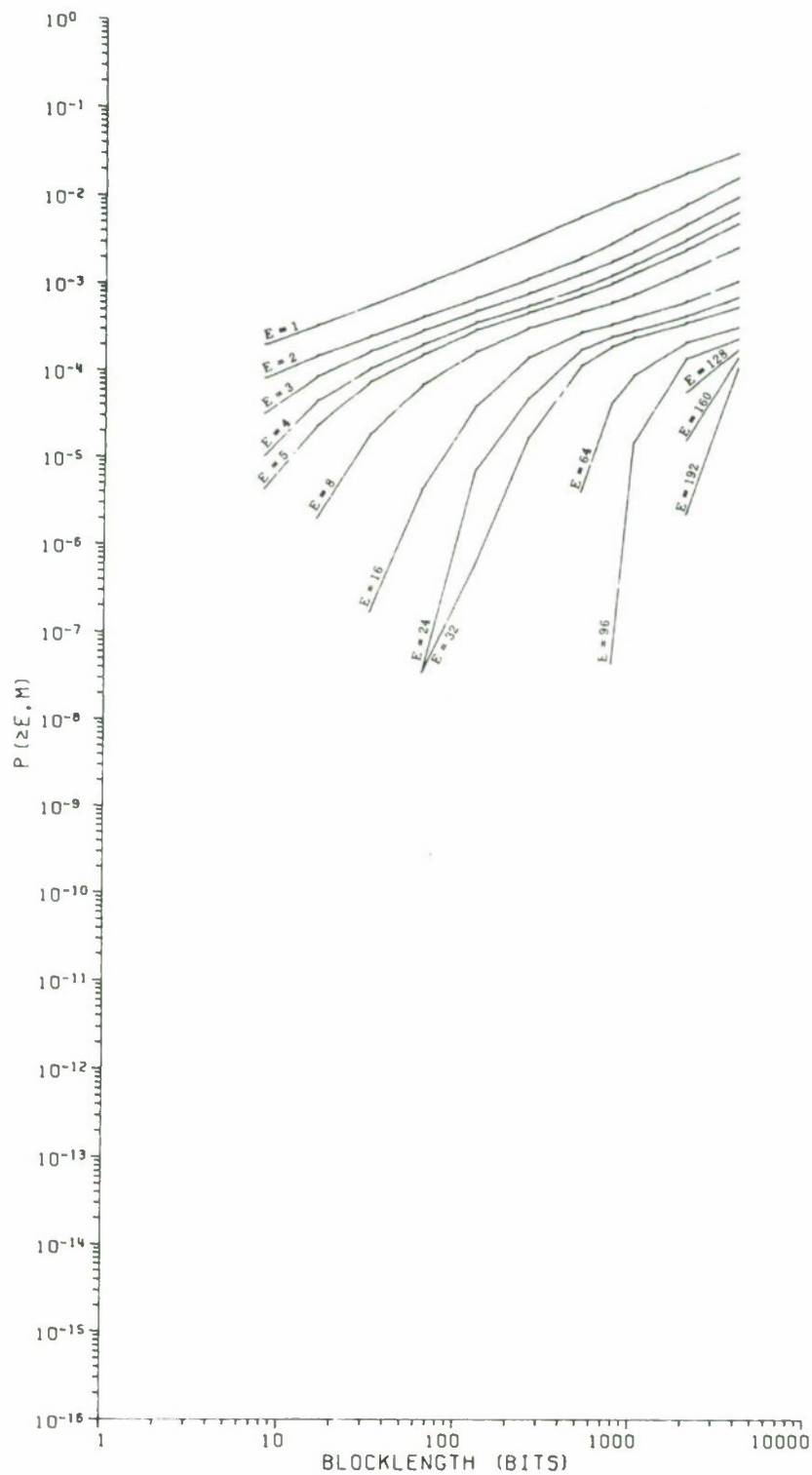


Figure 118. Probability of at Least E Errors in an M Bit Block — Loop to 2 Switches/4800 b/s

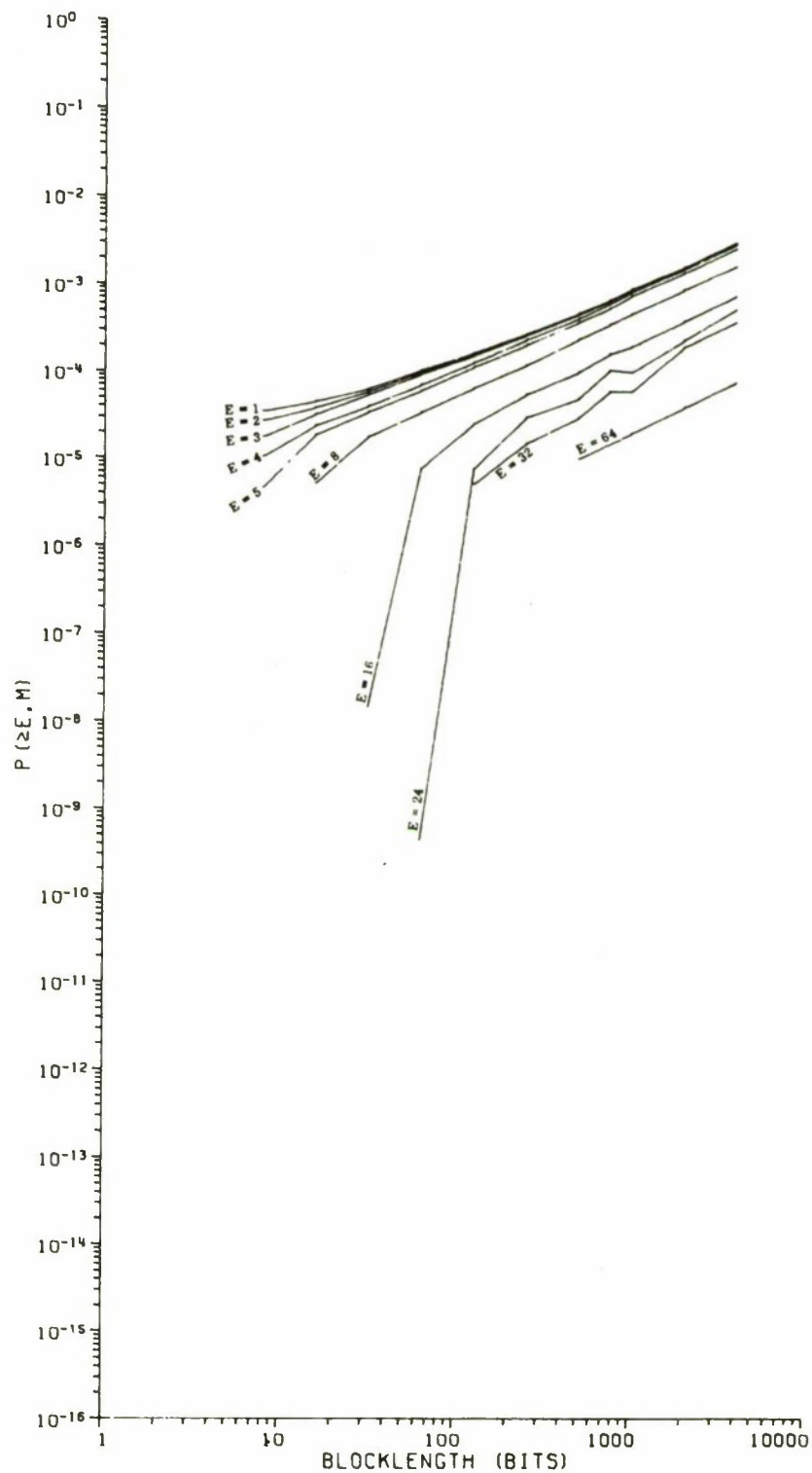


Figure 119. Probability of at Least E Errors in an M Bit Block — Loop to 2 Switches/Codex SS 4800 b/s

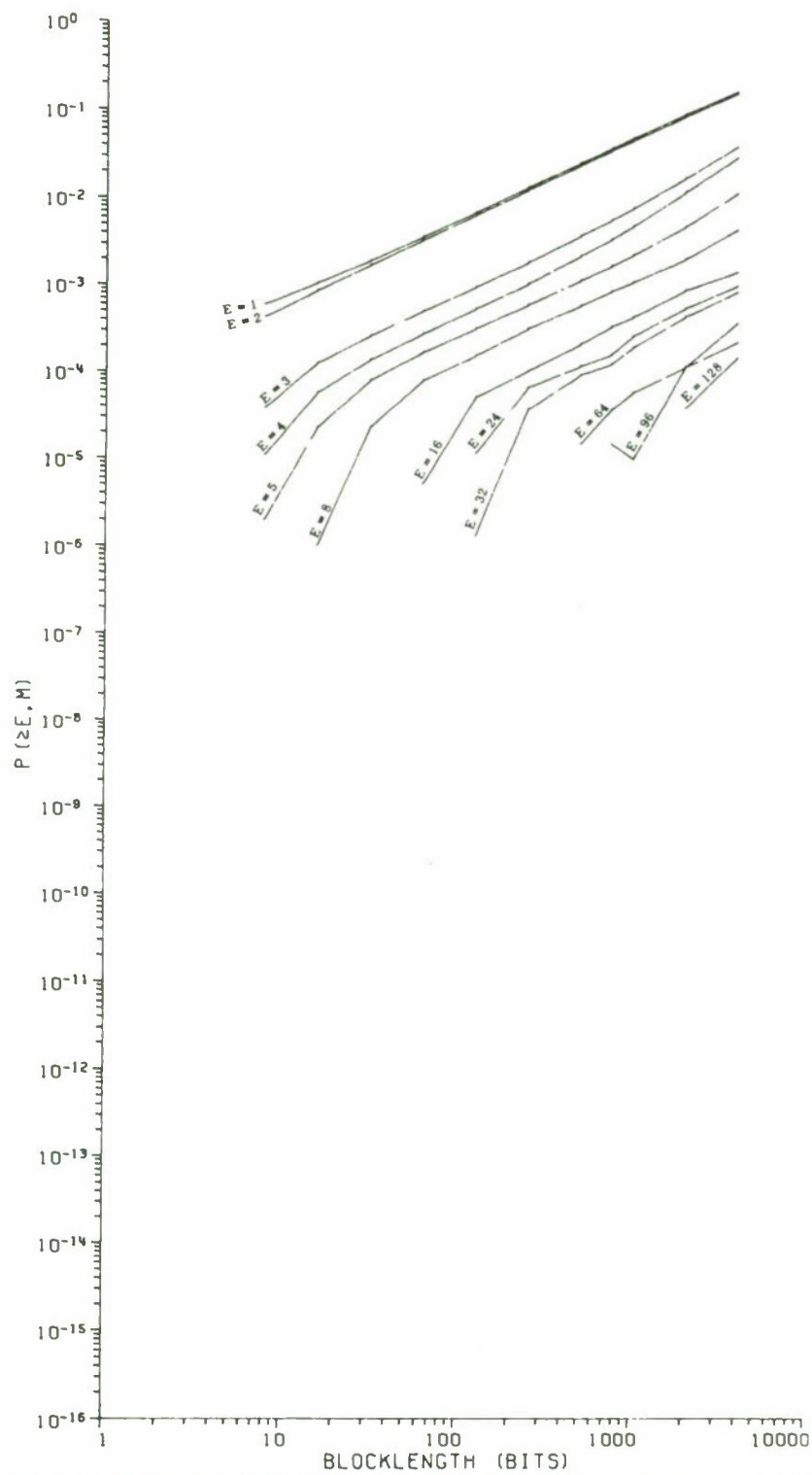


Figure 120. Probability of at Least E Errors in an M Bit Block — Loop to 2 Switches/9600 b/s

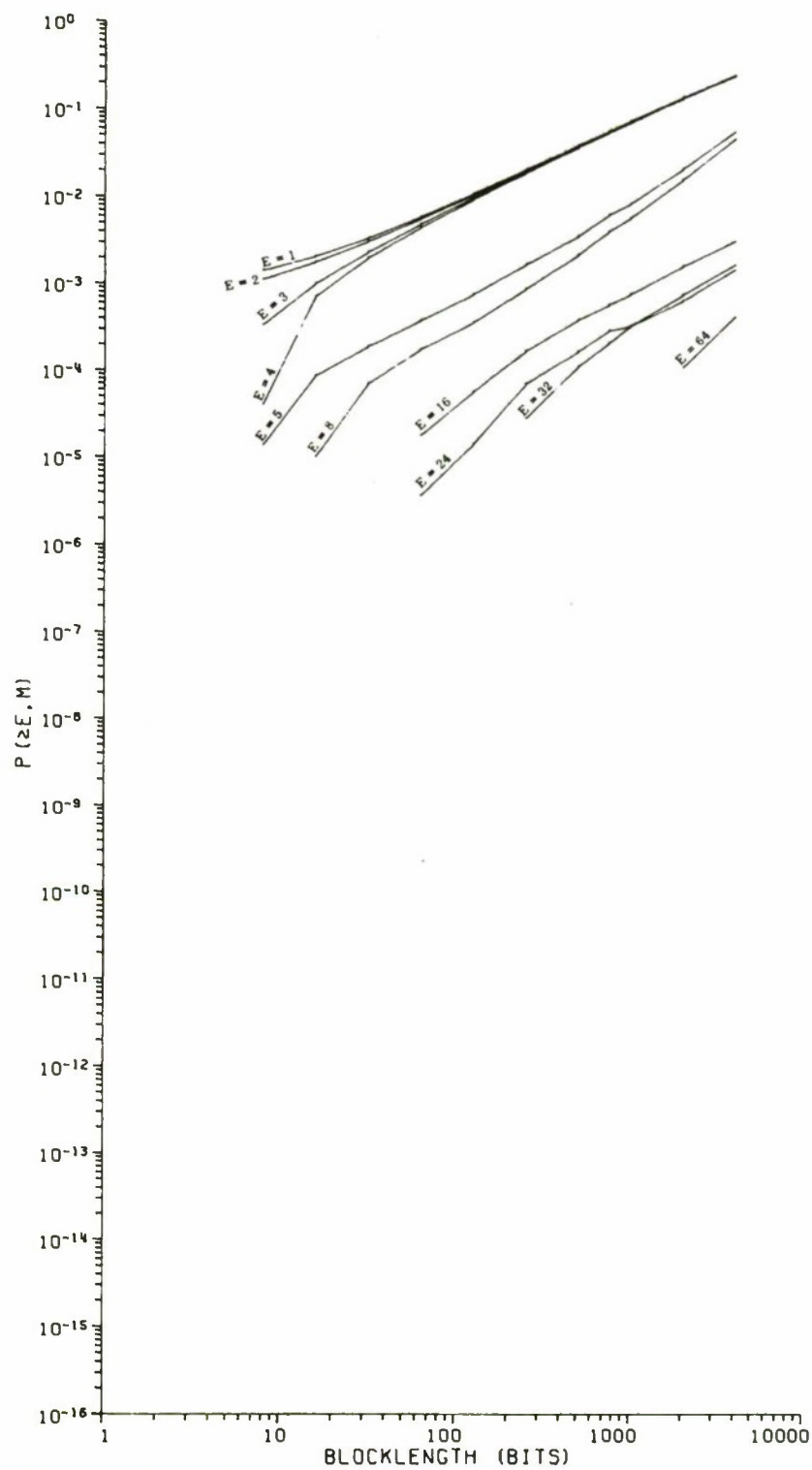


Figure 121. Probability of at Least E Errors in an M Bit Block — Loop to 2 Switches/Codex SS 9600 b/s

REFERENCES

1. K. Brayer, "Error Patterns Measured on Transequential HF Communication Links," IEEE Trans. on Communication Technology, April 1968.
2. J.R. Lemon, Comparative Performance Evaluation of Common and Special Grade Conus AUTOVON Trunks, Phase II, RADC-TR-72-317, December 1972.
3. J. L. Hammond, J. E. Brown, and S. S. Liu, Development of a Transmission Error Model and an Error Control Model, RADC-TR-75-138, June 1975.
4. B. D. Fritchman, "A Binary Channel Characterization Using Partitioned Markov Chains with Applications to Error Correcting Codes," Lehigh University, Bethlehem, Pa. , June 1967.
5. Bell System Technical Reference, Data Set 208A Interface Specification, PUB 41209, October 1972, p. 10.